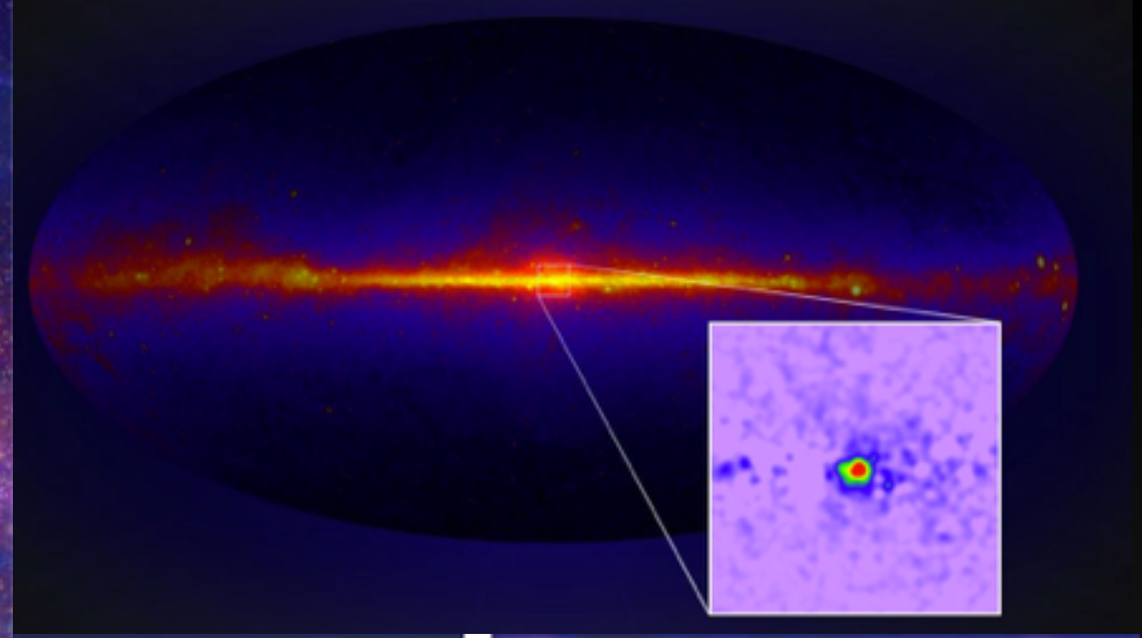

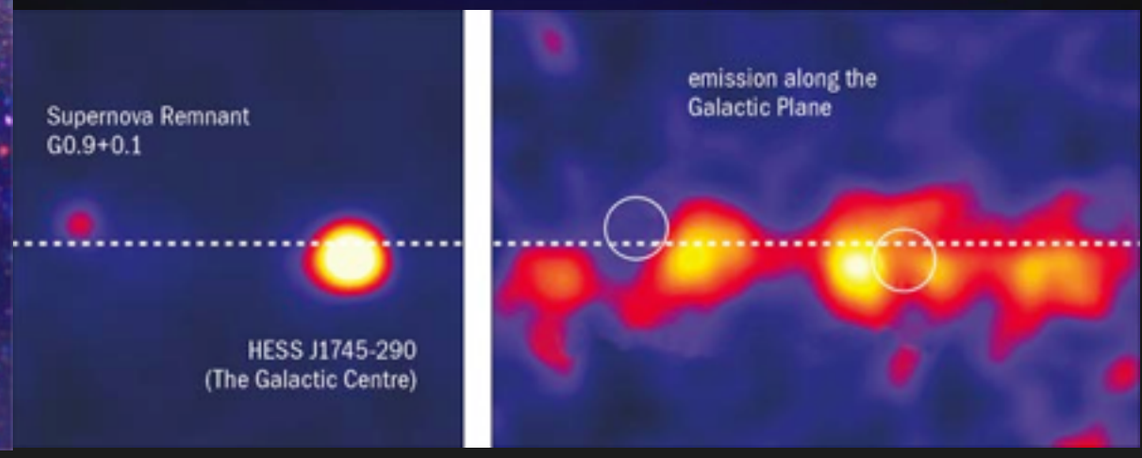

The Galactic Center Environment and Dark Matter Annihilation

Tim Linden

CCAPP Postdoctoral Fellow
Center for Cosmology and Astro-Particle Physics
The Ohio State University

CCAPP Summer Seminar 8/16/16

The Central Molecular Zone

- 400 pc x 80 pc
- 10^7 $M_\odot$ of gas in Molecular Clouds
- Conditions similar to nearby starburst galaxies

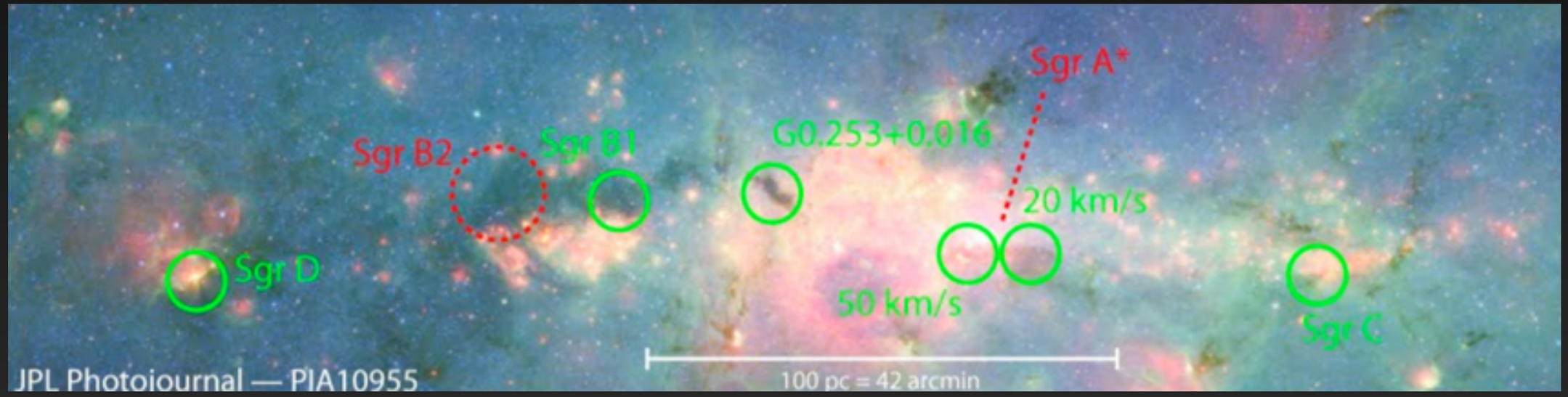

- Molecular Gas clouds in the Central Molecular Zone are hot (~100K)
- Indicative of heating by a significant cosmic-ray population confined in the central molecular zone. (Yusef-Zadeh et al. 2013)

What Generates these Cosmic-Rays?

The Galactic center region is known to contain nearly every known cosmic-ray acceleration mechanism.

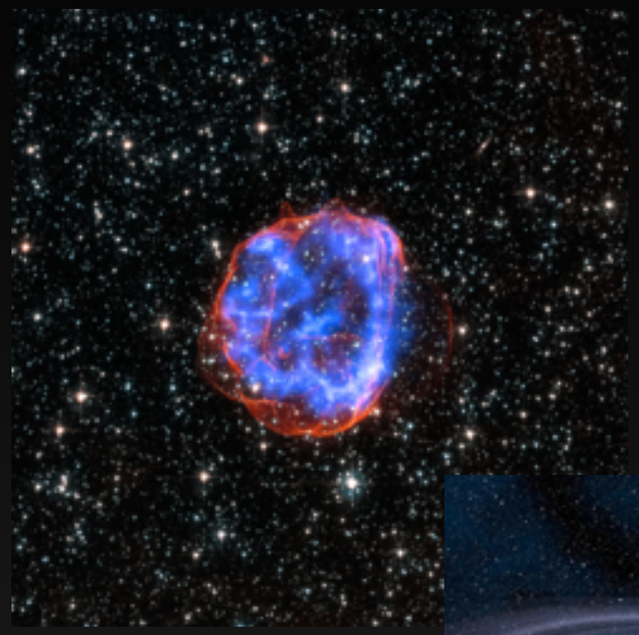

1.) Supernovae
2.) Pulsars
3.) Sgr A*
4.) Reacceleration
5.) Dark Matter Annihilation?

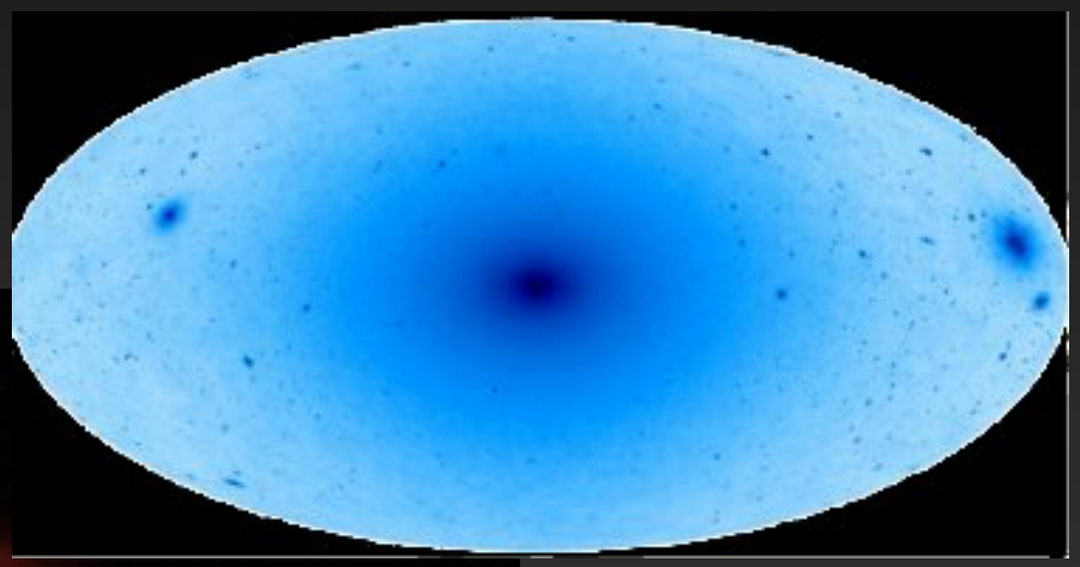

The Galactic Center Supernovae

Multiwavelength observations indicate that the Galactic Center is a dense star-forming environment.

3-20% of the total Galactic Star Formation Rate is contained within the Central Molecular Zone.

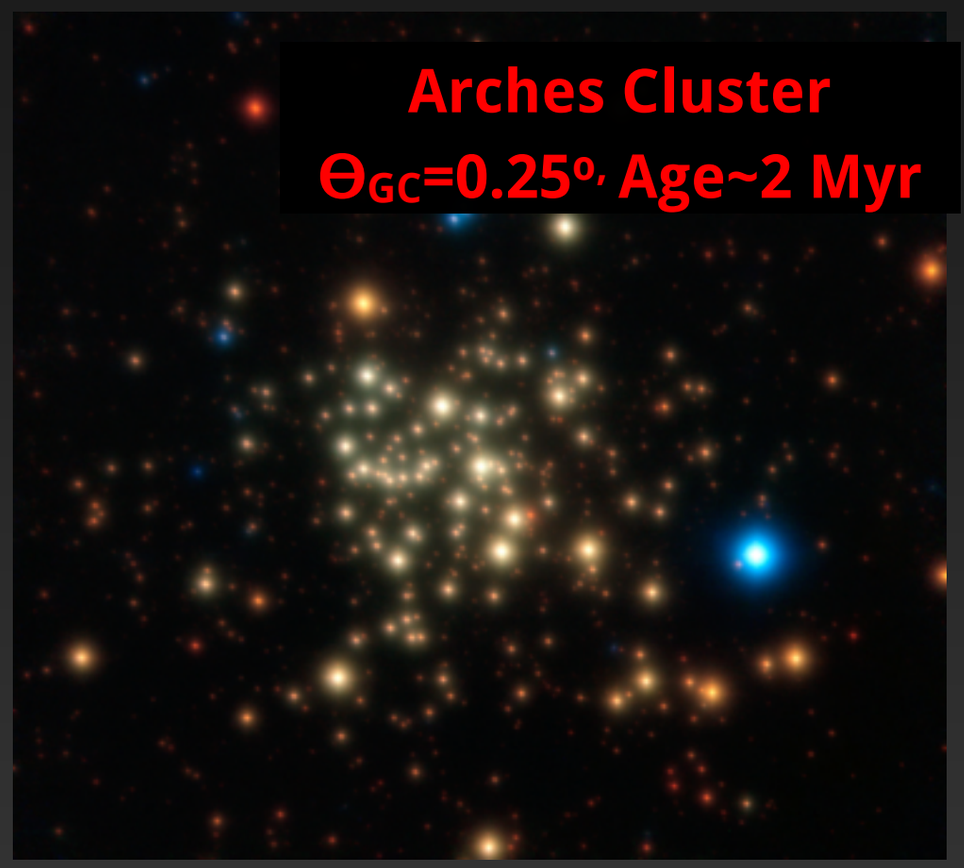

2-4% - ISOGAL Survey Immer et al. (2012)
2.5-5% - Young Stellar Objects Yusef-Zadeh et al. (2009)
5-10% - Infrared Flux Longmore et al. (2013)
10-20% - Wolf-Rayet Stars Rosslowe & Crowther (2014)
2% - Far-IR Flux Thompson et al. (2007)
2.5-6% - SN1a Schanne et al. (2007)

Galactic Center Pulsars

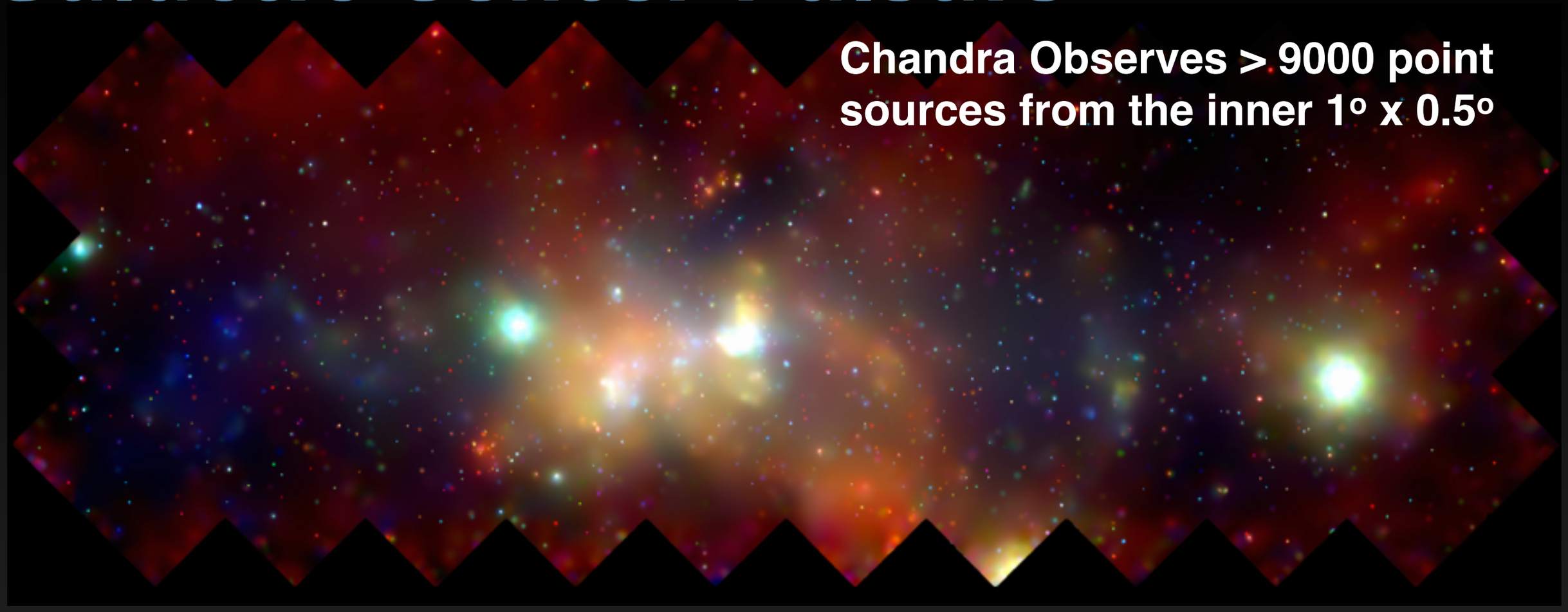

The Galactic Center is expected to host a significant population of both young pulsars (due to its high SFR), and millisecond pulsars (in part from the disruption of Globular Clusters).

Over the lifetime of a young (recycled) pulsar, ~10^{50} erg of energy our released, primarily in the form of relativistic e^+e^- pairs.

The Sgr A* Source

see slides by: R. Chaves, R. Parsons

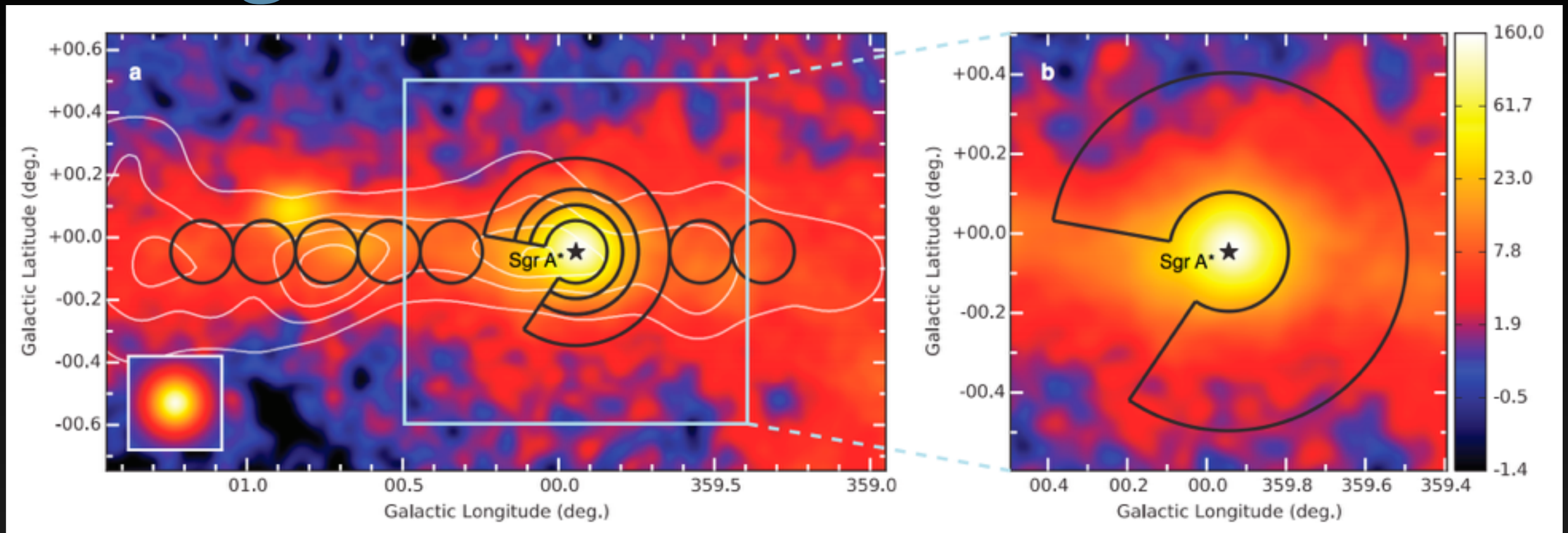

HESS has detected diffuse gamma-ray emission at energies ~100 TeV.

This is not observed in even the youngest supernova remnants.

The emission profile is indicative of diffusion from the central BH.

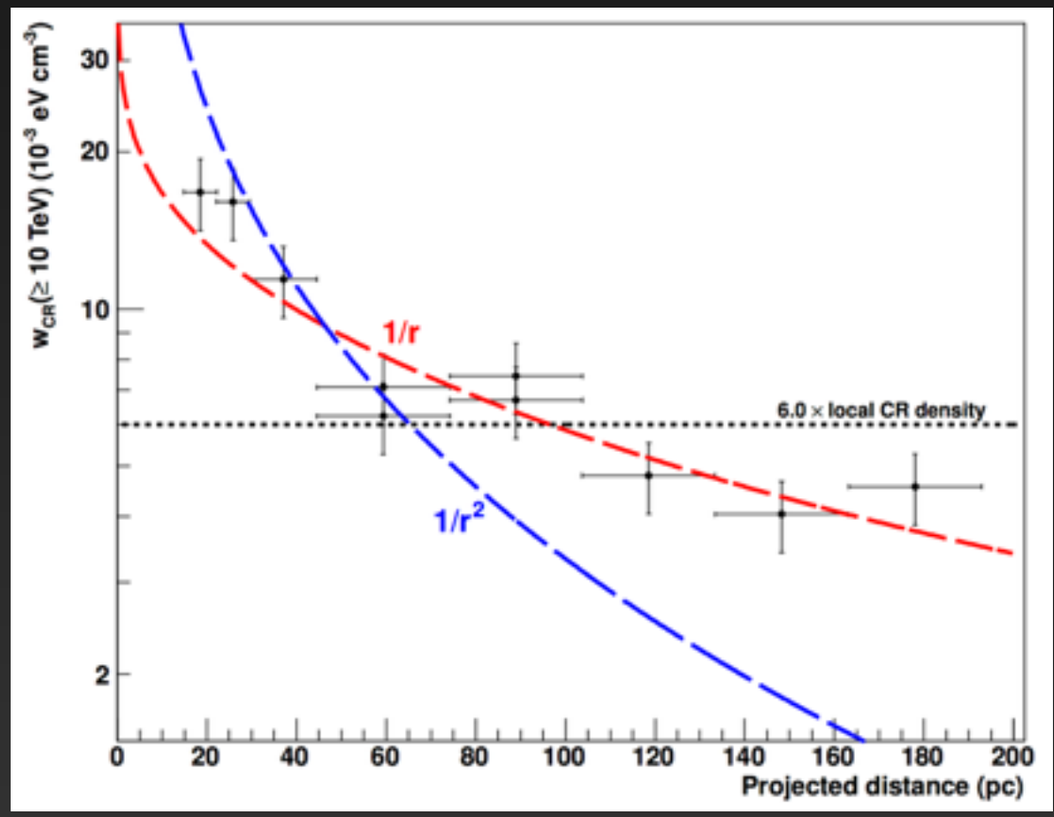

Dark Matter Annihilation?

WIMPs are currently among the most well-motivated dark matter models.

WIMP annihilation naturally produces a significant cosmic-ray (and gamma-ray) flux.

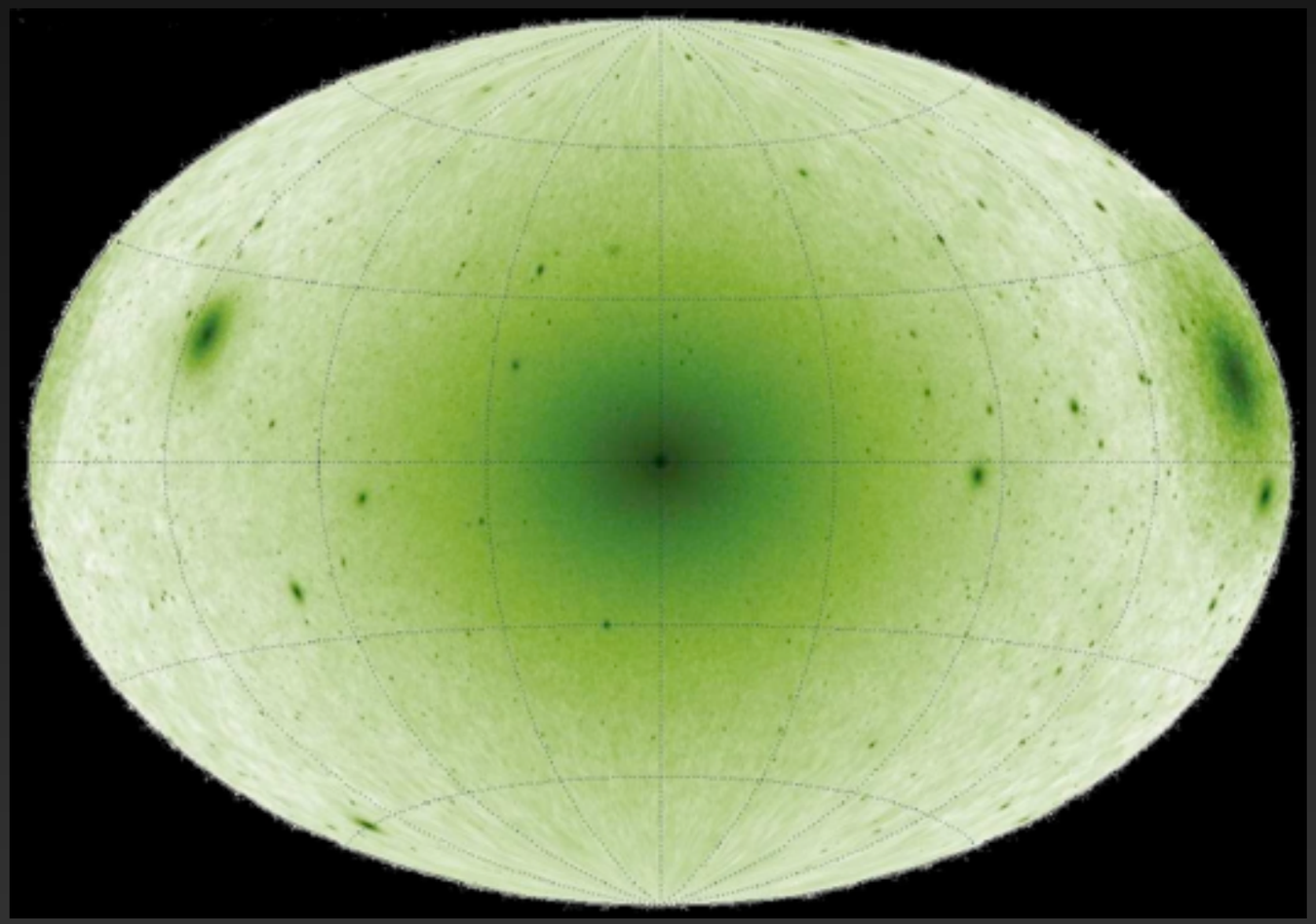

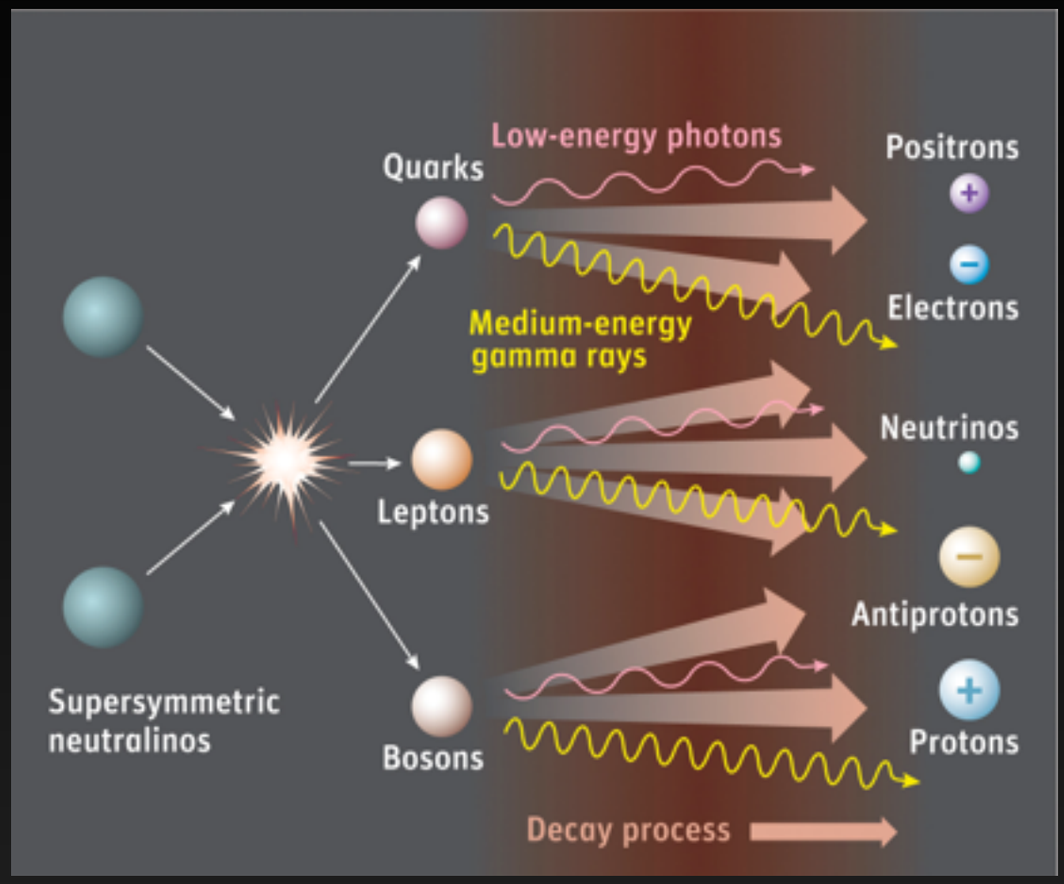

Dark Matter structure simulations uniformly predict that the GC is the brightest source of WIMP annihilations.

Standard scenarios predict the flux from the GC exceeds dSphs by a factor of ~100 – 1000.

Reacceleration

More than 80 filamentary structures identified in the central 2° x 1°.

The filaments are observed as highly polarized, hard-spectrum synchrotron sources – indicative of strongly ordered magnetic fields and hard injected electron spectra.

The best astrophysical explanation involves significant re-acceleration via magnetic reconnection (Lesch & Riech 1992, Lieb et al. (2004).

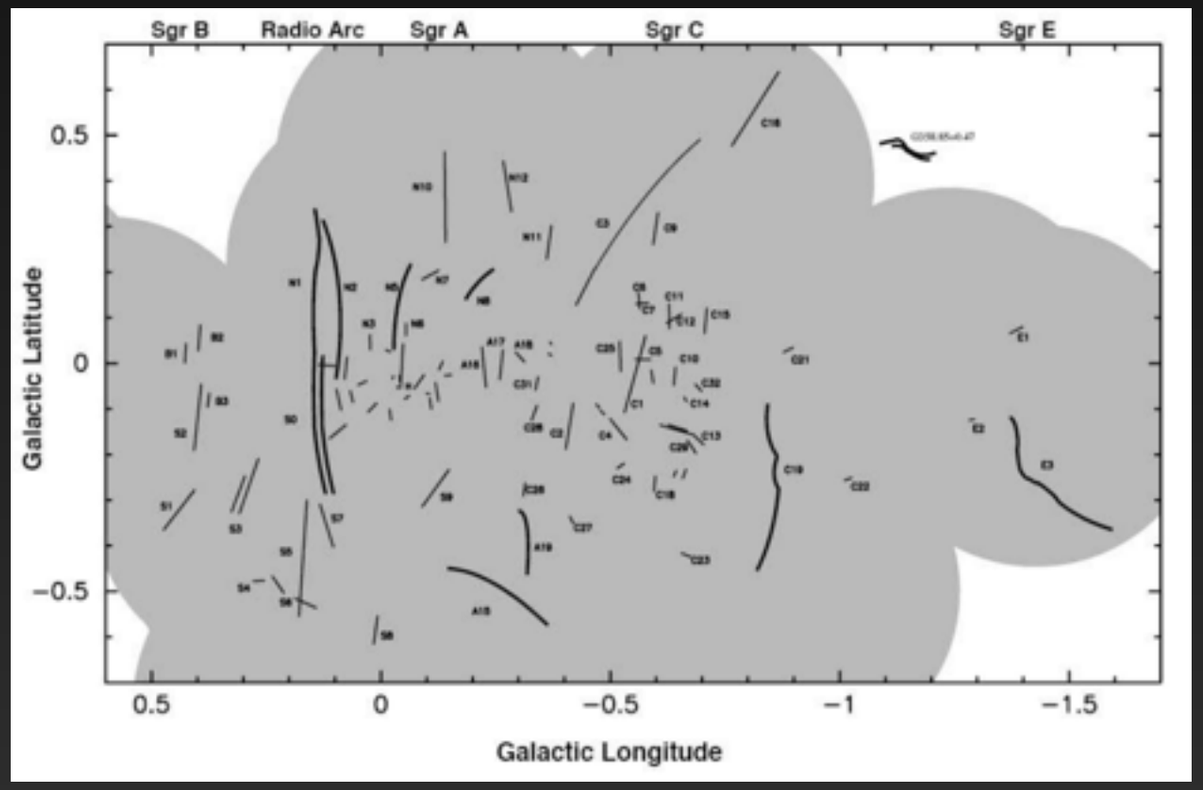

Yusef-Zadeh et al. (2004)

Non-Thermal Emission (Observables)

Fermi Bubbles

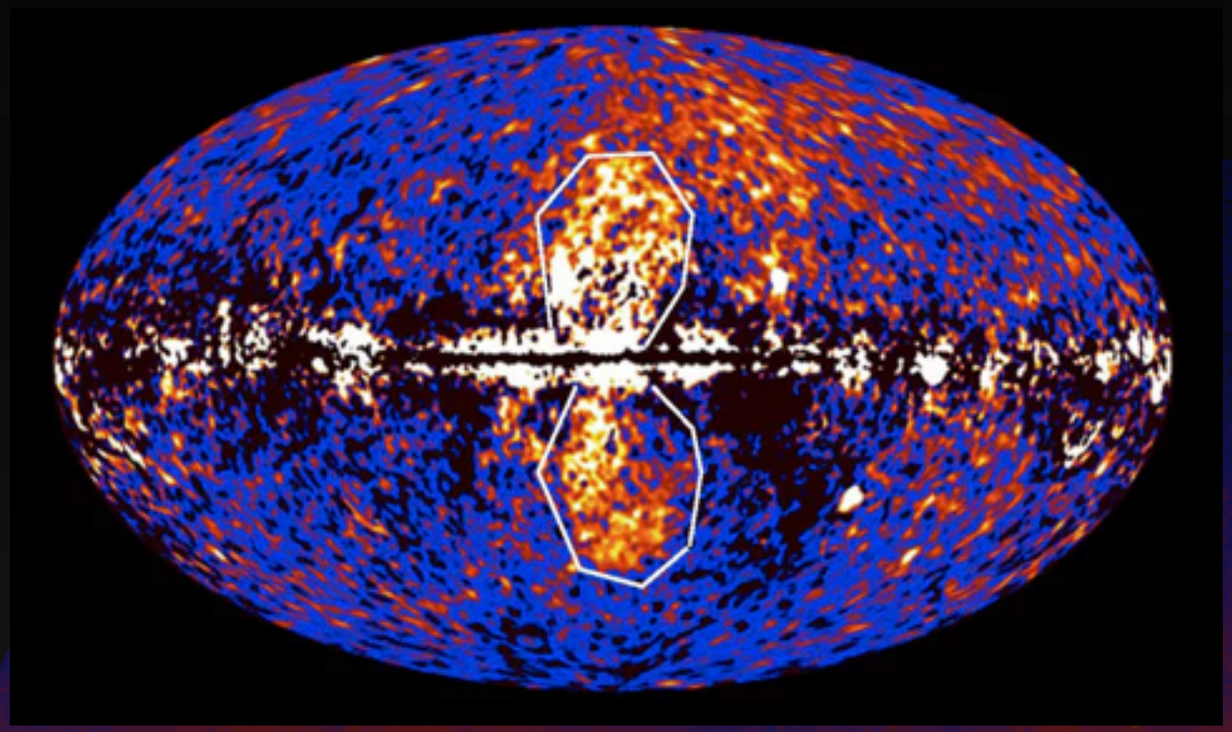

GeV Excess

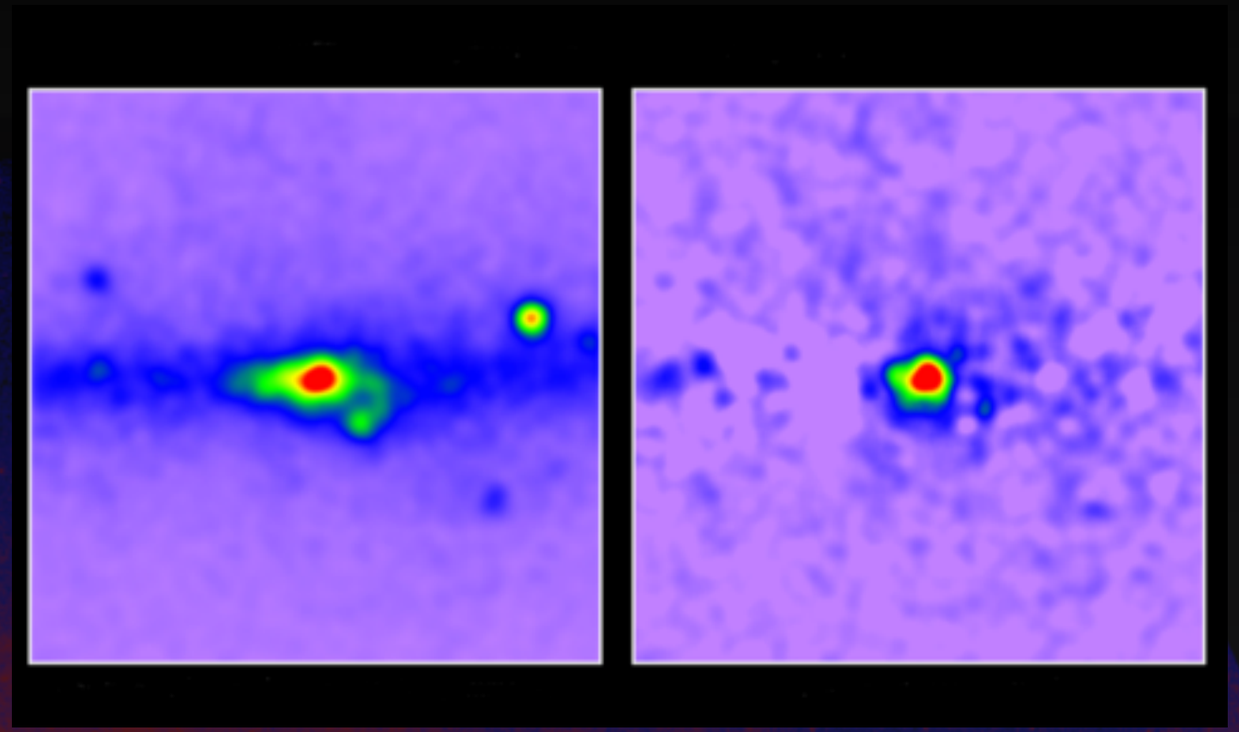

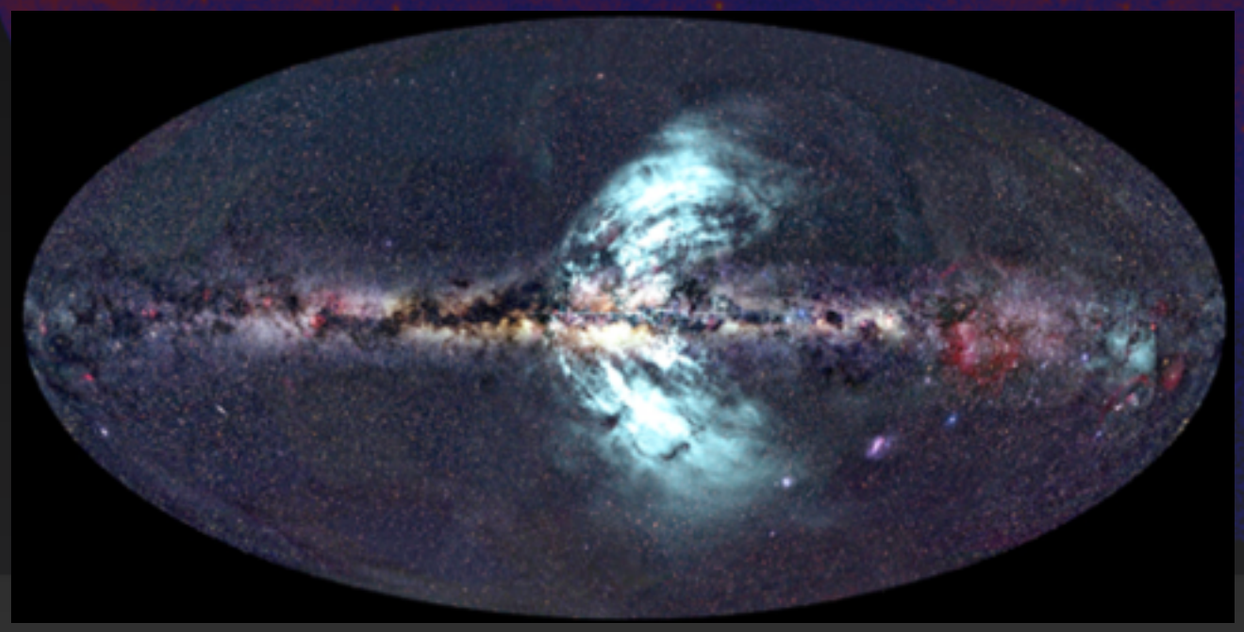

WMAP/PLANCK Haze

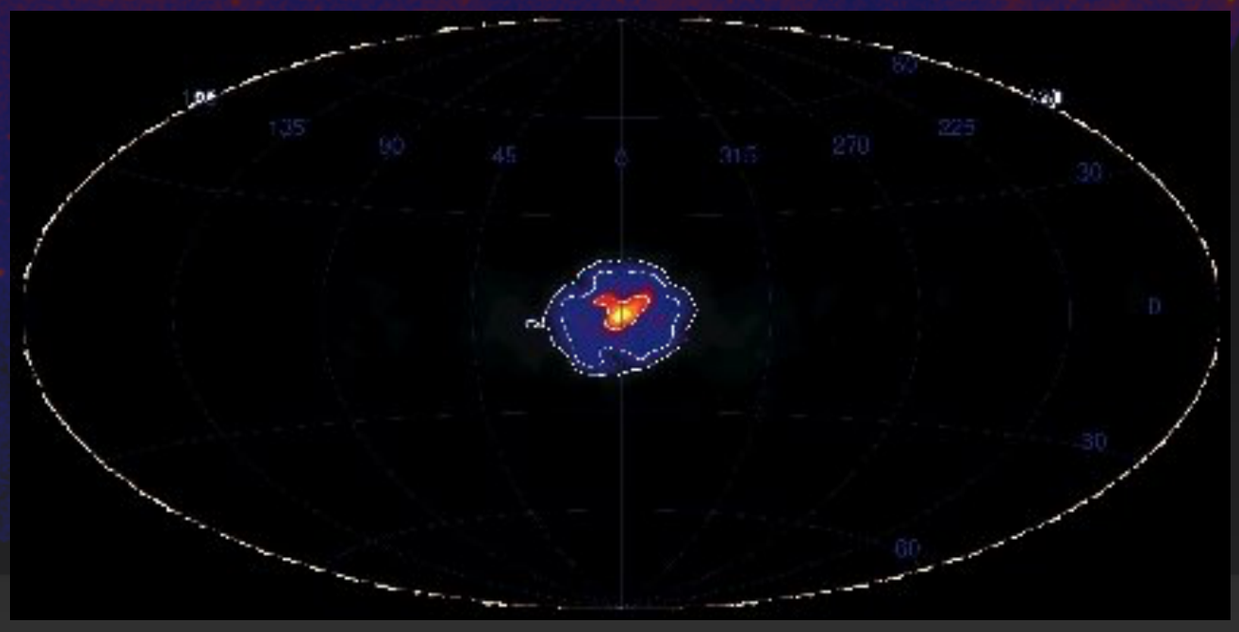

Integral 511 keV Excess

Non-Thermal Emission (Observables)

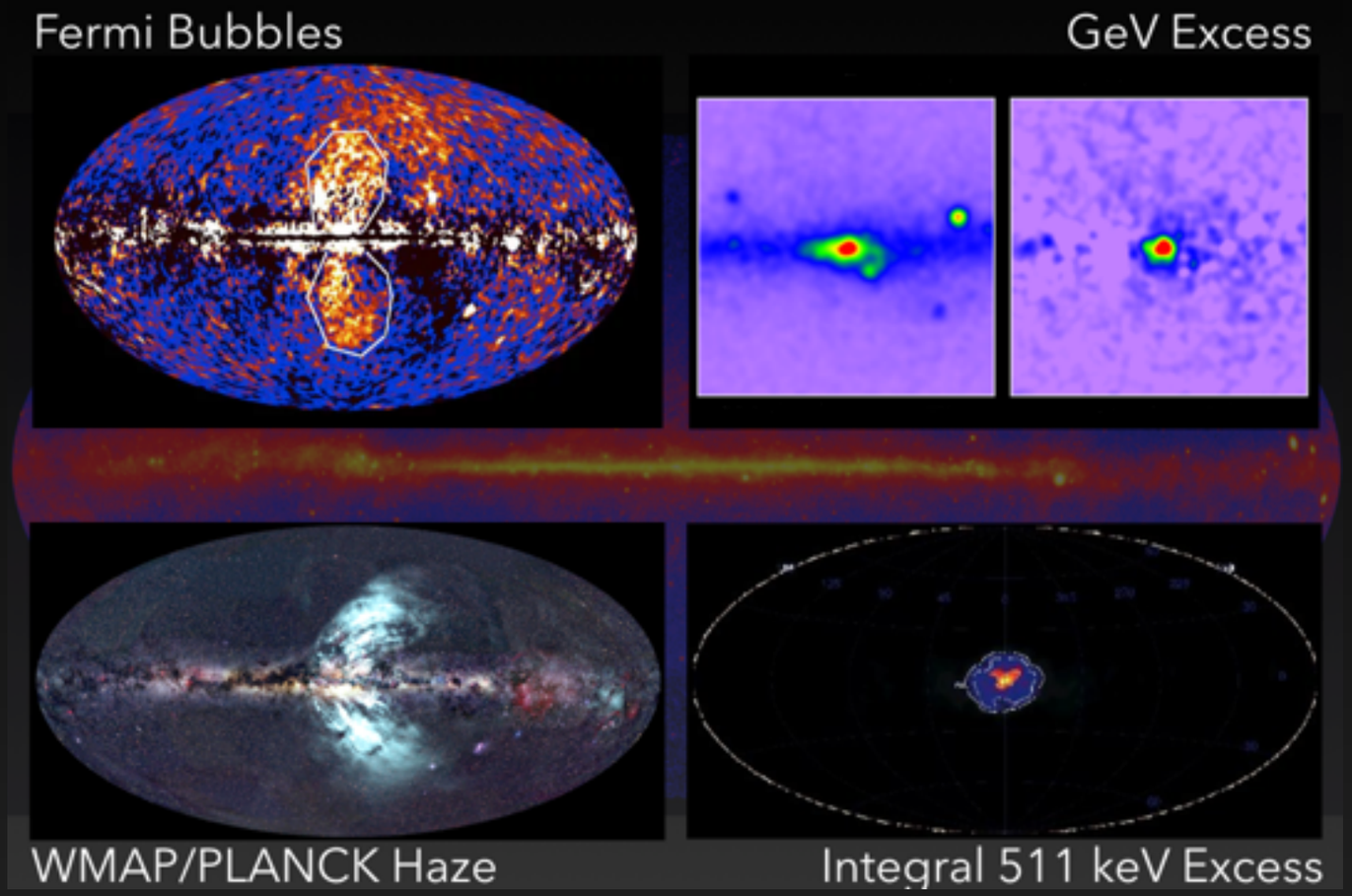

The photon excesses extend very far from the central molecular region!

This:

(a) Indicates the relative power of Galactic center accelerators, compared to the Galactic plane.

(b) Provides a large field of view for studies of GC emission.

(c) Implies that propagation is important!

Cosmic-Ray Propagation

Start with a source of relativistic cosmic-rays

Cosmic-Ray Propagation

Start with a source of relativistic cosmic-rays

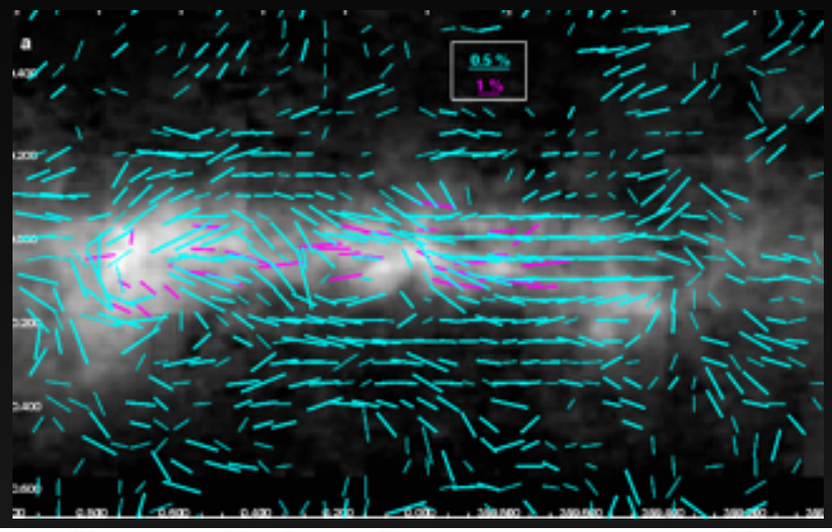

cosmic rays propagate

$$\frac{\partial \psi}{\partial t} = q(\vec{r},p) + \vec{\nabla}\cdot(D_{xx}\vec{\nabla}\psi - \vec{V}\psi) + \frac{\partial}{\partial p}p^2 D_{pp}\frac{\partial}{\partial p}\frac{1}{p^2}\psi - \frac{\partial}{\partial p}\left[\dot{p}\psi - \frac{p}{3}(\vec{\nabla}\cdot\vec{V})\psi\right] - \frac{1}{\tau_f}\psi - \frac{1}{\tau_r}\psi$$

Solved Numerically:
e.g. Galprop

Cosmic-Ray Propagation

Start with a source of relativistic cosmic-rays

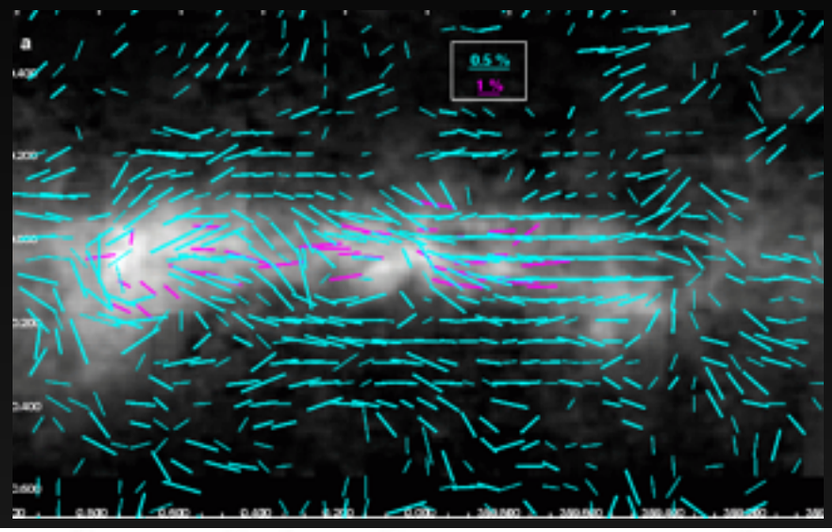

cosmic rays propagate

$$\frac{\partial \psi}{\partial t} = q(\vec{r},p) + \vec{\nabla}\cdot(D_{xx}\vec{\nabla}\psi - \vec{V}\psi) + \frac{\partial}{\partial p}p^2 D_{pp}\frac{\partial}{\partial p}\frac{1}{p^2}\psi - \frac{\partial}{\partial p}\left[\dot{p}\psi - \frac{p}{3}(\vec{\nabla}\cdot\vec{V})\psi\right] - \frac{1}{\tau_f}\psi - \frac{1}{\tau_r}\psi$$

Solved Numerically:
e.g. Galprop

Gas/ISRF

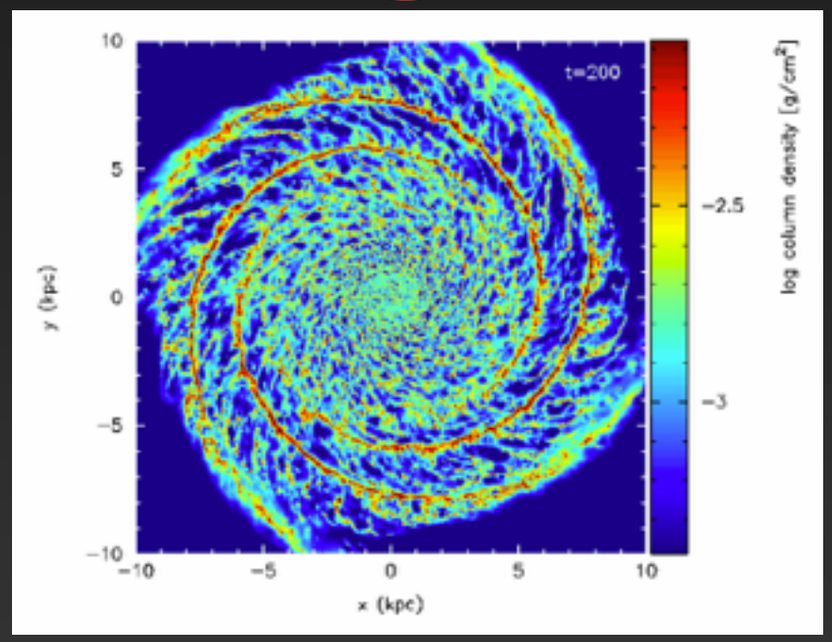

Cosmic-Ray Propagation

Start with a source of relativistic cosmic-rays

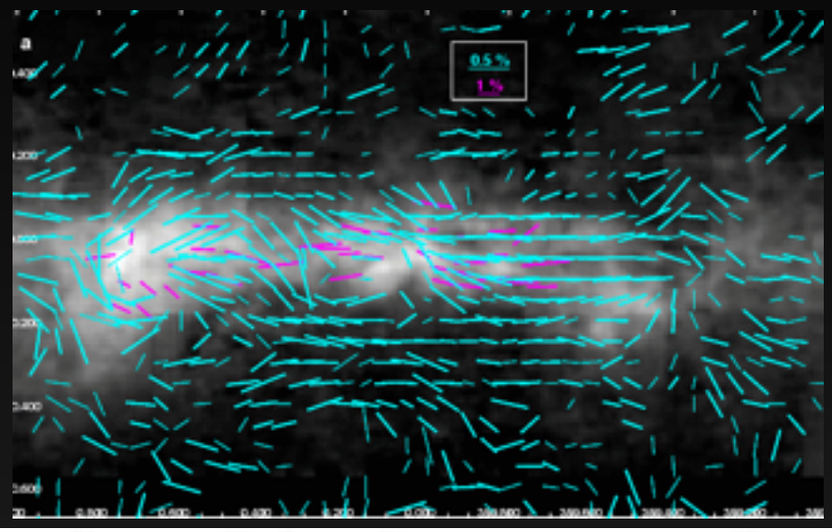

cosmic rays propagate

$$\frac{\partial \psi}{\partial t} = q(\vec{r},p) + \vec{\nabla}\cdot(D_{xx}\vec{\nabla}\psi - \vec{V}\psi) + \frac{\partial}{\partial p}p^2 D_{pp}\frac{\partial}{\partial p}\frac{1}{p^2}\psi - \frac{\partial}{\partial p}\left[\dot{p}\psi - \frac{p}{3}(\vec{\nabla}\cdot\vec{V})\psi\right] - \frac{1}{\tau_f}\psi - \frac{1}{\tau_r}\psi$$

Solved Numerically:
e.g. Galprop

Gas/ISRF

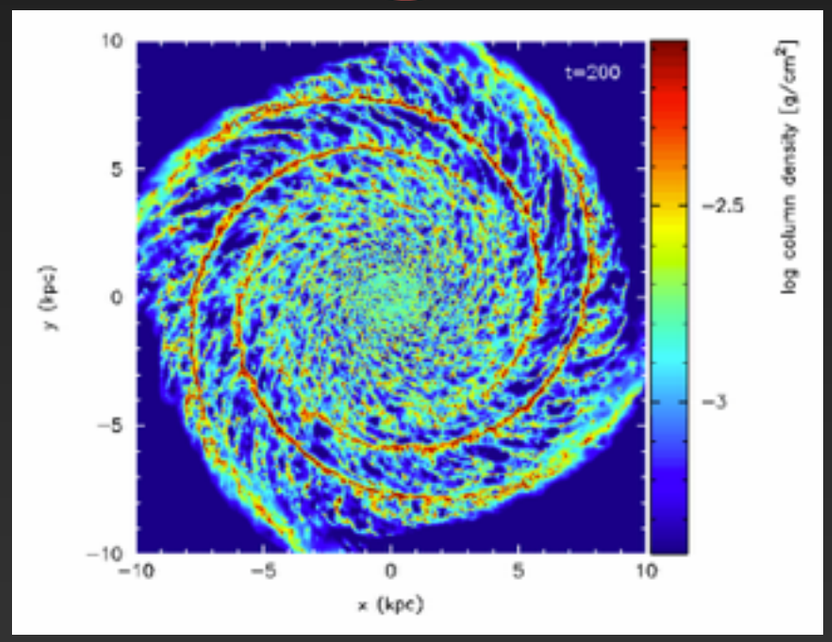

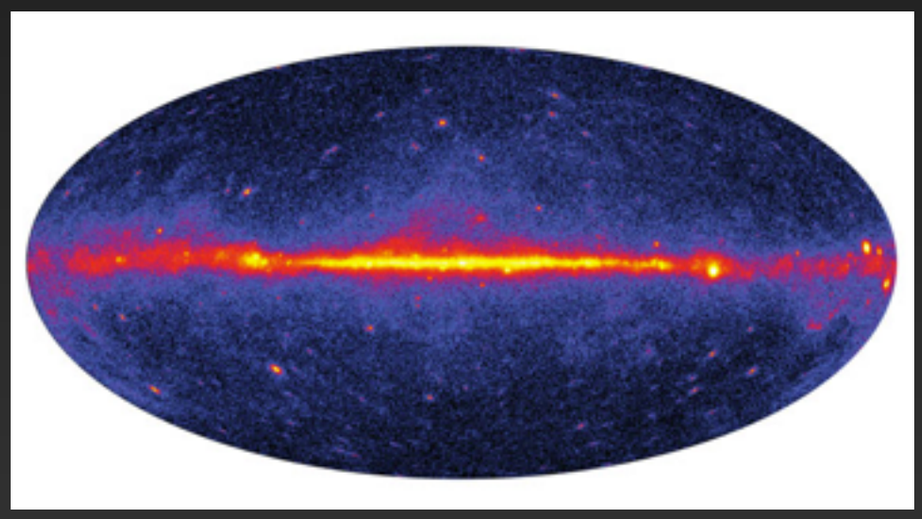

A Fermi-LAT Based Example

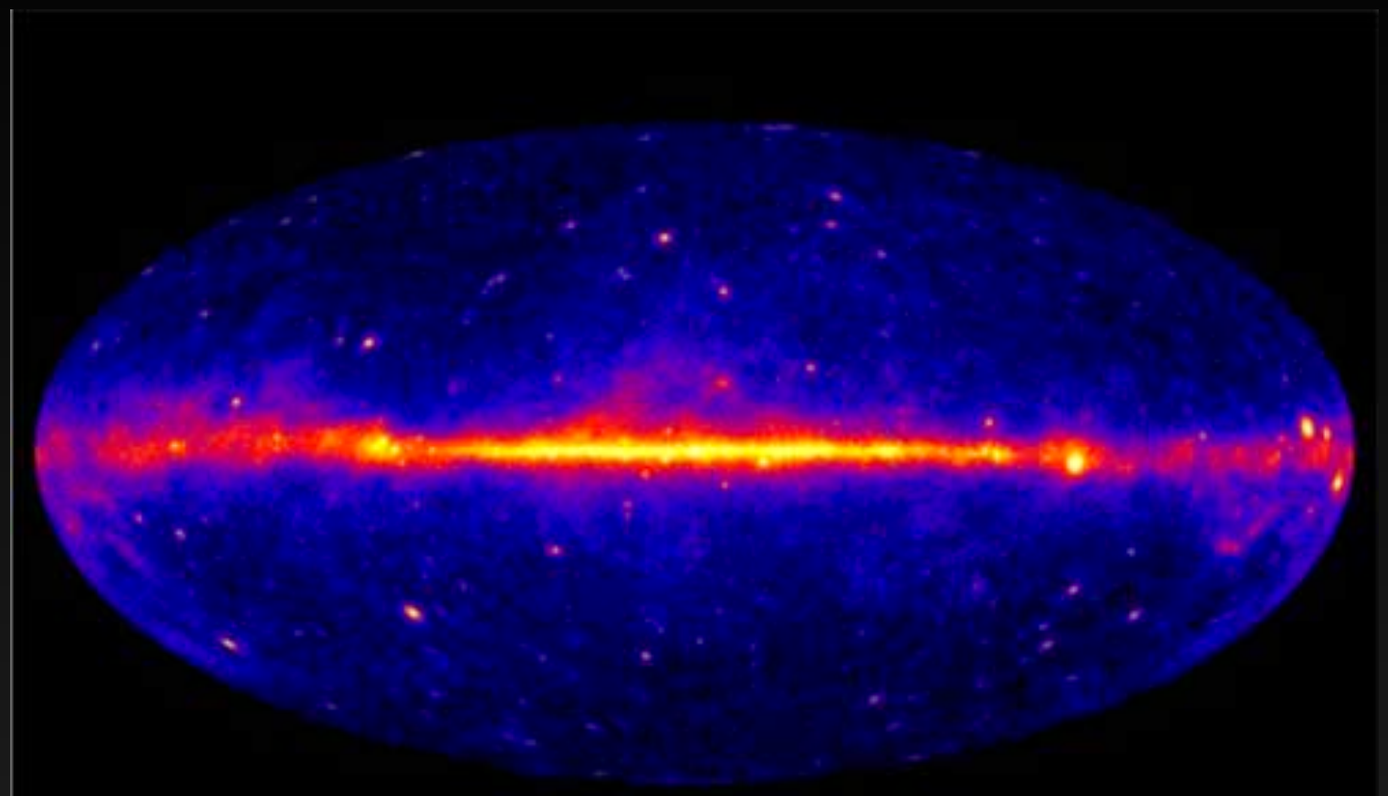

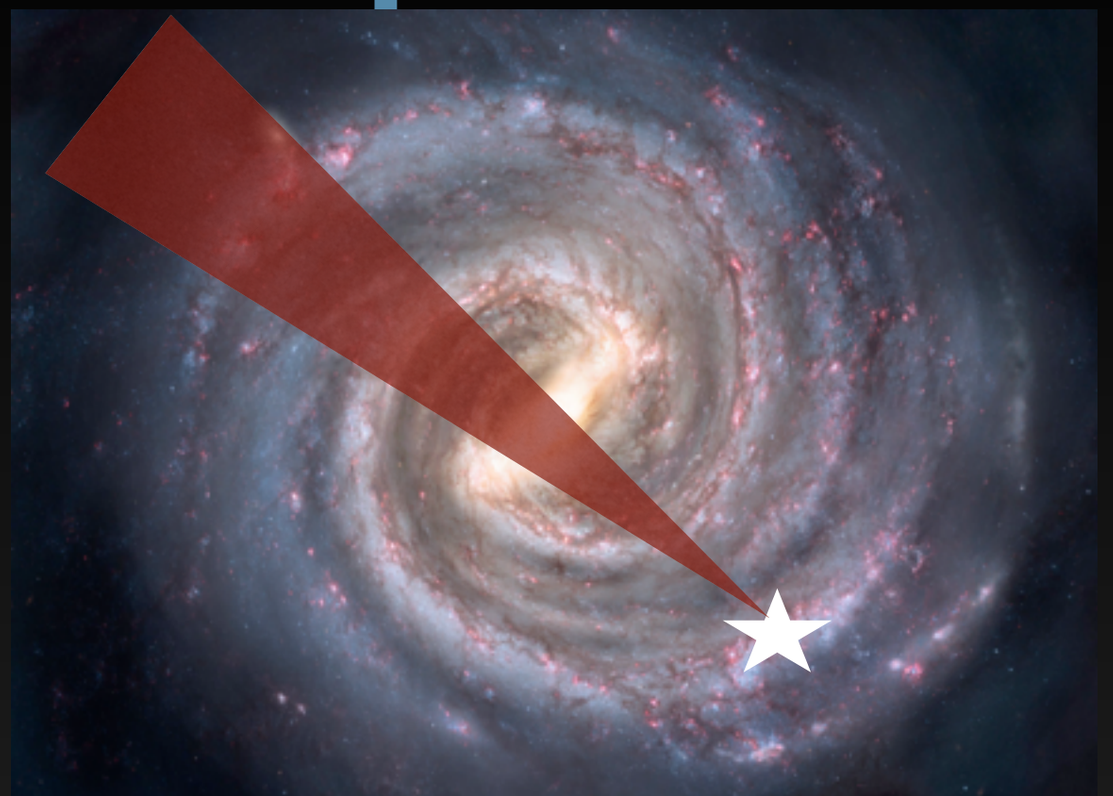

Total Gamma-Ray Flux (>1 GeV) in inner 1° is **1.1×10^{-9} erg cm^2 s^{-1}**

Approximately half of this emission is produced along the line of sight towards the GC, and thus we approximate the total gamma-ray luminosity of the central one degree to be **5×10^{36} erg s^{-1}**

What models can power this emission?

A Fermi-LAT Based Example

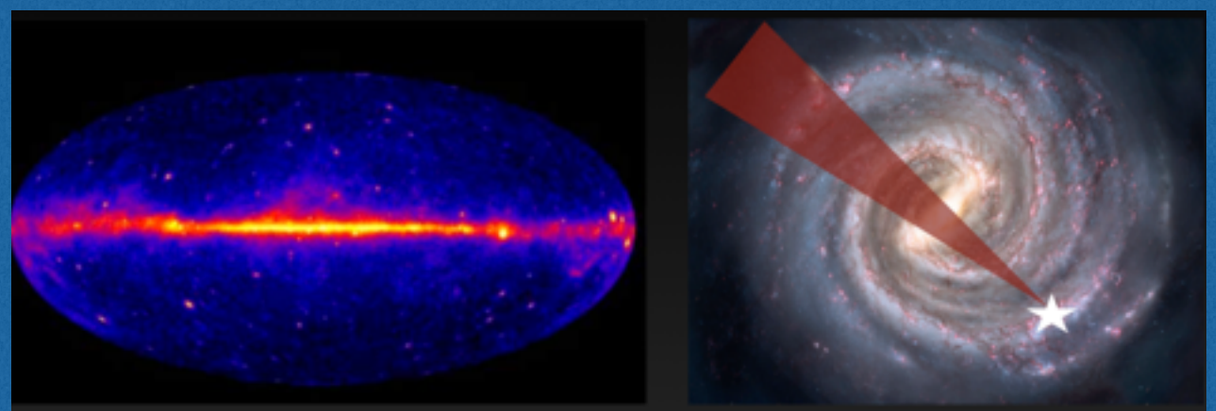

Total Gamma-Ray Flux (>1 GeV) in inner 1° is 1.1×10^{-9} erg cm^2 s^{-1}

Approximately half of this emission is produced along the line of sight towards the GC, and thus we approximate the total gamma-ray luminosity of the central one degree to be 5×10^{36} erg s^{-1}

Supernovae:

A Supernovae produces ~10^{51} erg of energy.

~10% to CR protons.

Assuming 1 Galactic center SN every 250 years (10% the Galactic Rate), this provides an energy flux of 1.3×10^{40} erg s^{-1}.

If these cosmic-rays are trapped for 10 kyr in a 100 pc box ($D_0 = 5 \times 10^{28}$ cm^2 s-1), filled with Hydrogen gas at density 100 cm^{-2}, this will produce a total gamma-ray emission:

A Fermi-LAT Based Example

Total Gamma-Ray Flux (>1 GeV) in inner 1° is 1.1×10^{-9} erg cm^2 s^{-1}

Approximately half of this emission is produced along the line of sight towards the GC, and thus we approximate the total gamma-ray luminosity of the central one degree to be 5×10^{36} erg s^{-1}

Supernovae:

A Supernovae produces ~10^{51} erg of energy.

~10% to CR protons.

Assuming 1 Galactic center SN every 250 years (10% the Galactic Rate), this provides an energy flux of 1.3×10^{40} erg s^{-1}.

If these cosmic-rays are trapped for 10 kyr in a 100 pc box ($D_0 = 5 \times 10^{28}$ cm^2 s-1), filled with Hydrogen gas at density 100 cm^{-2}, this will produce a total gamma-ray emission:

6.7×10^{37} erg s^{-1} ✔

A Fermi-LAT Based Example

Total Gamma-Ray Flux (>1 GeV) in inner 1° is 1.1×10^{-9} erg cm^2 s^{-1}

Approximately half of this emission is produced along the line of sight towards the GC, and thus we approximate the total gamma-ray luminosity of the central one degree to be 5×10^{36} erg s^{-1}

Sgr A*:

A tidal disruption event releases ~10^{45} erg s^{-1} for a period of ~0.2 yr.

Sgr A* is expected to produce a tidal disruption event every ~10^5 yr, producing a time-averaged energy output of 2×10^{39} erg s^{-1}.

If these CRs are primarily leptonic, and the electrons remain trapped in a region with a 40 eV cm^{-3} ISRF and a 200 μG magnetic field the gamma-ray flux from inverse Compton scattering is:

A Fermi-LAT Based Example

Total Gamma-Ray Flux (>1 GeV) in inner 1° is 1.1×10^{-9} erg cm^2 s^{-1}

Approximately half of this emission is produced along the line of sight towards the GC, and thus we approximate the total gamma-ray luminosity of the central one degree to be 5×10^{36} erg s^{-1}

Sgr A*:

A tidal disruption event releases ~10^{45} erg s^{-1} for a period of ~0.2 yr.

Sgr A* is expected to produce a tidal disruption event every ~10^5 yr, producing a time-averaged energy output of 2×10^{39} erg s^{-1}.

If these CRs are primarily leptonic, and the electrons remain trapped in a region with a 40 eV cm^{-3} ISRF and a 200 μG magnetic field the gamma-ray flux from inverse Compton scattering is:

7.0×10^{37} erg s^{-1} ✔

A Fermi-LAT Based Example

Total Gamma-Ray Flux (>1 GeV) in inner 1° is 1.1×10^{-9} erg cm^2 s^{-1}

Approximately half of this emission is produced along the line of sight towards the GC, and thus we approximate the total gamma-ray luminosity of the central one degree to be 5×10^{36} erg s^{-1}

Pulsars

MSPs observed in the galactic field are fit by a population with a mean gamma-ray flux of 3×10^{34} erg s^{-1}. (Hooper & Mohlabeng 2015)

Given the population of 129 MSPs among 124 globular clusters (with a total stellar mass ~5×10^7 $M_\odot$). For the 1×10^9 $M_\odot$ of stars formed in the inner degree of the Milky Way, we get:

A Fermi-LAT Based Example

Total Gamma-Ray Flux (>1 GeV) in inner 1° is 1.1×10^{-9} erg cm^2 s^{-1}

Approximately half of this emission is produced along the line of sight towards the GC, and thus we approximate the total gamma-ray luminosity of the central one degree to be 5×10^{36} erg s^{-1}

Pulsars

MSPs observed in the galactic field are fit by a population with a mean gamma-ray flux of 3×10^{34} erg s^{-1}. (Hooper & Mohlabeng 2015)

Given the population of 129 MSPs among 124 globular clusters (with a total stellar mass ~5×10^7 $M_\odot$). For the 1×10^9 $M_\odot$ of stars formed in the inner degree of the Milky Way, we get:

7.7×10^{37} erg s^{-1} ✔

A Fermi-LAT Based Example

Total Gamma-Ray Flux (>1 GeV) in inner 1° is 1.1×10^{-9} erg cm^2 s^{-1}

Approximately half of this emission is produced along the line of sight towards the GC, and thus we approximate the total gamma-ray luminosity of the central one degree to be 5×10^{36} erg s^{-1}

Dark Matter

For a 35 GeV dark matter particle annihilating at the thermal cross-section to bb, and a slightly adiabatically contracted $r^{-1.35}$ density profile.

The dark matter annihilation rate is 8.6×10^{38} ann s^{-1}, which produces a gamma-ray flux of:

A Fermi-LAT Based Example

Total Gamma-Ray Flux (>1 GeV) in inner 1° is 1.1×10^{-9} erg cm^2 s^{-1}

Approximately half of this emission is produced along the line of sight towards the GC, and thus we approximate the total gamma-ray luminosity of the central one degree to be 5×10^{36} erg s^{-1}

Dark Matter

For a 35 GeV dark matter particle annihilating at the thermal cross-section to bb, and a slightly adiabatically contracted $r^{-1.35}$ density profile.

The dark matter annihilation rate is 8.6×10^{38} ann s^{-1}, which produces a gamma-ray flux of:

6.9×10^{36} erg s^{-1} ✔

Conclusion:
Every Model is Correct

Conclusion:
Every Model is Correct

Is this (theorist) heaven?
or is this hell?

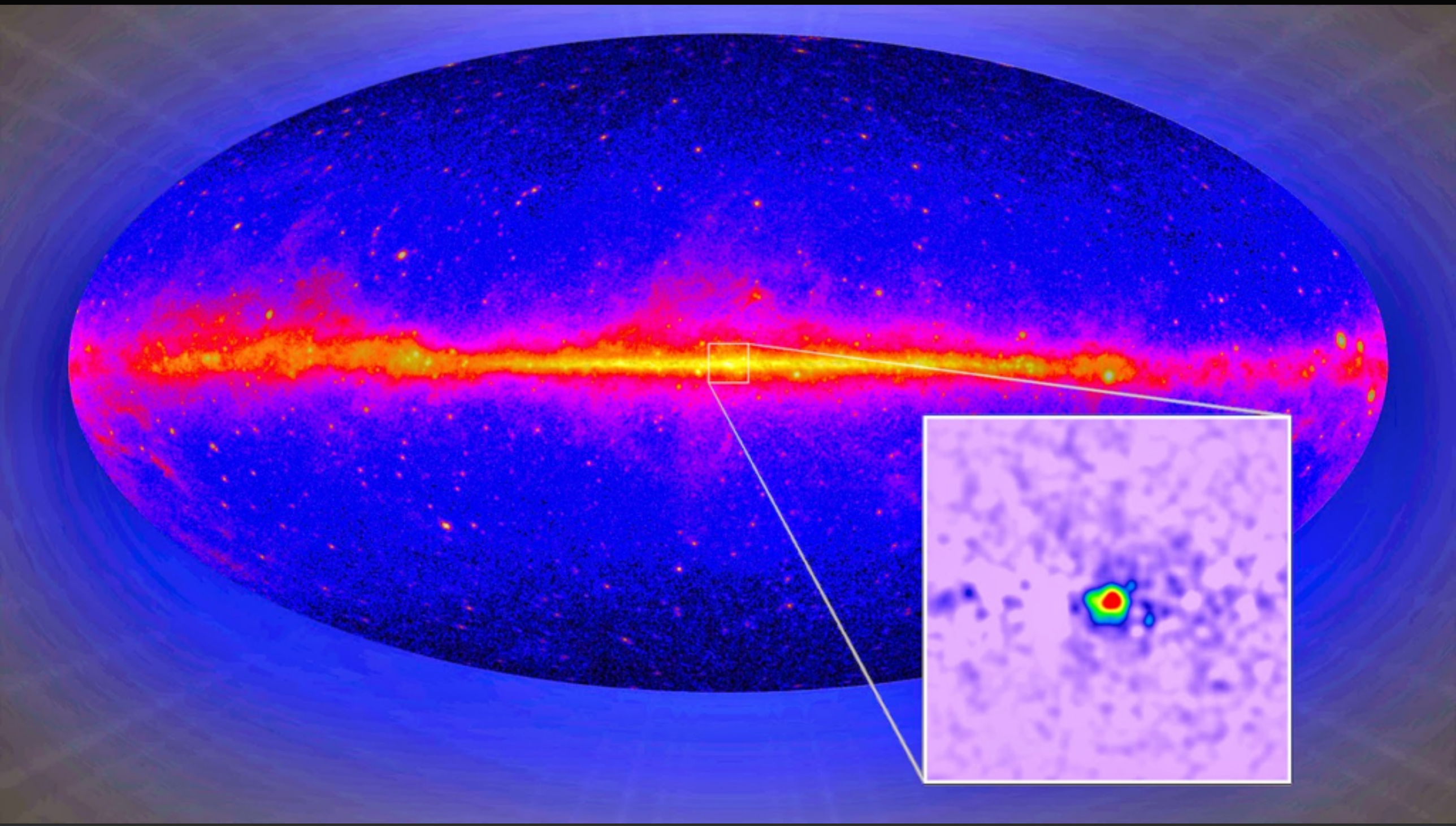

Modeling the Galactic Center

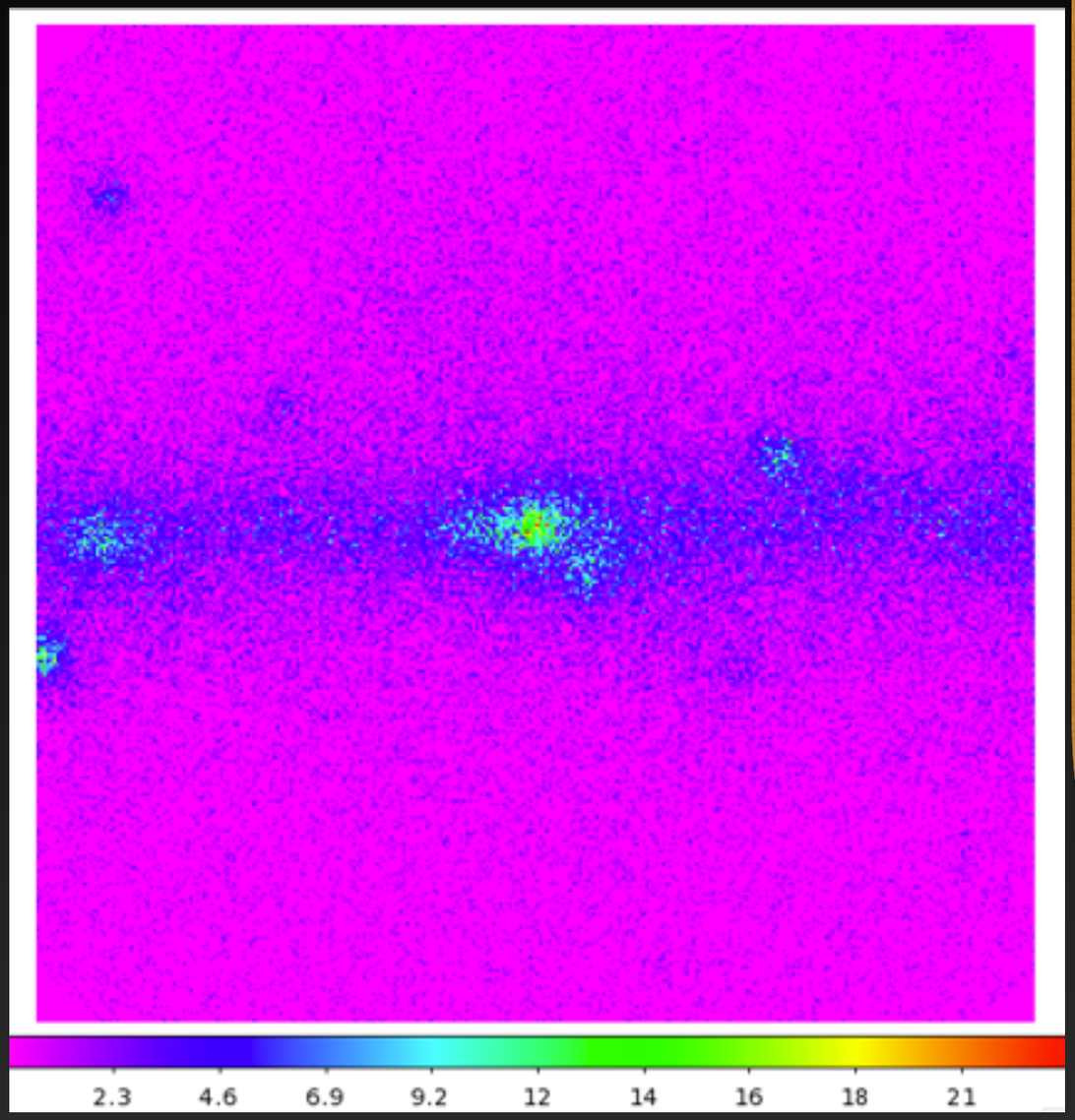

Data

750 — 950 MeV

Best Angular Resolution Cut

10^{o} x 10^{o} ROI

=

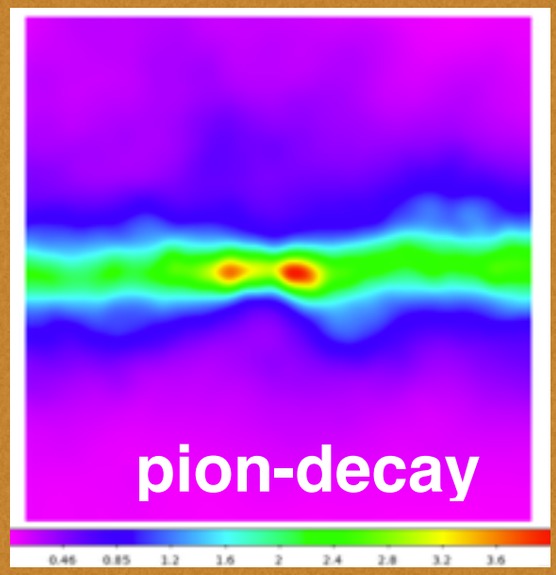

+

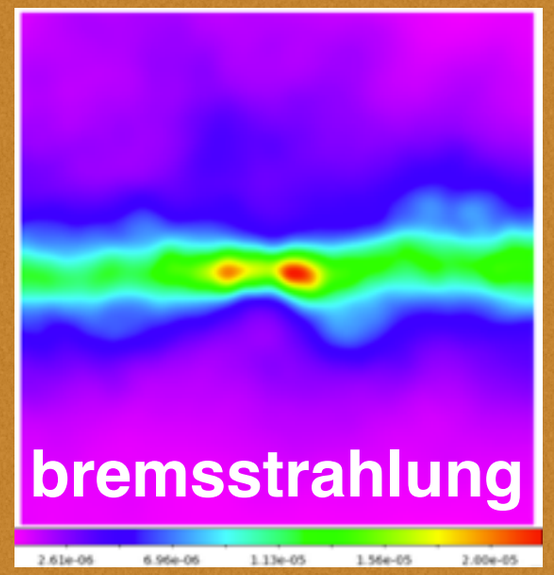

+

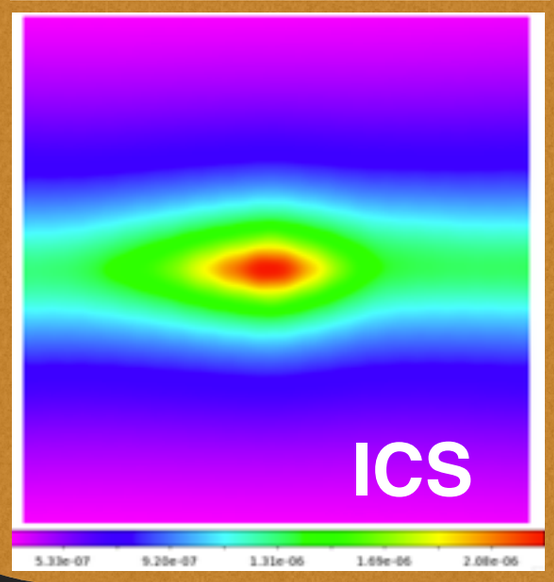

+

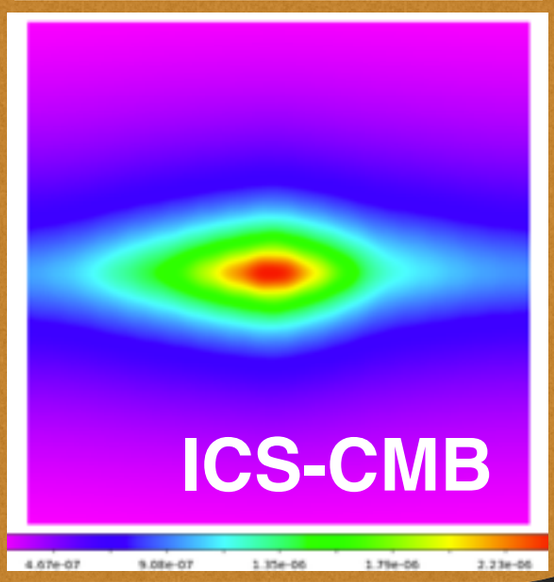

+

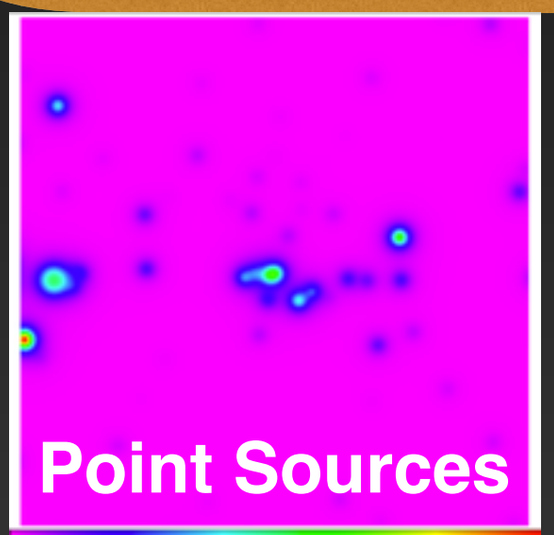

+

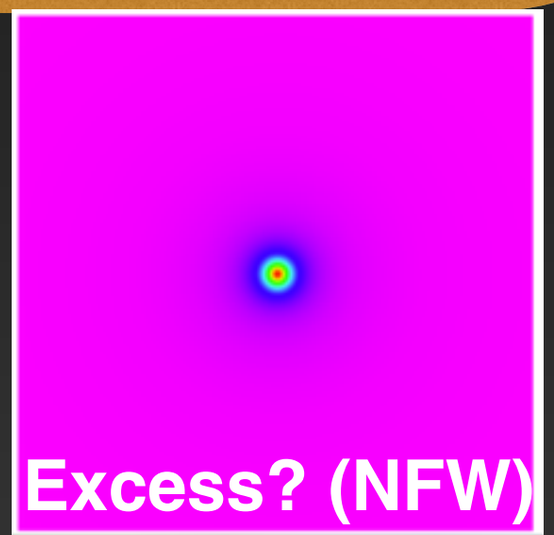

Two Analyses of the Gamma-Ray Excess

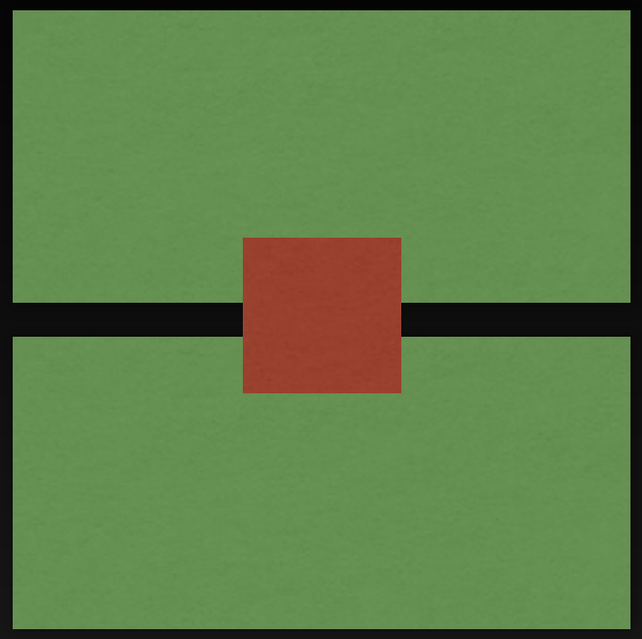

INNER GALAXY

- Mask galactic plane (e.g. $|b| > 1^o$), and consider 40^o x 40^o box
- Bright point sources masked at 2^o
- Use likelihood analysis, allowing the diffuse templates to float in each energy bin
- Background systematics controlled

GALACTIC CENTER

- Box around the GC (10^o x 10^o)
- Include and model all point sources
- Use likelihood analysis to calculate the spectrum and intensity of each source
- Bright Signal

The Galactic Center Excess

IG

Utilizing different models for removing astrophysical and point source foregrounds. Multiple studies have consistently observed a gamma-ray excess.

Goodenough & Hooper (2009, 0910.2998)
Hooper & Goodenough (2010, 1010.2752)
Hooper & Linden (2011, 1110.0006)
Abazajian & Kaplinghat (2012, 1207.6047)
Gordon & Macias (2013, 1306.5725)
Gordon & Macias (2013, 1312.6671)
Abazajian et al. (2014, 1402.4090)
Daylan et al. (2014, 1402.6703)
Calore et al. (2014, 1409.0042)
Abazajian et al. (2014, 1410.6168)
Bartels et al. (2015, 1506.05104)
Lee et al. (2015, 1506.05124)
Gaggero et al. (2015, 1507.06129)
Carlson et al. (2015, 1510.04698)
The Fermi-LAT Collaboration (2015, 1511.02938)
Yang & Aharonian (2016, 1602.06764)
Carlson et al. (2016, 1603.06584)
Linden et al. (2016, 1604.01026)
Horiuichi et al. (2016, 1604.01402)

Daylan et al. (2014)

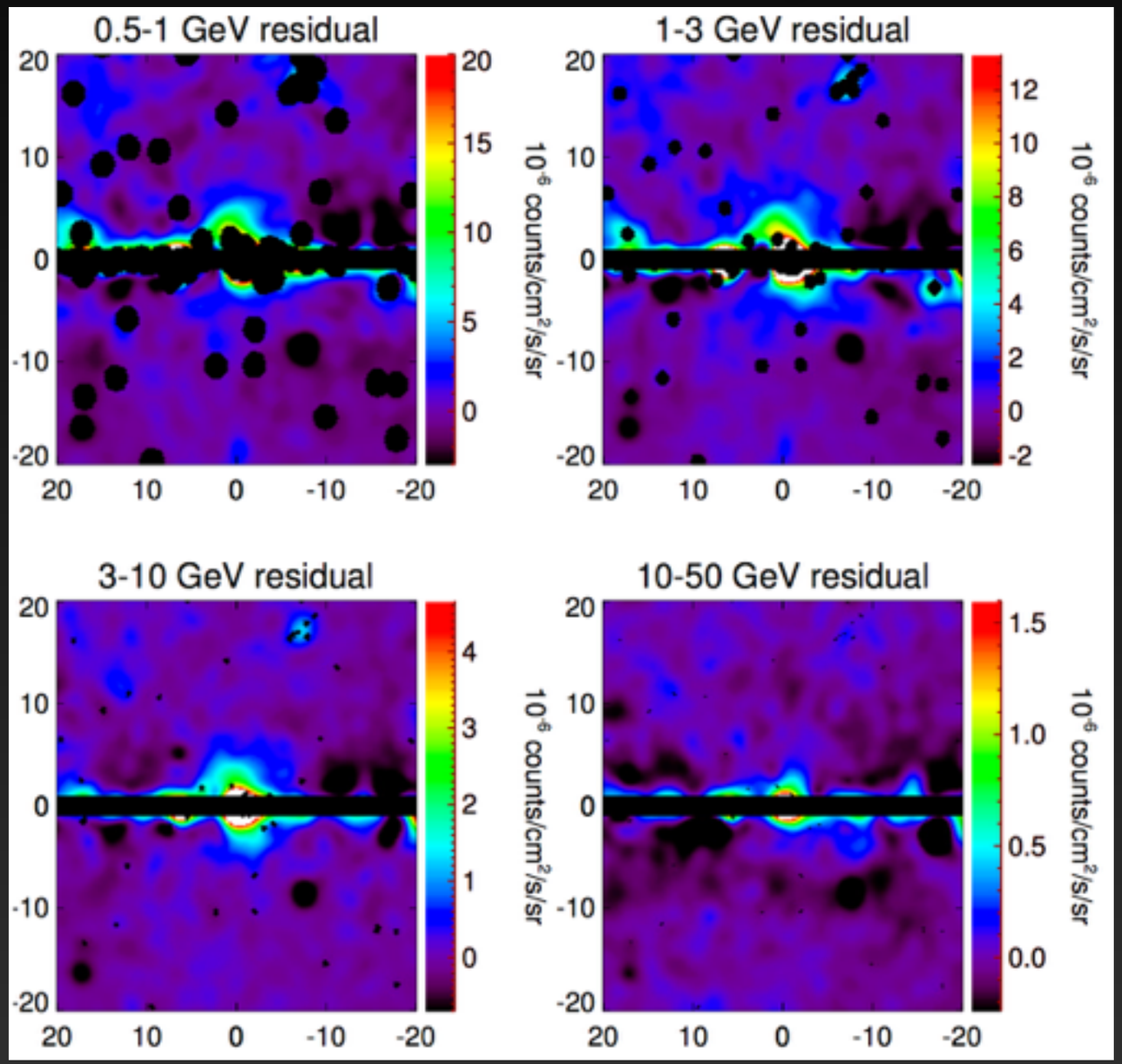

Observational Results

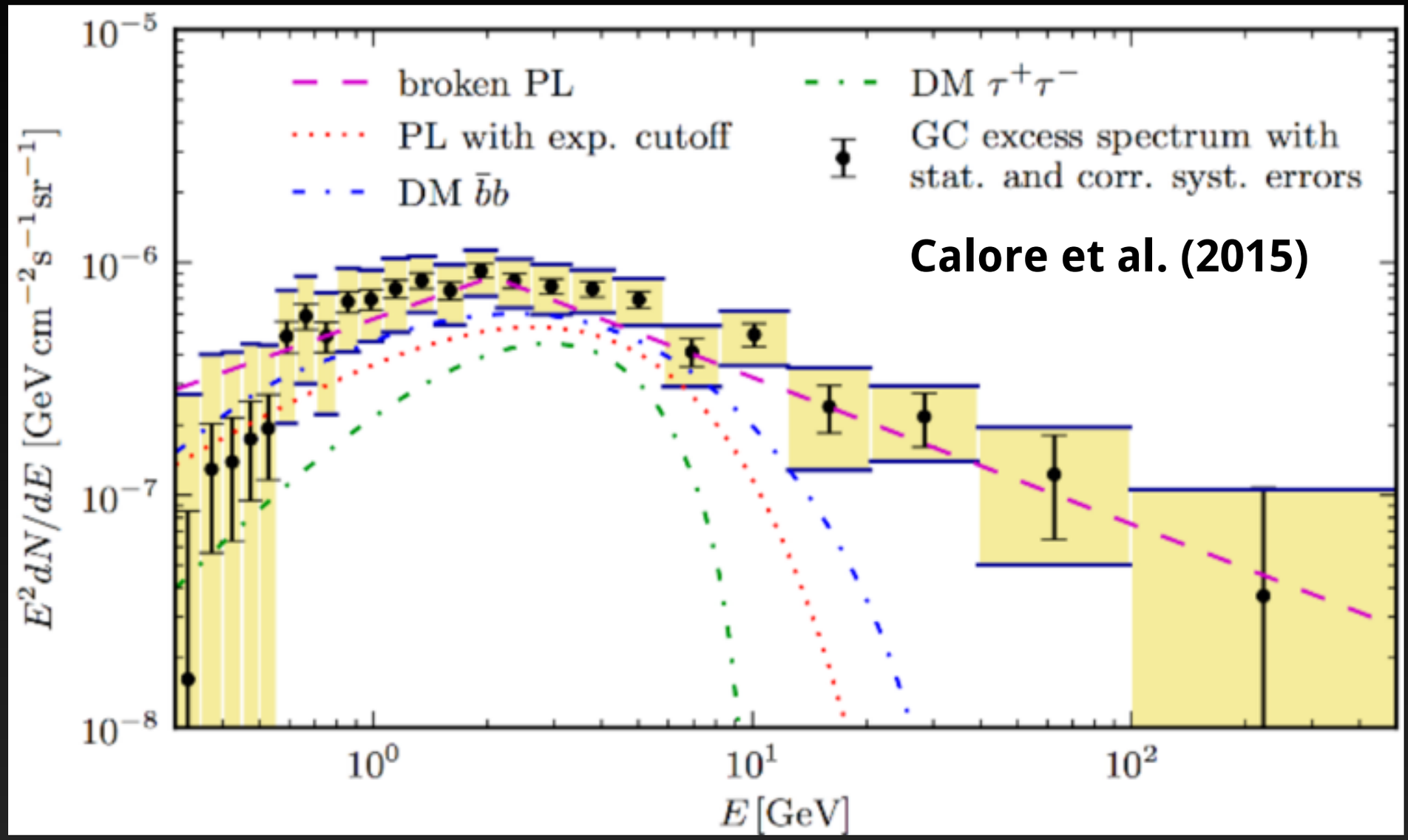

The excess has an unusual spectrum - highly peaked at an energy of ~2 GeV.

This spectrum is significantly harder than expected from astrophysical diffuse emission.

Observational Results

GC/IG

Daylan et al. (2014)

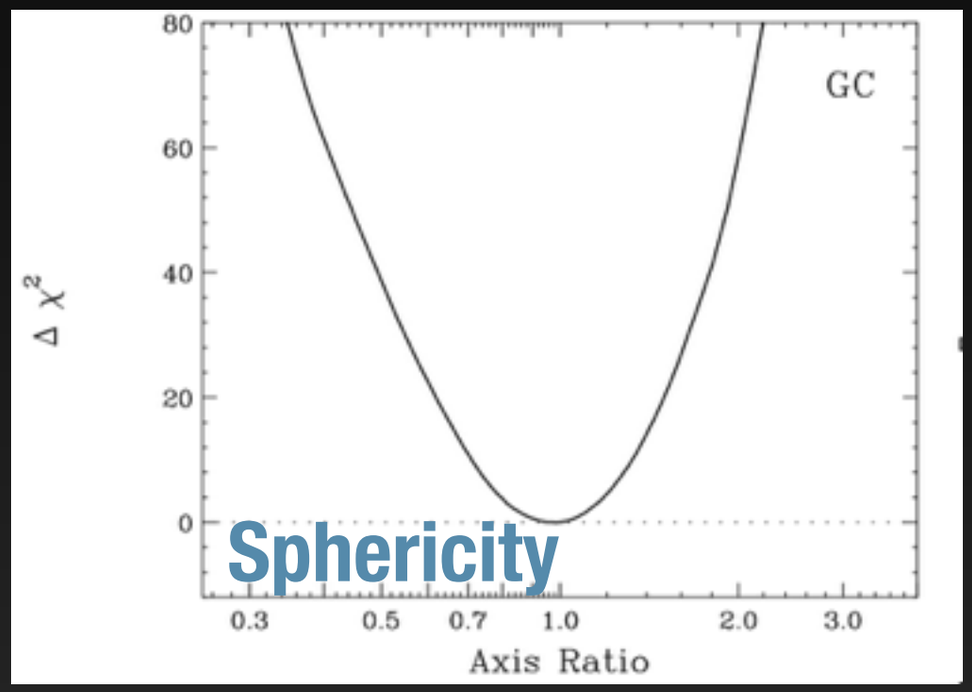

Calore et al. (2014b)

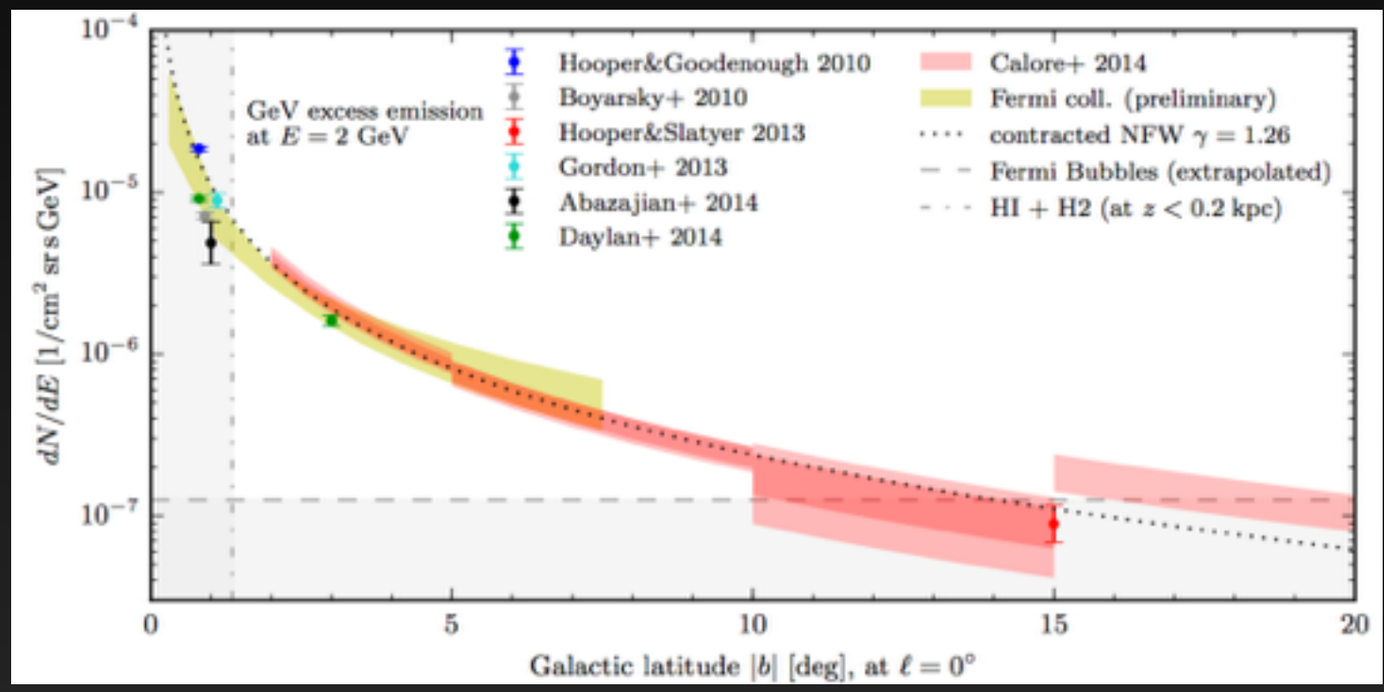

The GeV excess spherically symmetric, and is statistically significant from 0.1° – 10° from the Galactic Center.

Observational Results

<u>These are the three resilient features of the GeV Excess:</u>

1.) Hard Gamma-Ray Spectrum peaking at ~2 GeV
2.) Spherically Symmetric Emission Morphology
3.) Extension to >10° from the GC.

<u>How could we model this with:</u>

1.) Dark Matter annihilation
2.) Millisecond Pulsars
3.) Leptonic Outbursts from Sgr A*
4.) Changes in Diffuse Emission Modeling

Dark Matter Model Fitting?

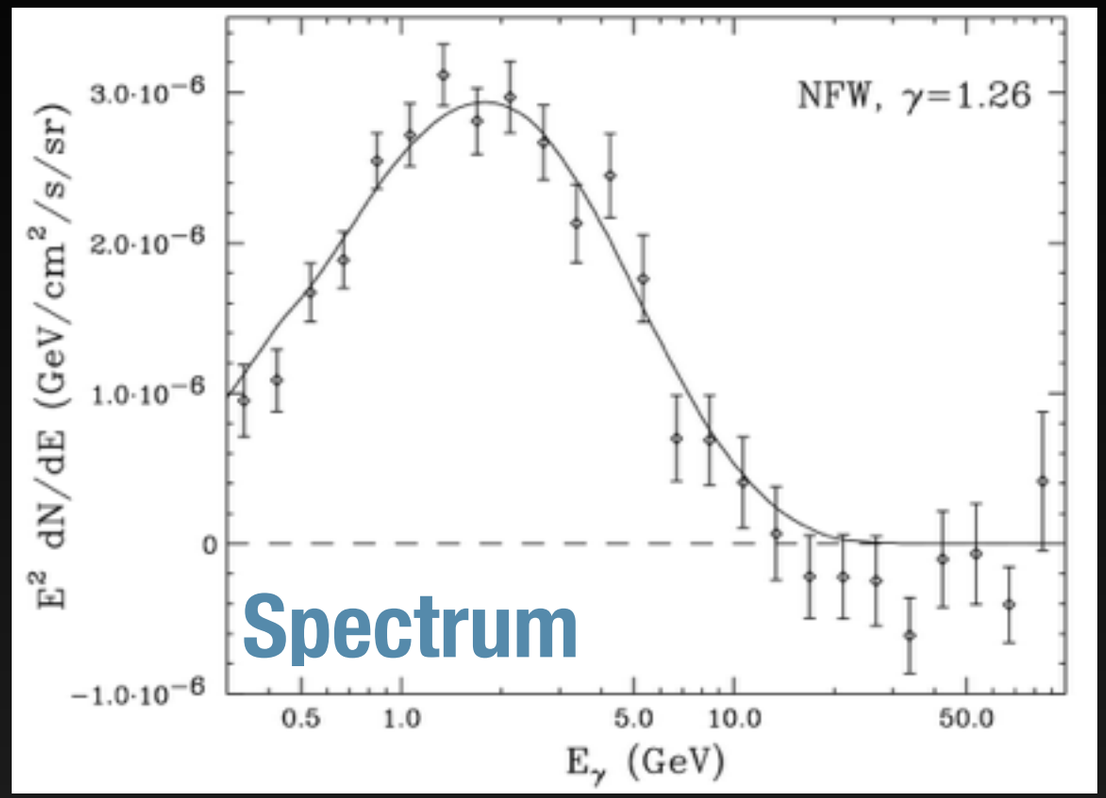

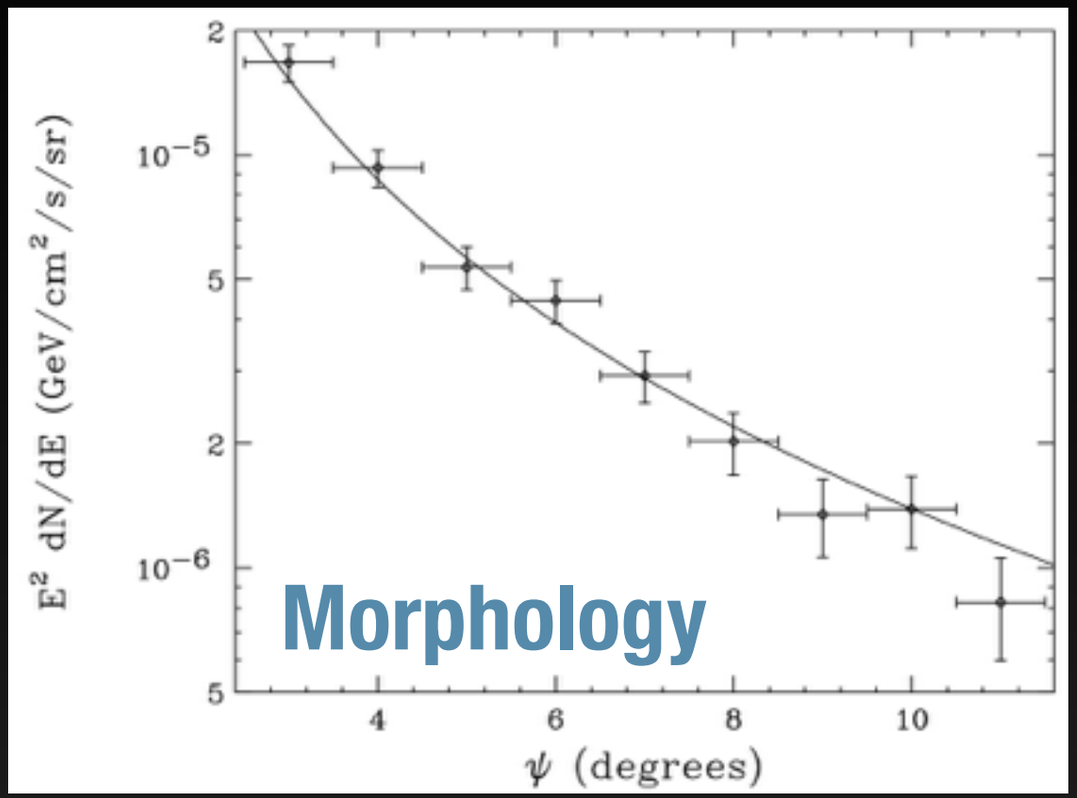

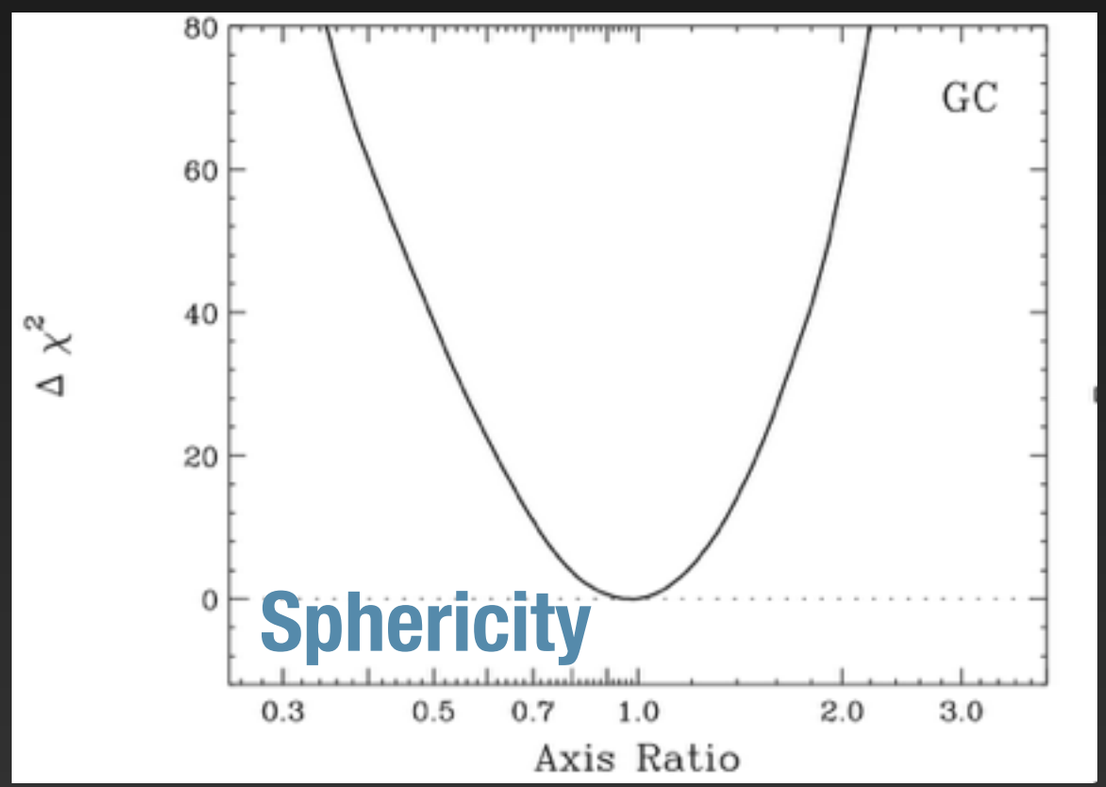

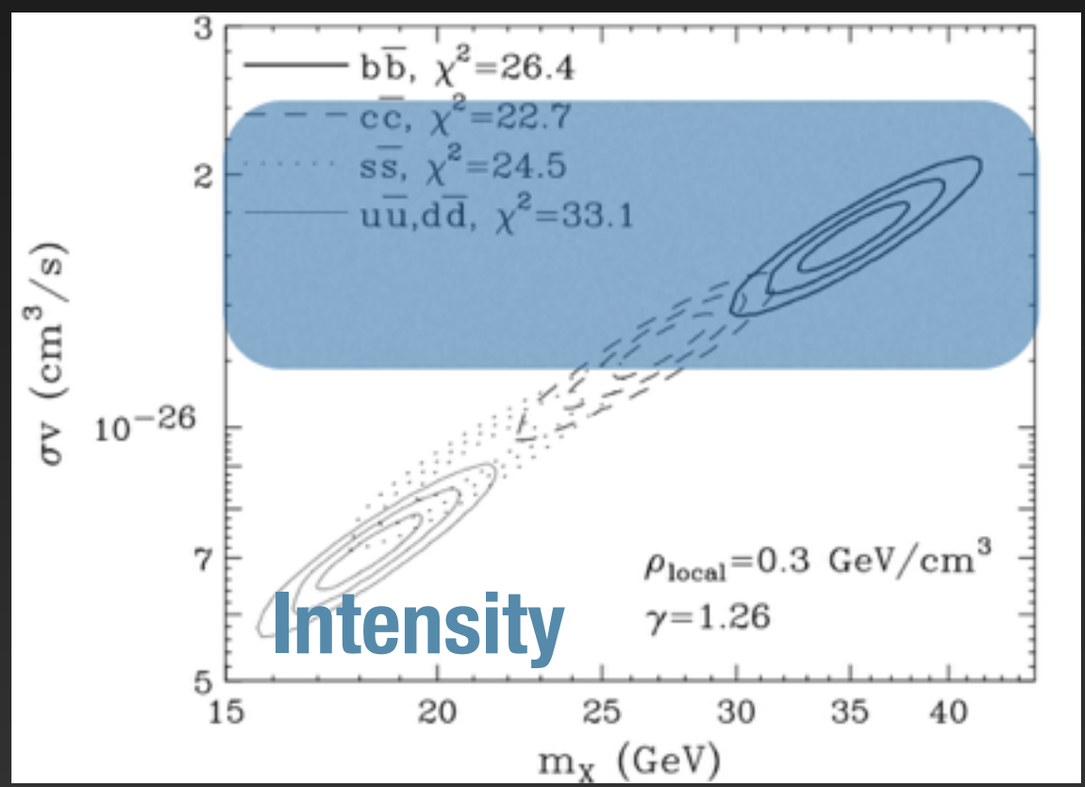

Particle Physics Models Exist...

Chan (1607.02246)
Jia (1607.00737)
Barrau et al. (1606.08031)
Huang et al. (1605.09018)
Cui et al. (1605.08138)
Krauss et al. (1605.05327)
Kumar et al. (1605.00611)
Biswas et al. (1604.06566)
Sage et al. (1604.04589)
Choquette et al. (1604.01039)
Cuoco et al. (1603.08228)
Chao et al. (1602.05192)
Horiuchi et al. (1602.04788)
Hektor et al. (1602.00004)
Freytsis et al. (1601.07556)
Kim et al. (1601.05089)
Huang et al. (1512.08992)
Kulkami et al. (1512.06836)
Tang et al. (1512.02899)
Cox et al. (1512.00471)
Cai et al. (1511.09247)
Agrawal et al. (1511.06293)
Duerr et al. (1510.07562)
Drozd et al. (1510.07053)
Arcadi et al. (1510.02297)
Williams (1510.00714)
Cai & Spray (1509.08481)
Freese et al. (1509.05076)
Bhattacharya et al. (1509.03665)
Algeri et al. (1509.01010)
Fox & Tucker-Smith (1509.00499)
Dutta et al. (1509.05989)
Liu et al. (1508.05716)
Berlin et al. (1508.05390)
Fan et al. (1507.06993)
Hektor et al. (1507.05096)
Achterbeg et al. (1507.04644)
Biswas et al. (1507.04543)

Butter et al. (1507.02288)
Mondal et al. (1507.01793)
Cao et al. (1506.06471)
Banik et al. (1506.05665)
Ipek (1505.07826)
Buchmueller et al. (1505.07826)
Balazs et al. (1505.06758)
Medina (1505.05565)
Kim et al. (1505.04620)
Ko et al. (1504.06944)
Ko & Tang (1504.03908)
Ghorbani & Ghorbani (1504.03610)
Fortes et al. (1503.08220)
Cline et al. (1503.08213)
Rajaraman et al. (1503.05919)
Bi et al. (1503.03749)
Kopp et al. (1503.02669)
Elor et al. (1503.01773)
Gherghetta et al. (1502.07173)
Berlin et al. (1502.06000)
Achterberg et al. (1502.05703)
Modak et al. (1502.05682)
Guo et al. (1502.00508)
Chen & Nomura (1501.07413)
Kozaczuk & Martin (1501.07275)
Berlin et al. (1501.03496)
Kaplinghat et al. (1501.03507)
Alves et al. (1501.03490)
Biswas et al. (1501.02666)
Biswas et al. (1501.02666)
Ghorbani & Ghorbani (1501.00206)
Cerdeno et al. (1501.01296)
Liu et al. (1412.1485)
Hooper (1411.4079)
Arcadi et al. (1411.2985)
Cheung et al. (1411.2619)
Agrawal et al. (1411.2592)
Kile et al. (1411.1407)

Buckley et al. (1410.6497)
Heikinheimo & Spethmann (1410.4842)
Freytsis et al. (1410.3818)
Yu et al. (1410.3347)
Cao et al. (1410.3239)
Guo et al. (1409.7864)
Yu (1409.3227)
Cahill-Rowley et al. (1409.1573)
Banik & Majumdar (1408.5795)
Bell et al. (1408.5142)
Ghorbani (1408.4929)
Okada & Seto (1408.2583)
Frank & Mondal (1408.2223)
Baek et al. (1407.6588)
Tang (1407.5492)
Balazs & Li (1407.0174)
Huang et al. (1407.0038)
McDermott (1406.6408)
Cheung et al. (1406.6372)
Arina et al. (1406.5542)
Chang & Ng (1406.4601)
Wang & Han (1406.3598)
Cline et al. (1405.7691)
Berlin et al. (1405.5204)
Mondal & Basak (1405.4877)
Martin et al. (1405.0272)
Ghosh et al. (1405.0206)
Abdullah et al. (1404.5503)
Park & Tang (1404.5257)
Cerdeno et al. (1404.2572)
Izaguirre et al. (1404.2018)
Agrawal et al. (1404.1373)
Berlin et al. (1404.0022)
Alves et al. (1403.5027)
Finkbeiner & Weiner (1402.6671)
Boehm et al. (1401.6458)
Kopp et al. (1401.6457)
Modak et al. (1312.7488)

Alves et al. (1312.5281)
Fortes et al. (1312.2837)
Banik et al. (1311.0126)
Arhrib et al. (1310.0358)
Kelso et al. (1308.6630)
Kozaczuk et al. (1308.5705)
Kumar (1308.4513)
Demir et al. (1308.1203)
Buckley et al. (1307.3561)
Cline et al. (1306.4710)
Cannoni et al. (1205.1709)
An et al. (1110.1366)
Buckley et al. (1106.3583)
Boucenna et al. (1106.3368)
Ellis et al. (1106.0768)
Cheung et al. (1104.5329)
Marshall et al. (1102.0492)
Abada et al. (1101.0365)
Tytgat (1012.0576)
Logan (1010.4214)
Barger et al. (1008.1796)
Raklev et al. (0911.1986)

Comparison to Dwarf Constraints

Ackermann et al. (2015)

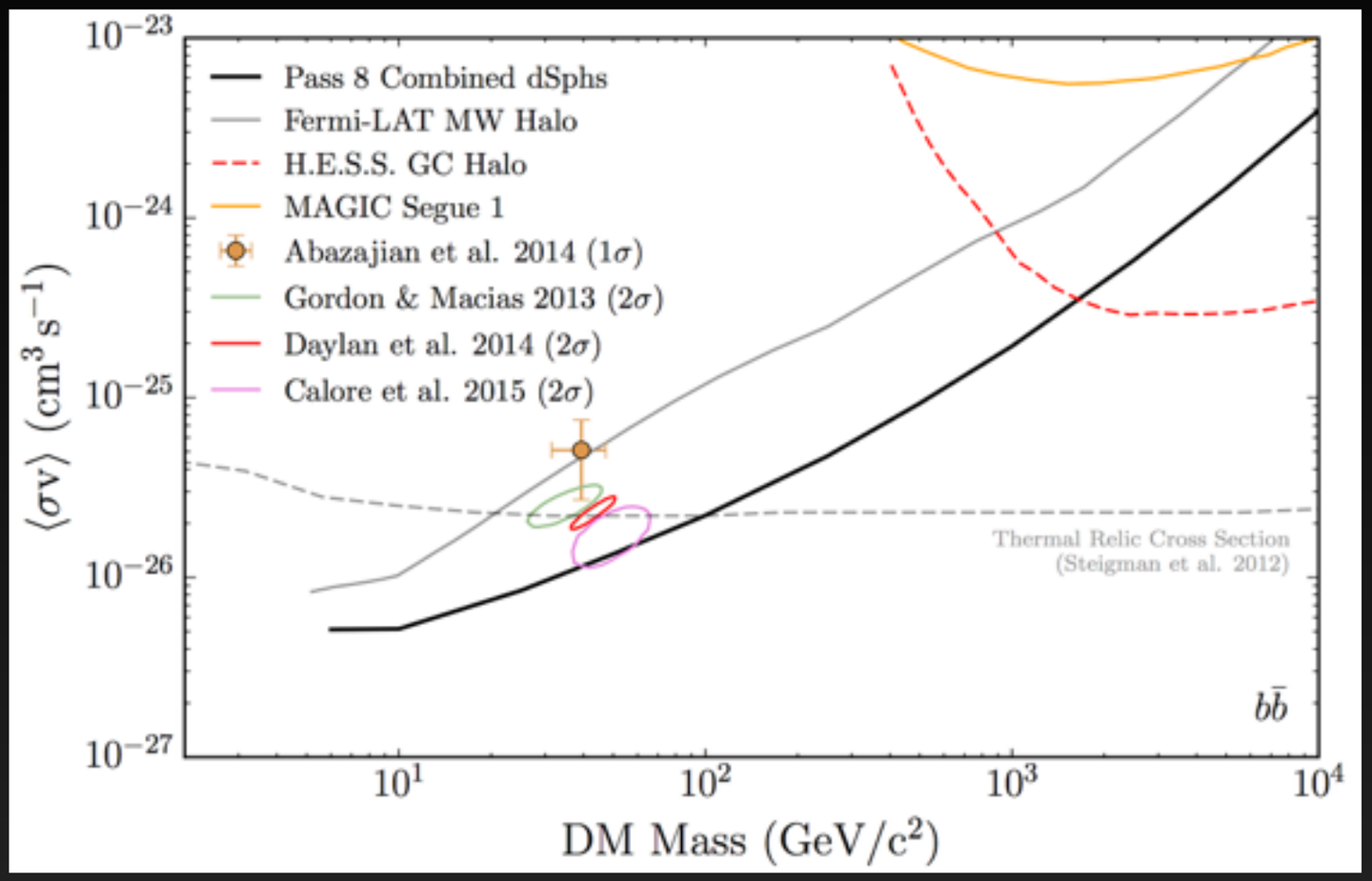

Constraints from dSphs are statistically in 1-2σ tension with the GC excess.

However, uncertainties in the dark matter density profile can easily resolve this tension.

credit: Kev Abazajian (2015)

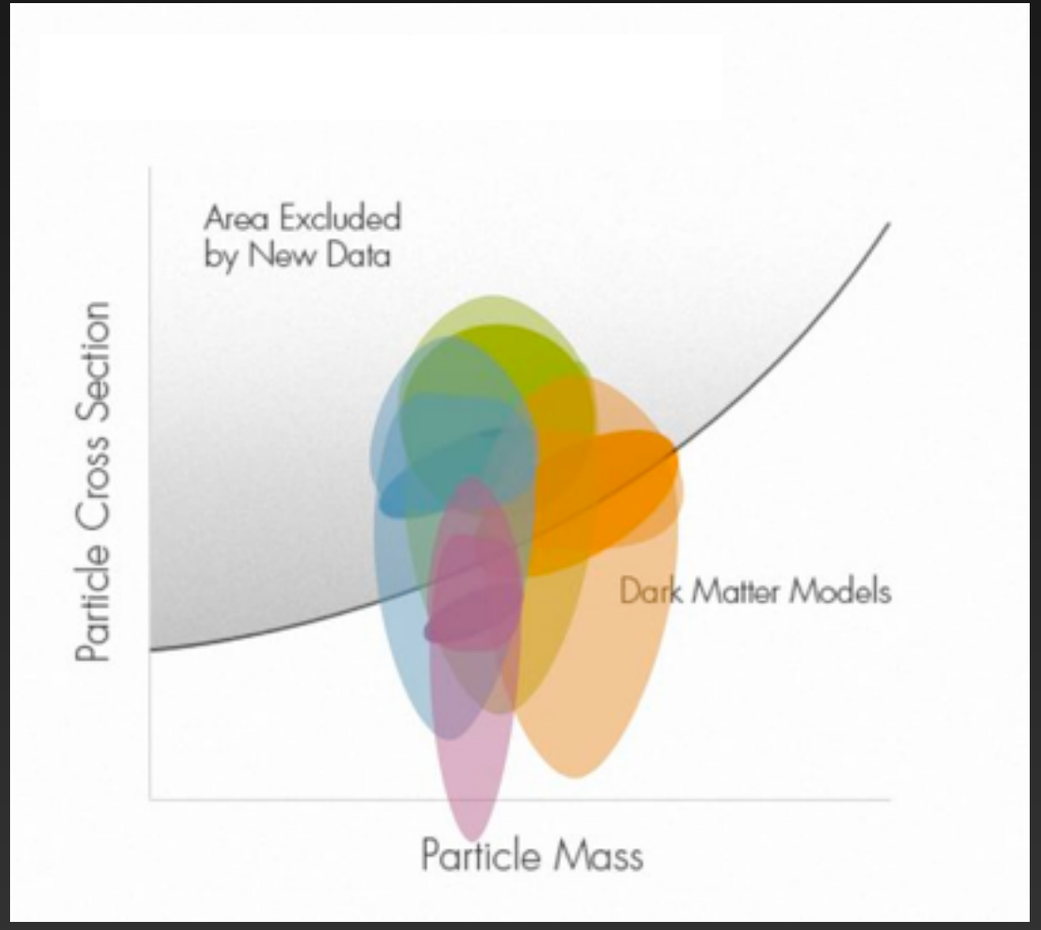

Millisecond Pulsar Fits

- The peak of the MSP energy spectrum matches the peak of the GeV excess

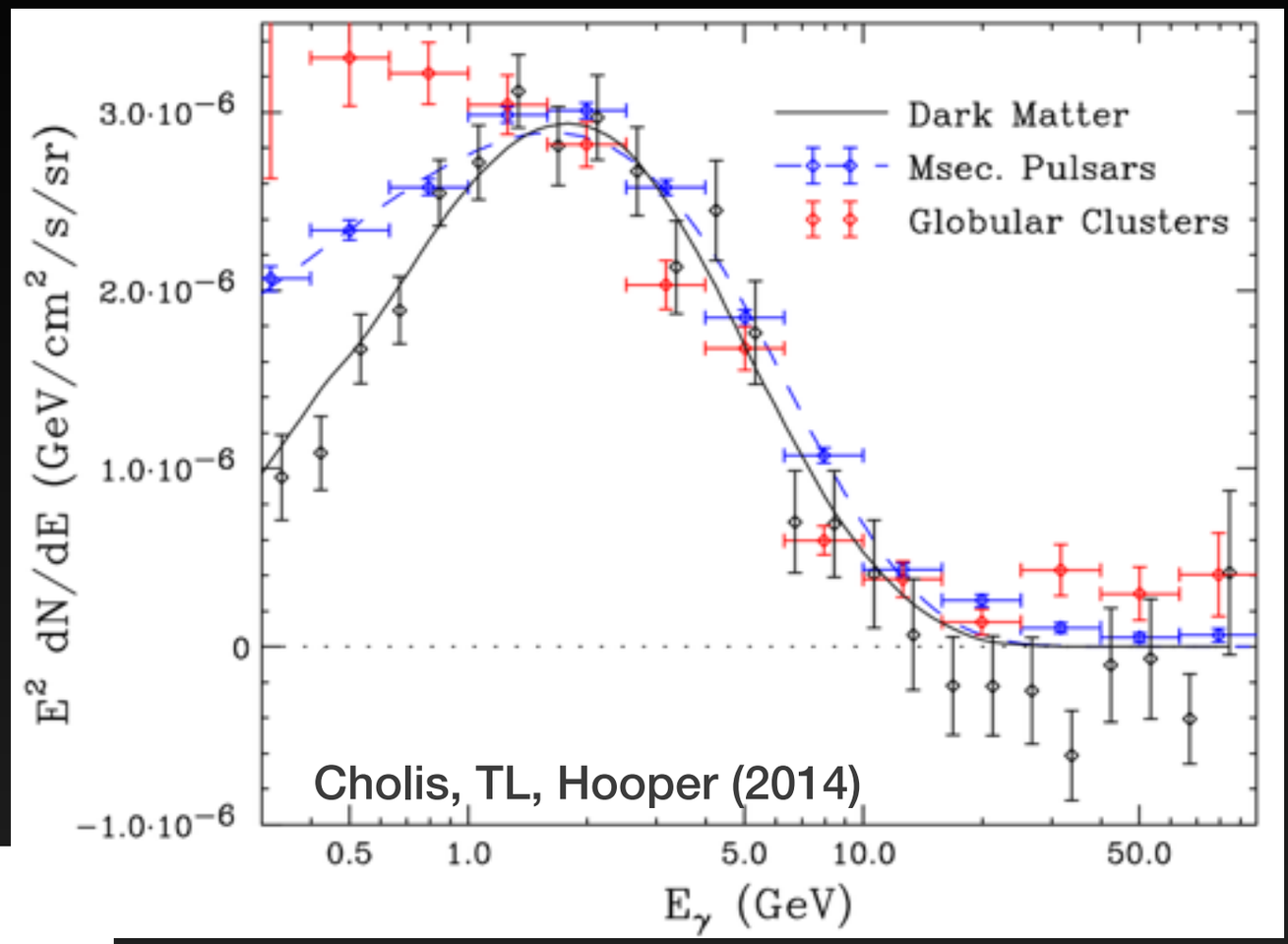

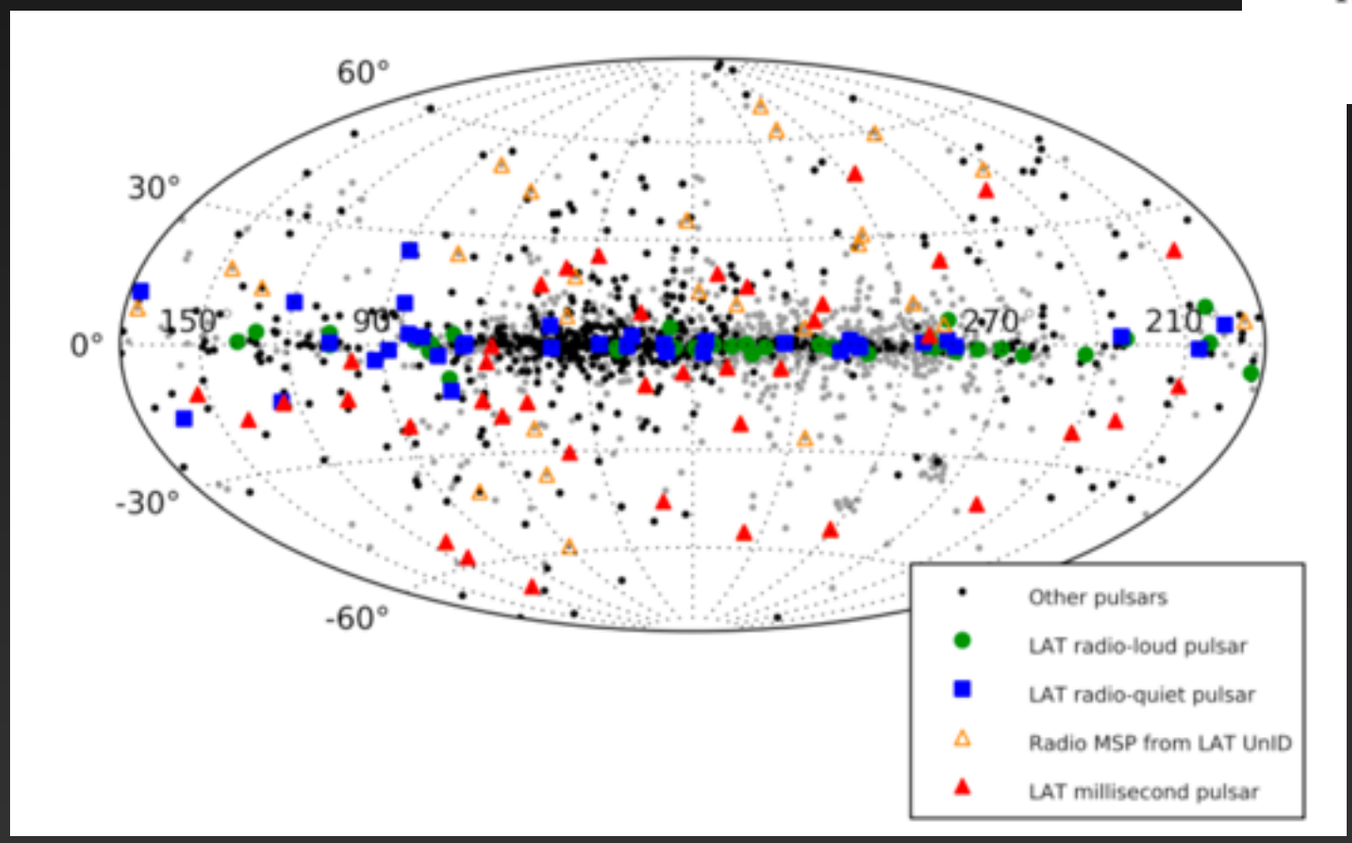

- MSPs are thought to be overabundant in dense star-forming regions like the Galactic Center

Millisecond Pulsar Fits

IG

Bartels et al. (2015)

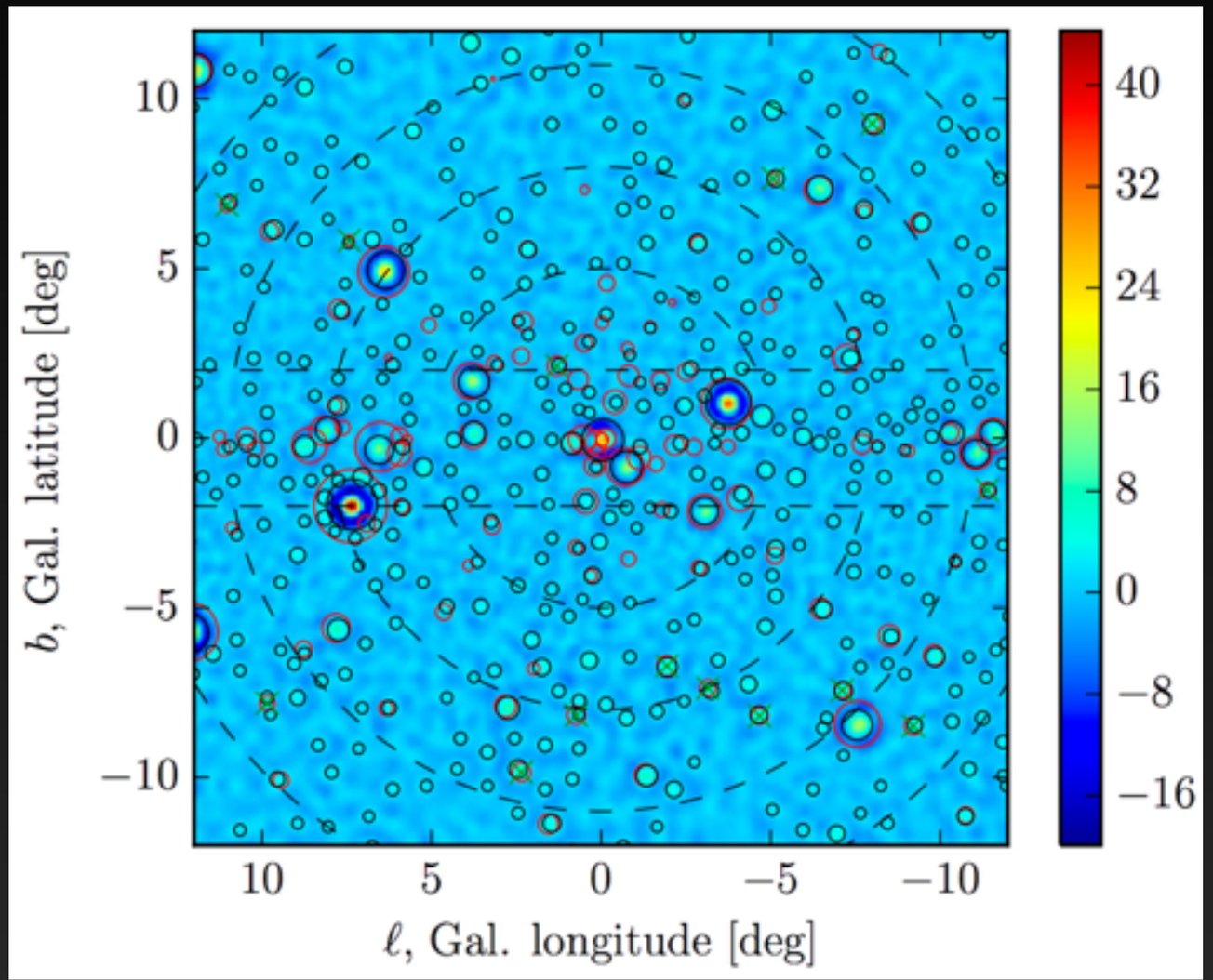

Lee et al. (2015)

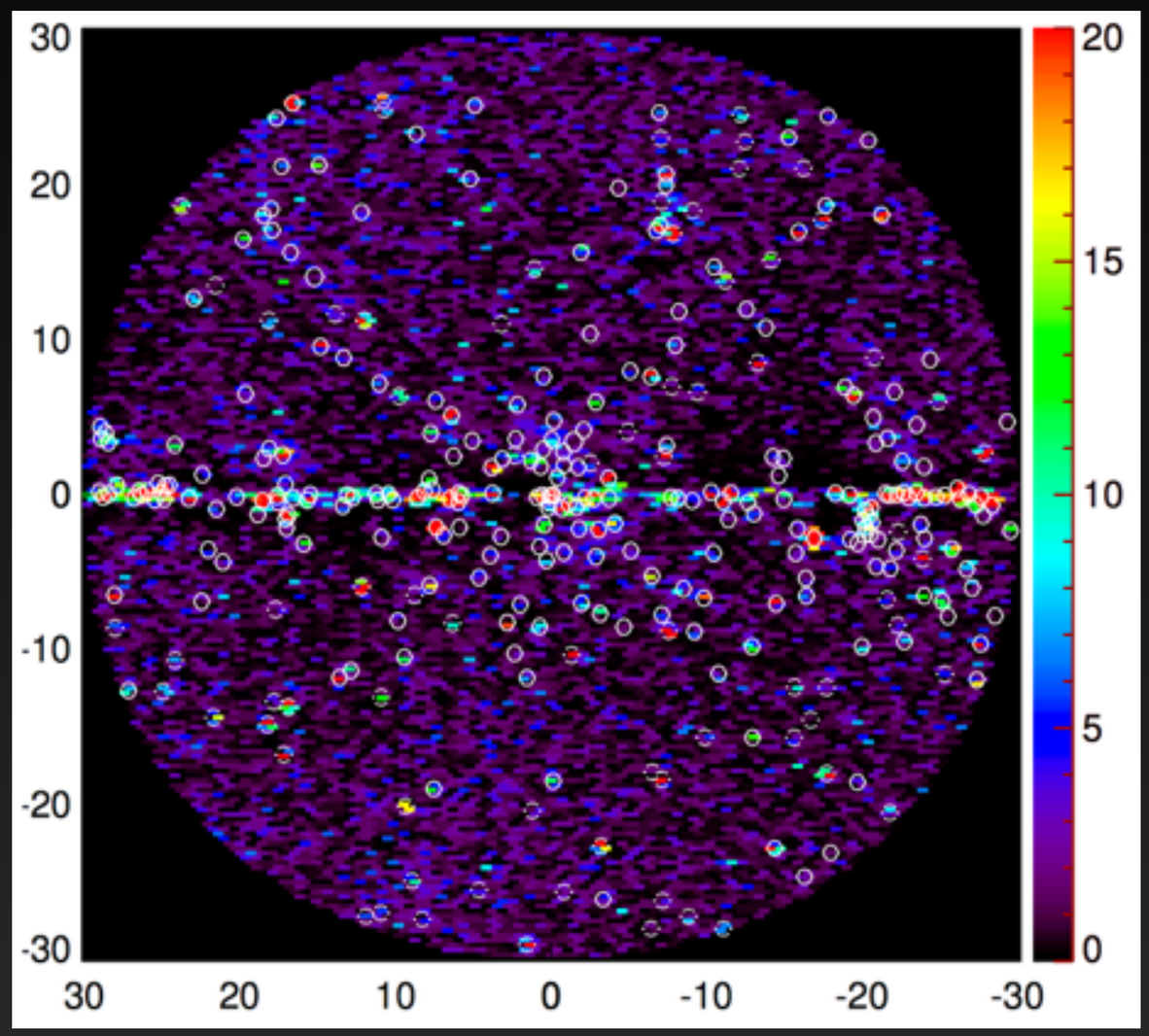

- **Recent analyses of hot-spots and cold spots in the GC region find evidence for the presence of a population of sub-threshold point sources.**

Millisecond Pulsar Fits

IG

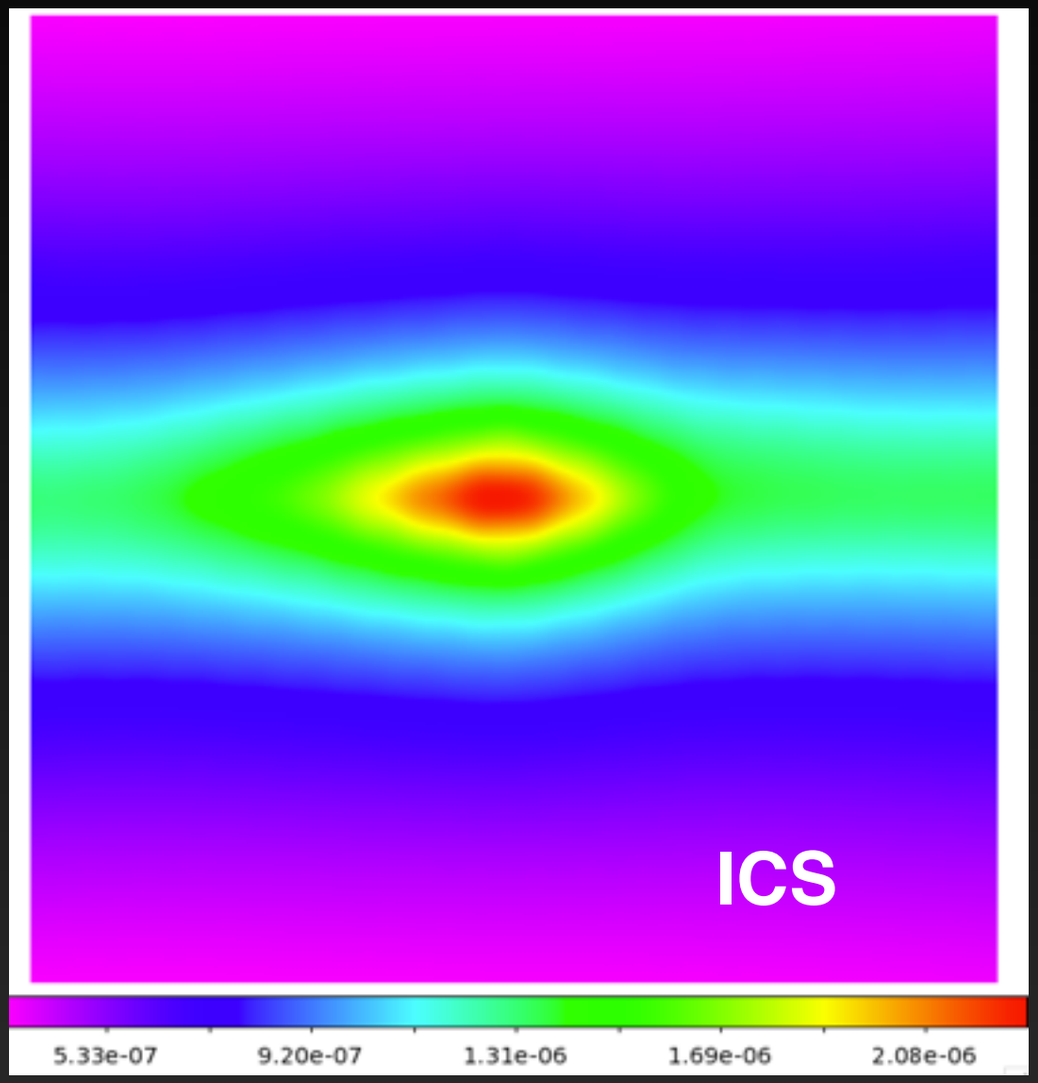

Ajello et al. (2015)

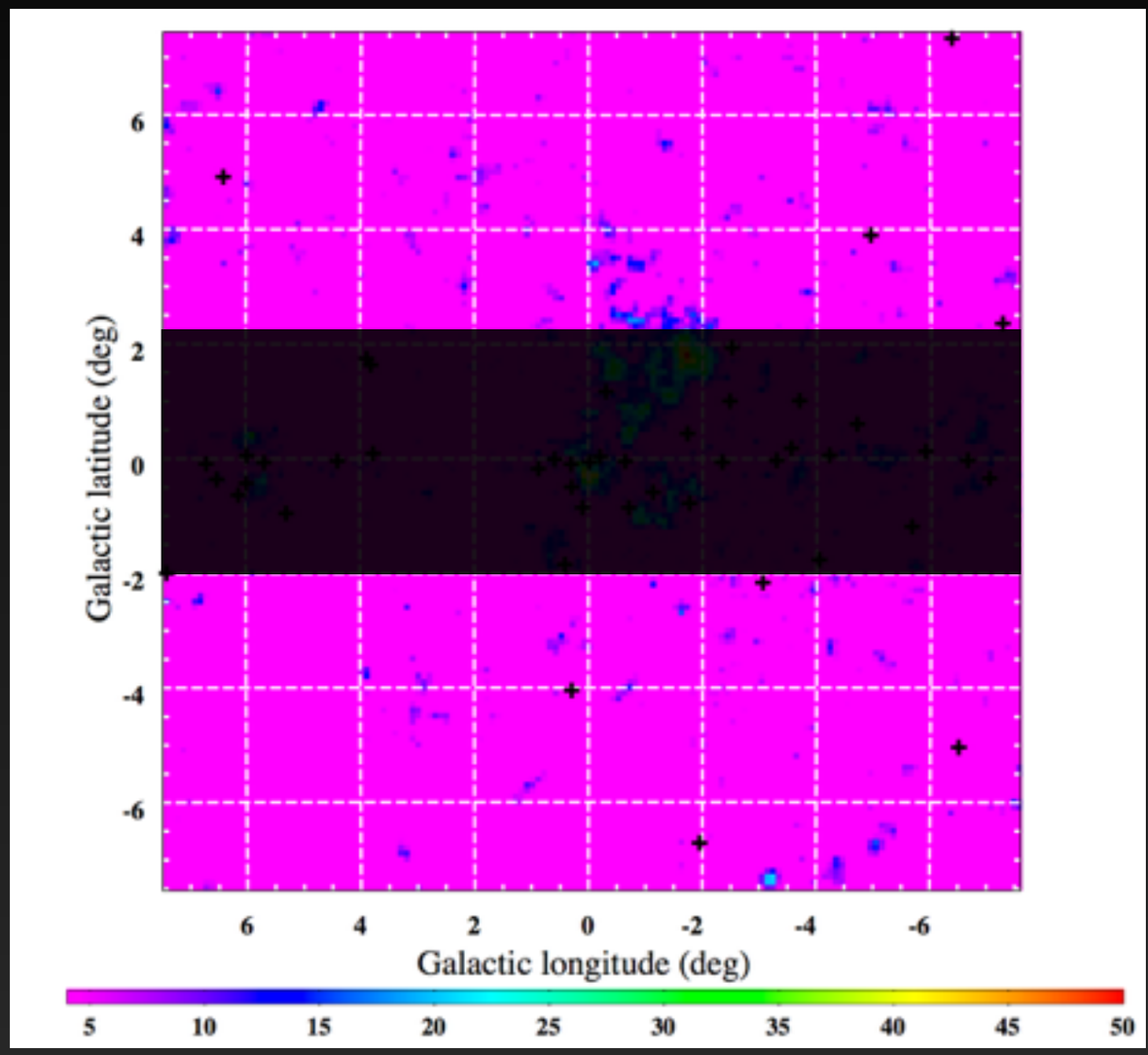

- However, these residuals are found once an extremely smooth diffuse emission model is subtracted - it remains to be seen whether the residuals are resilient to diffuse model changes.

Too Bright or Too Many?

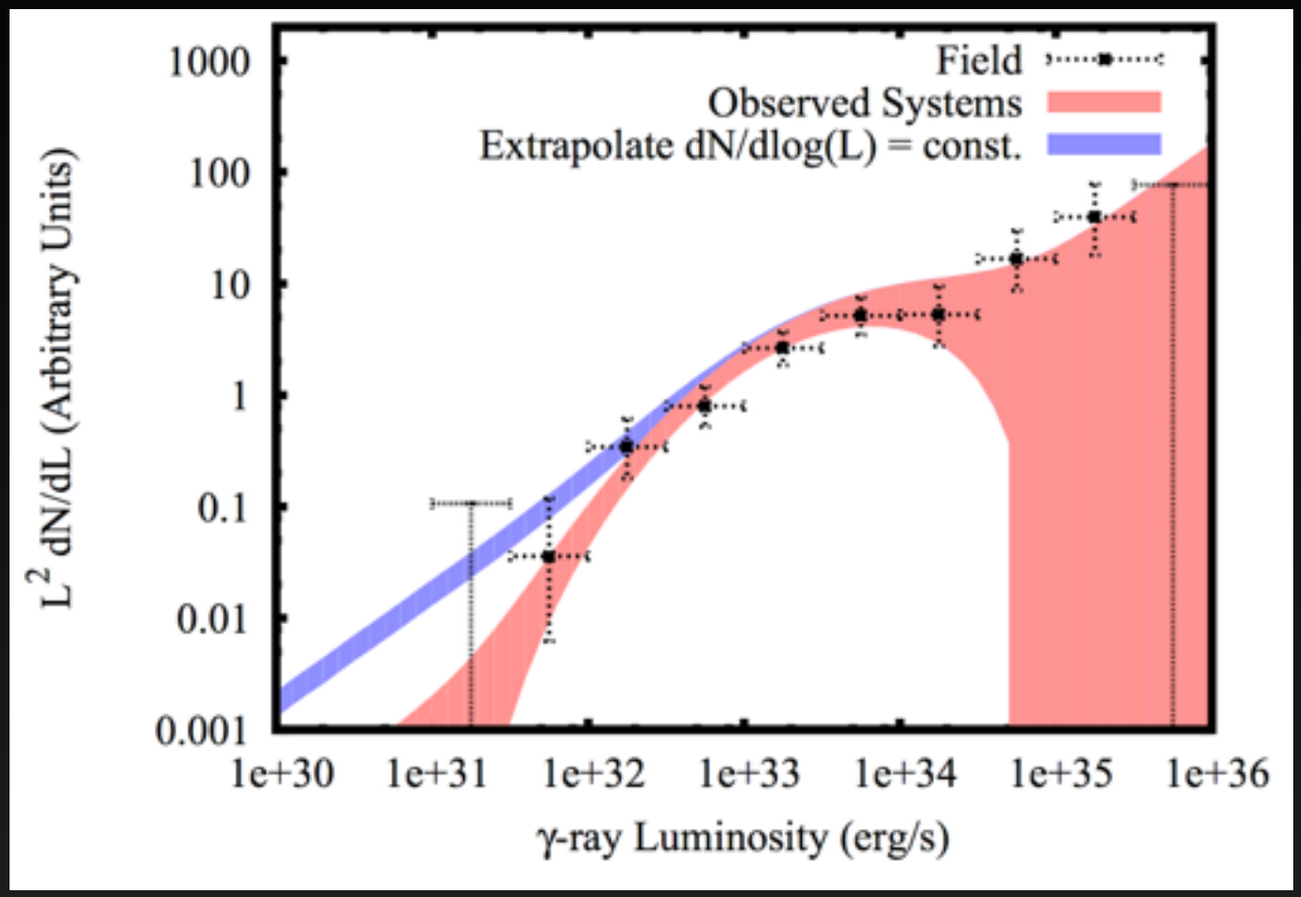

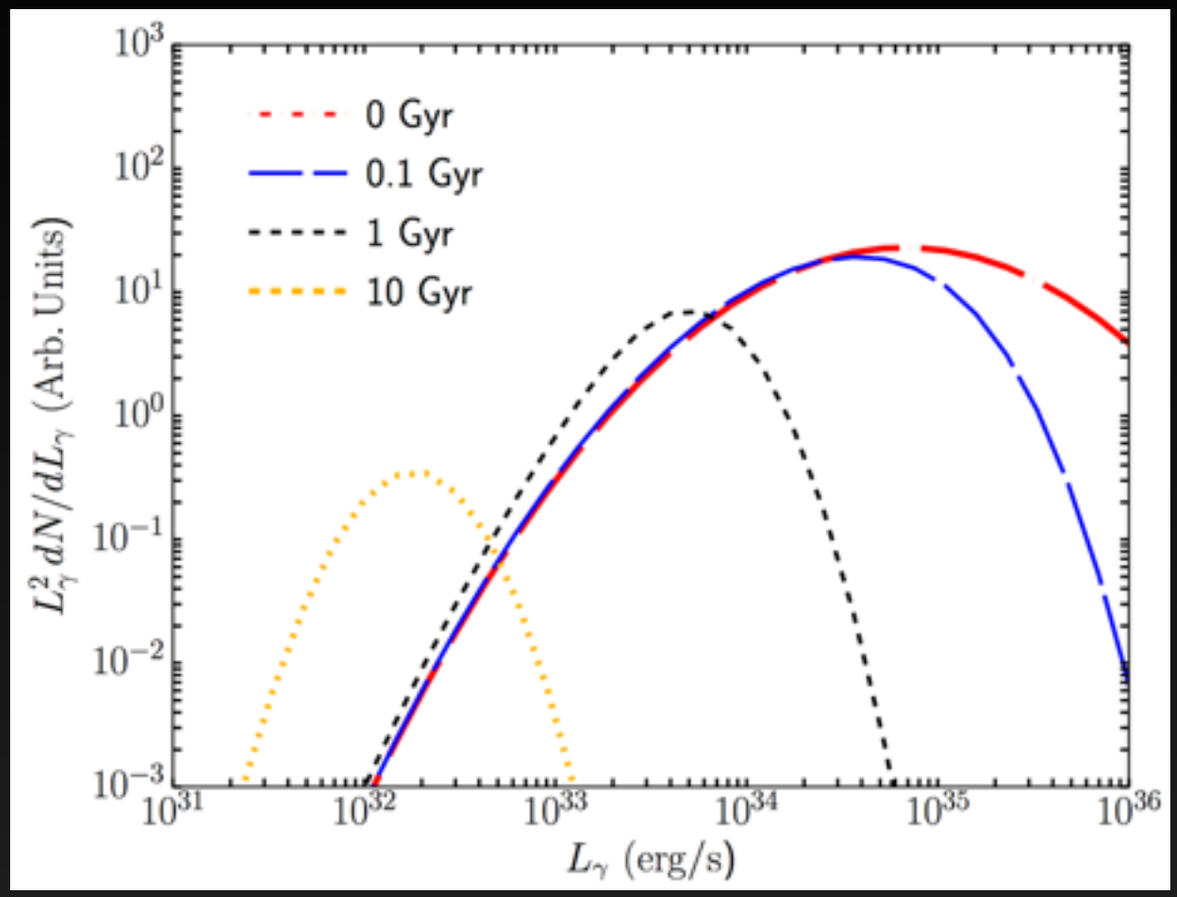

- Utilizing the luminosity distribution of pulsars in the field produces too many bright (detectable) pulsars, compared to observations. (Hooper et al. 2013, 2015)

- Evolving the pulsars (compared to the replenished field population) decreases the number of bright pulsars, but requires too many systems to explain the total luminosity. (Hooper & TL 2016)

Upcoming Work

1.) Utilizing deeper X-Ray observations of LMXBs in globular clusters to compare with the LMXB population of the Galactic center.

2.) Search for soft-spectrum radio sources in the Galactic center, which may be statistically correlated with MSPs.

3.) Direct Evaluation of the gamma-ray MSP luminosity function from point source searches at the positions of known radio MSPs.

MeerKAT and SKA

Calore et al. (2015)

- Radio Observations with GBT targeted at gamma-ray hotspots would be expected to find ~5-10 MSPs with a 200 hr commitment.

- Fortunately, SKA observations are likely to conclusively find MSPs in the GC, or rule out this scenario.

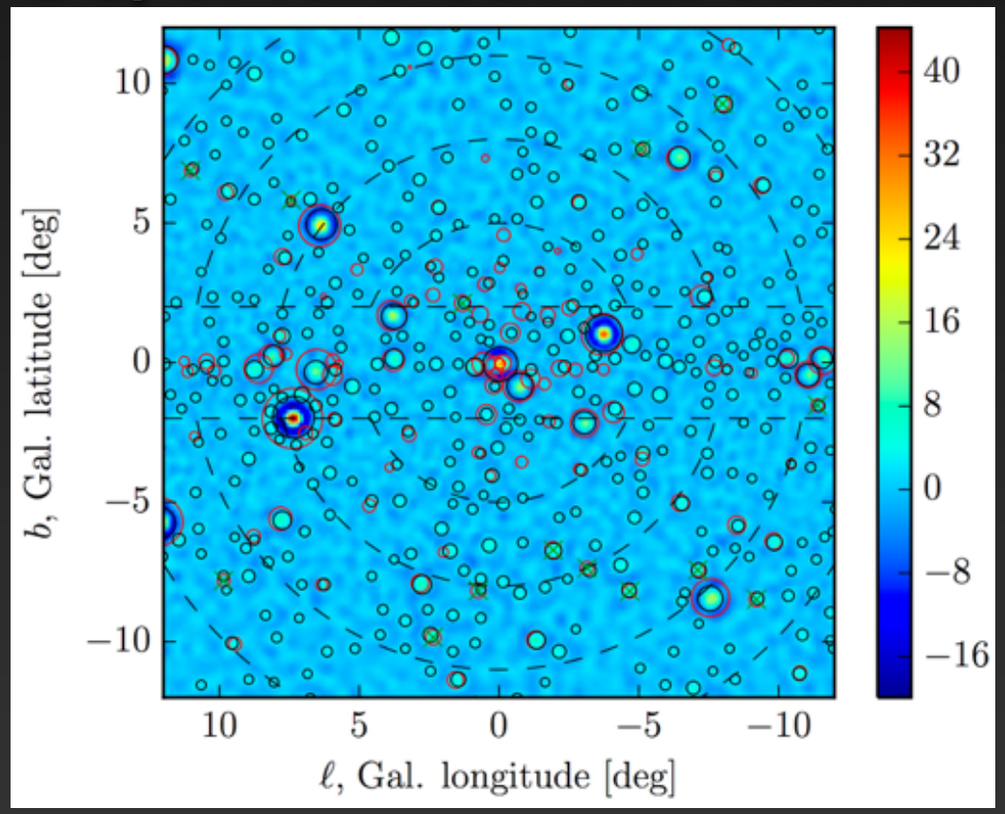

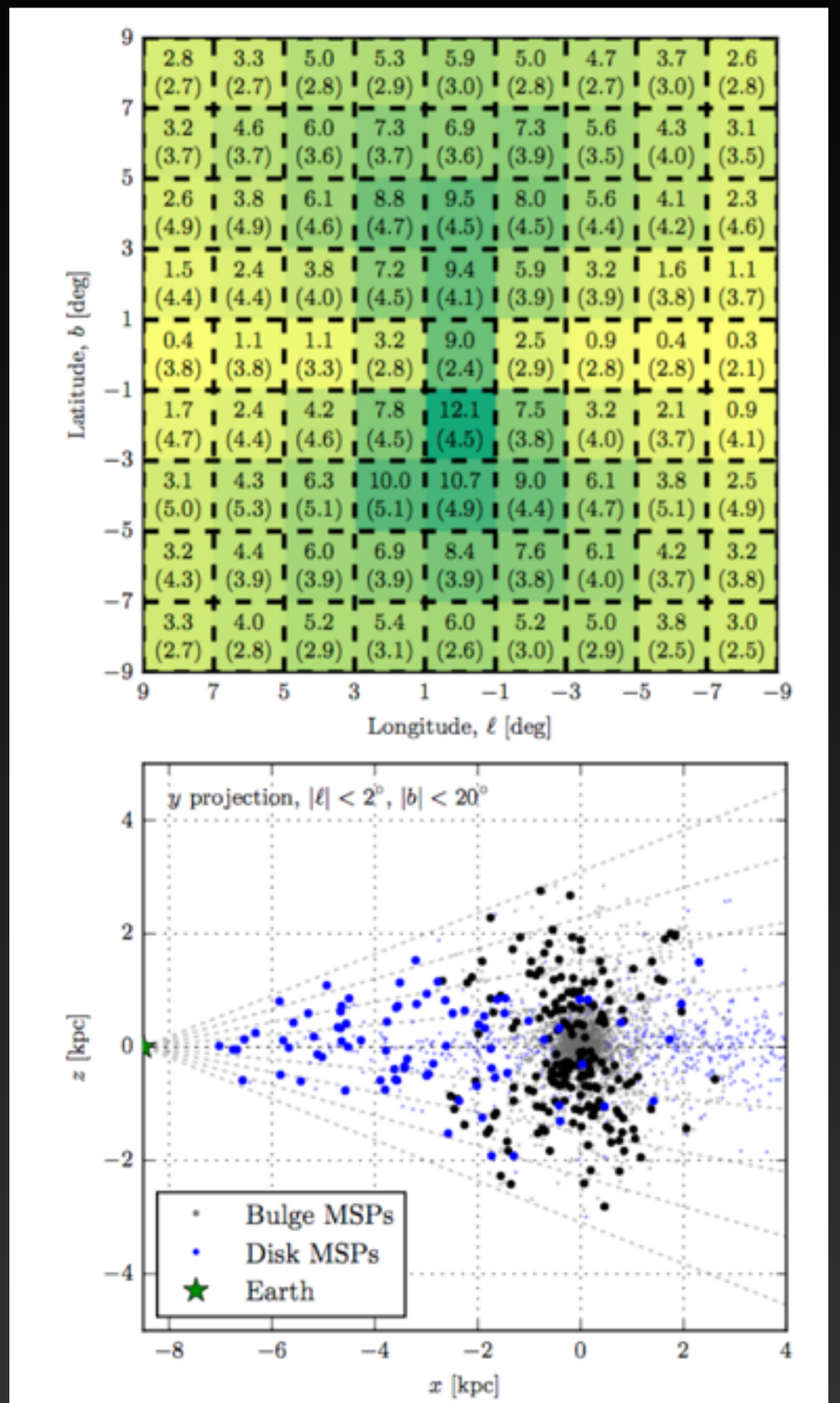

An Excess Compared to What?

Cosmic-Ray Propagation Codes (e.g. Galprop), generally utilize a cosmic-ray injection rate at the Galactic center that is identically 0.

These models were not produced to study the very center of the Galaxy!

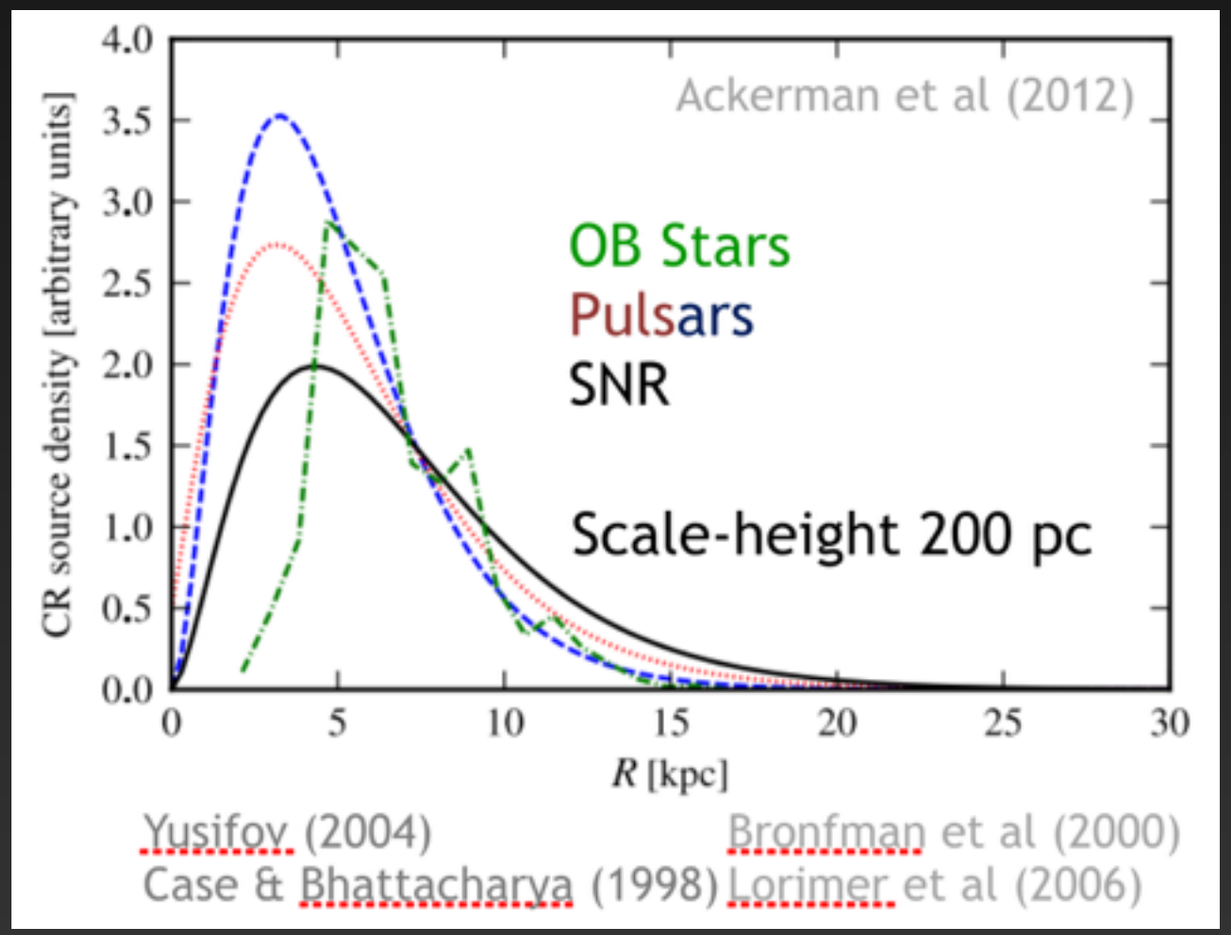

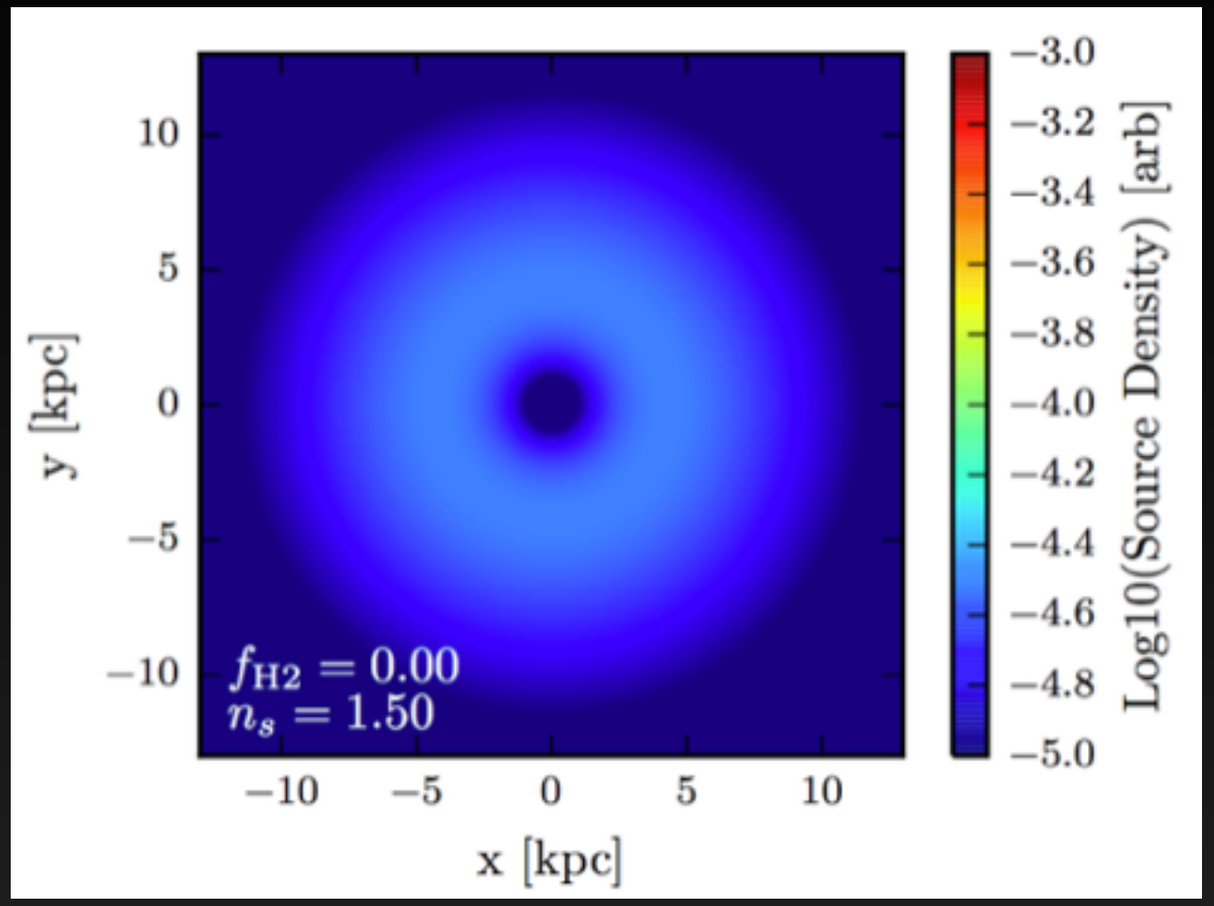

Results from these cosmic-ray propagation codes are used in many analyses of the Galactic center region.

Carlson et al. (2016a, 2016b)
1510.04698
1603.06584

The Solution

Solution: Add a new cosmic-ray injection morphology tracing the molecular gas density.

Observationally Resilient: Several tracers of molecular gas are sensitive to the galactic center region.

Theoretically Motivated: Molecular Gas is the seed of star formation, the Schmidt Law gives

$$\Sigma_{\rm SFR} \propto \Sigma_{\rm Gas}^{1.4\pm.15}$$

Specifically we inject a fraction of cosmic-rays ($0 < f_{H2} < 1$) following:

$$Q_{\rm CR}(\vec{r}) \propto \begin{cases} 0 & \rho_{\rm H2} \leq \rho_s \\ \rho_{\rm H2}^{n_s} & \rho_{\rm H2} > \rho_s \end{cases}$$

1510.04698

The Solution

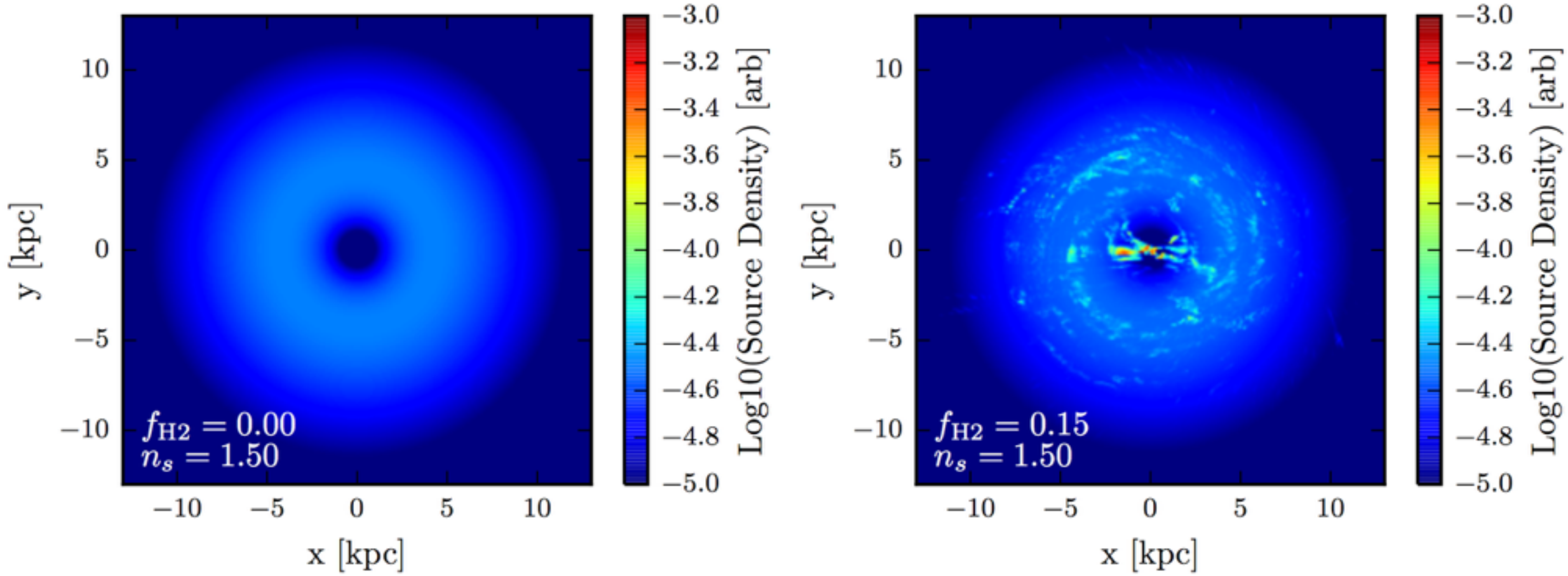

Two features leap out immediately:

1.) Spiral Arms

2.) A bright bar in the Galactic Center

The Solution

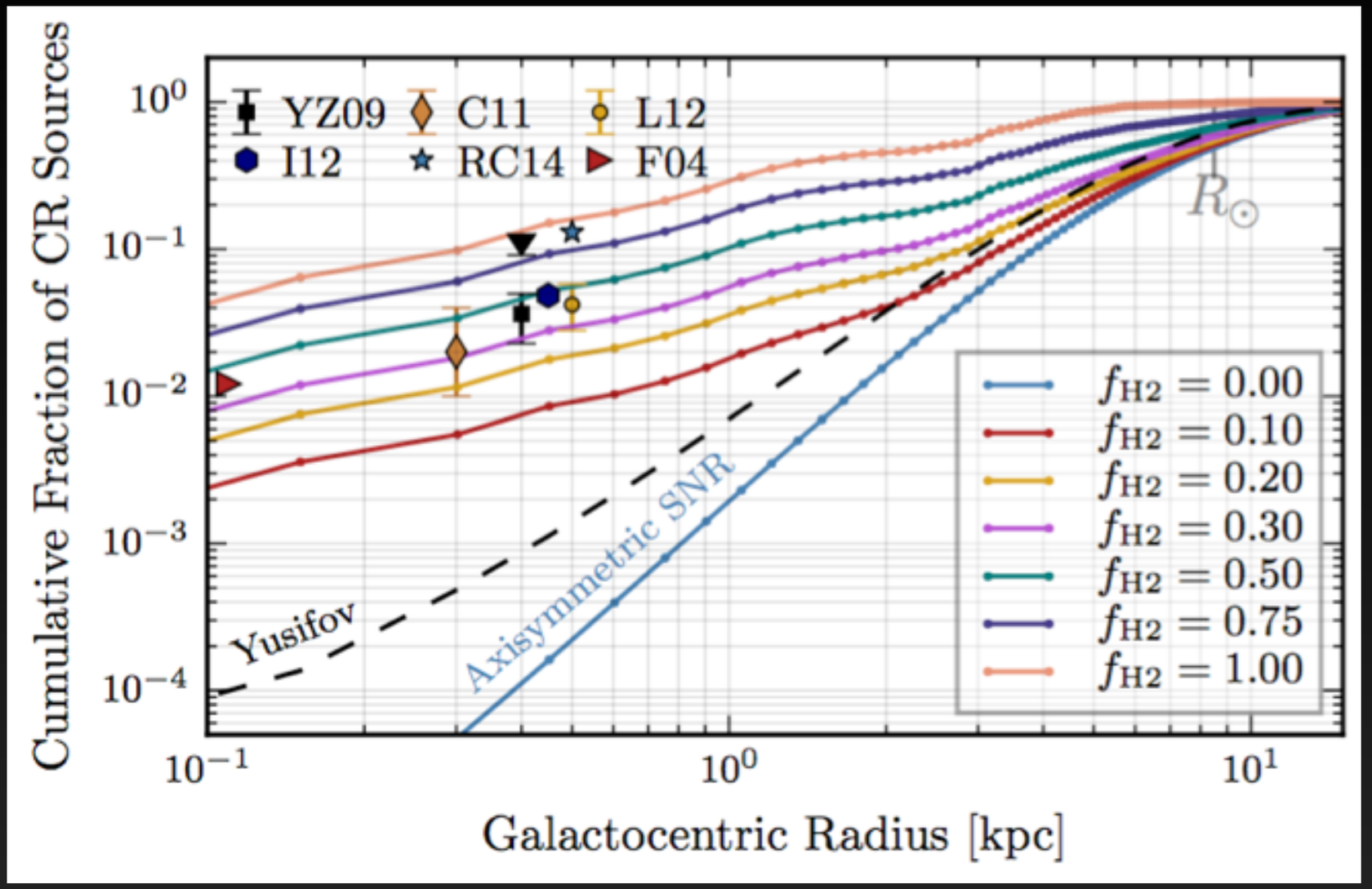

Adds a new, and significant, cosmic-ray injection component, in particular near the Galactic Center.

The cosmic-ray injection rate now matches observational constraints.

Simulations!

Add the new cosmic-ray injection models into Galprop to produce a new steady-state cosmic-ray distribution.

Parameter	Units	Canonical	Mod A	Description
D_0	$\mathrm{cm^2\ s^{-1}}$	7.2×10^{28}	5.0×10^{28}	Diffusion constant at $\mathcal{R} = 4$ GV
δ	–	0.33	0.33	Index of diffusion constant energy dependence
$z_{\rm halo}$	kpc	3	4	Half-height of diffusion halo
$R_{\rm halo}$	kpc	20	20	Radius diffusion halo
v_a	$\mathrm{km\ s^{-1}}$	35	32.7	Alfvén velocity
dv/dz	$\mathrm{km\ s^{-1}\ kpc^{-1}}$	0	50	Vertical convection gradient
$\alpha_{\rm p}$	–	1.88 (2.39)	1.88 (2.47)	p injection index below (above) $\mathcal{R} = 11.5$ GV
$\alpha_{\rm e}$	–	1.6 (2.42)	1.6 (2.43)	e^- injection index below (above) $\mathcal{R} = 2$ GV
Source	–	SNR	SNR	Distribution of $(1 - f_{\rm H2})$ primary sources*
$f_{\rm H2}$	–	.20	N/A	Fraction of sources in star formation model*
n_s	–	1.5	N/A	Schmidt Index*
ρ_c	$\mathrm{cm^{-3}}$	0.1	N/A	Critical H_2 density for star formation*
B_0	μG	7.2	9.0	Local ($r = R_\odot$) magnetic field strength
r_B, z_B	kpc	5, 1	5, 2	Scaling radius and height for magnetic field
ISRF	–	(1.0,.86,.86)	(1.0,.86,.86)	Relative CMB, Optical, FIR density
dx, dy	kpc	0.5, 0.5	1 (2D)	x, y (3D) or radial (2D) cosmic-ray grid spacing
dz	kpc	0.125	.1	z-axis cosmic-ray grid spacing

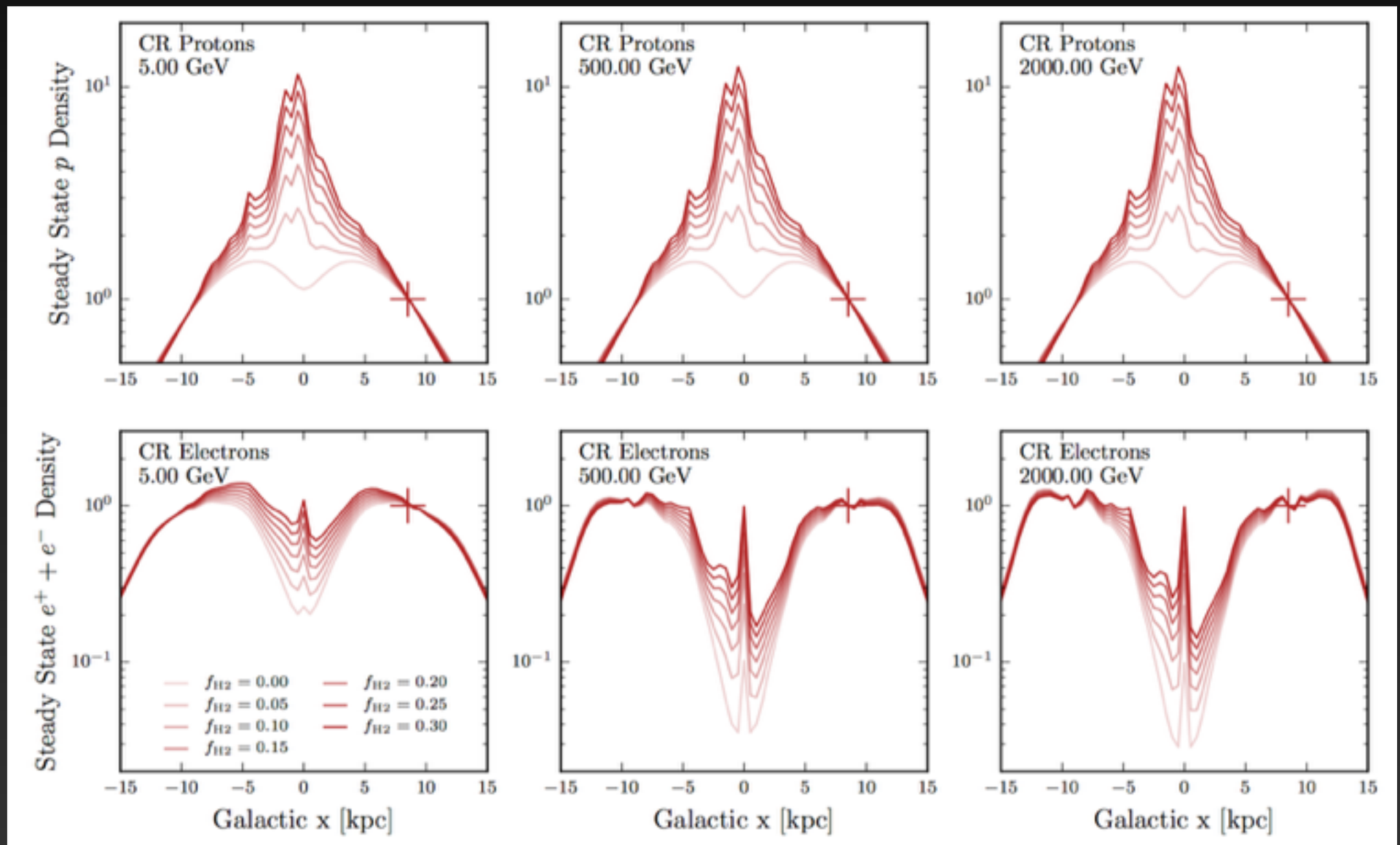

A Better fit to the Gamma-Ray Sky

1.) Adding a cosmic-ray injection component tracing f_{H2} improves the full-sky fit to the gamma-ray data.

2.) The best fit value over the full sky is $f_{H2} = 0.25$

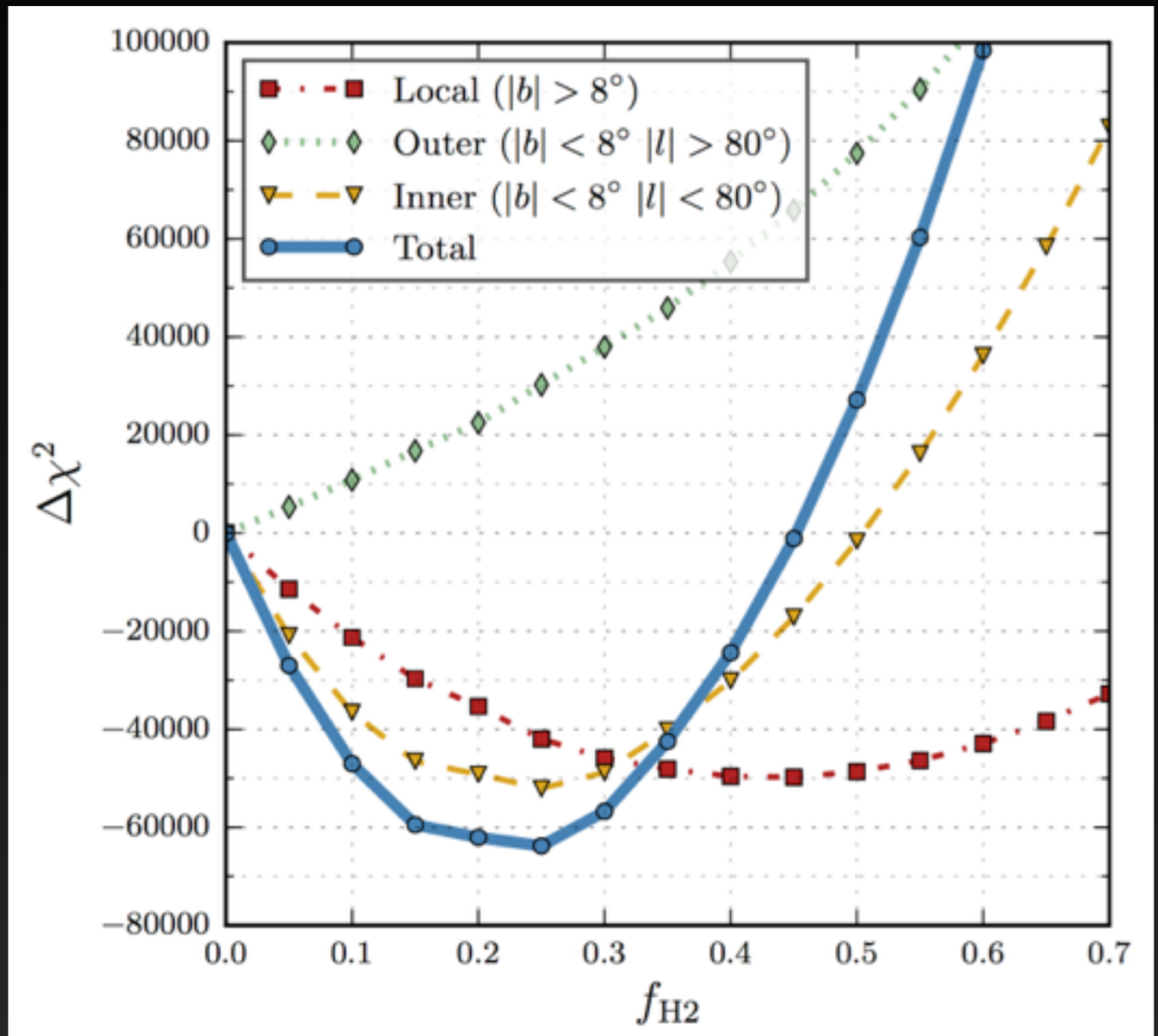

3.) Technique will become more powerful with the introduction of 3D gas and dust maps in the near future.

A Better fit to the Gamma-Ray Sky

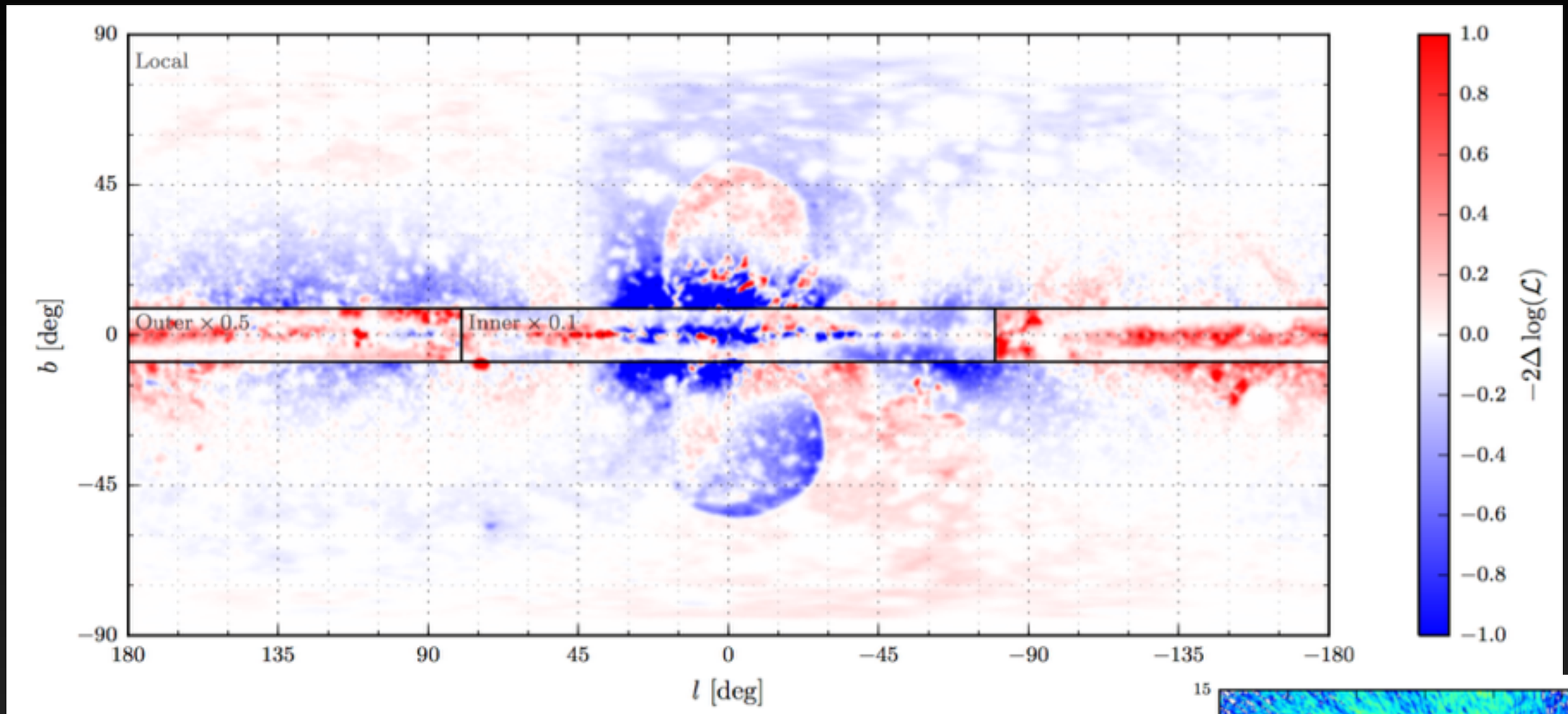

Fits are significantly improved, in particular in regions near the Galactic Center where there is significant kinematic gas information.

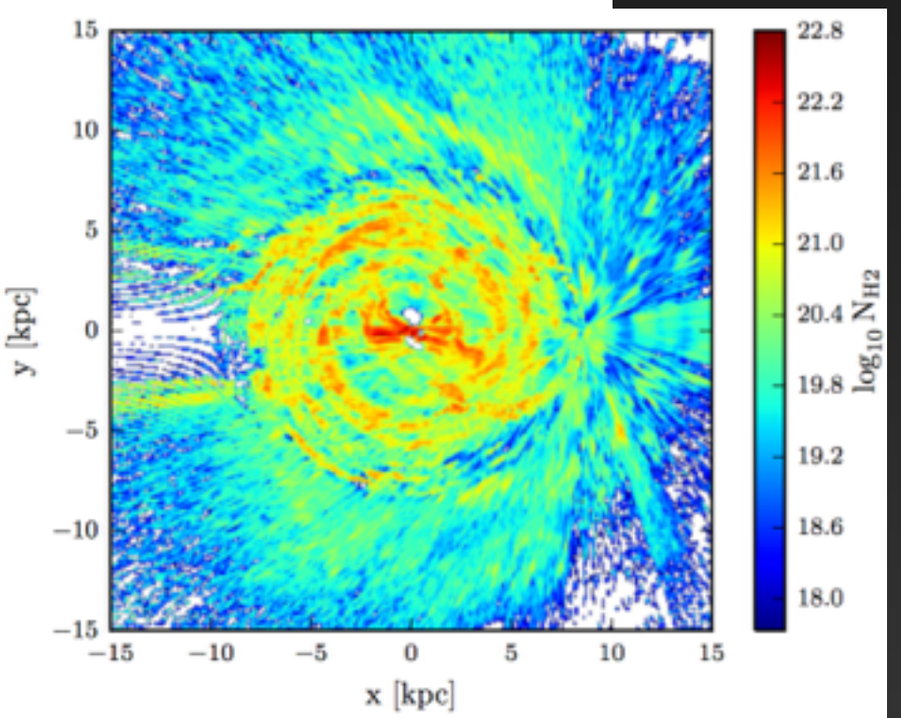

Application to the Galactic Center

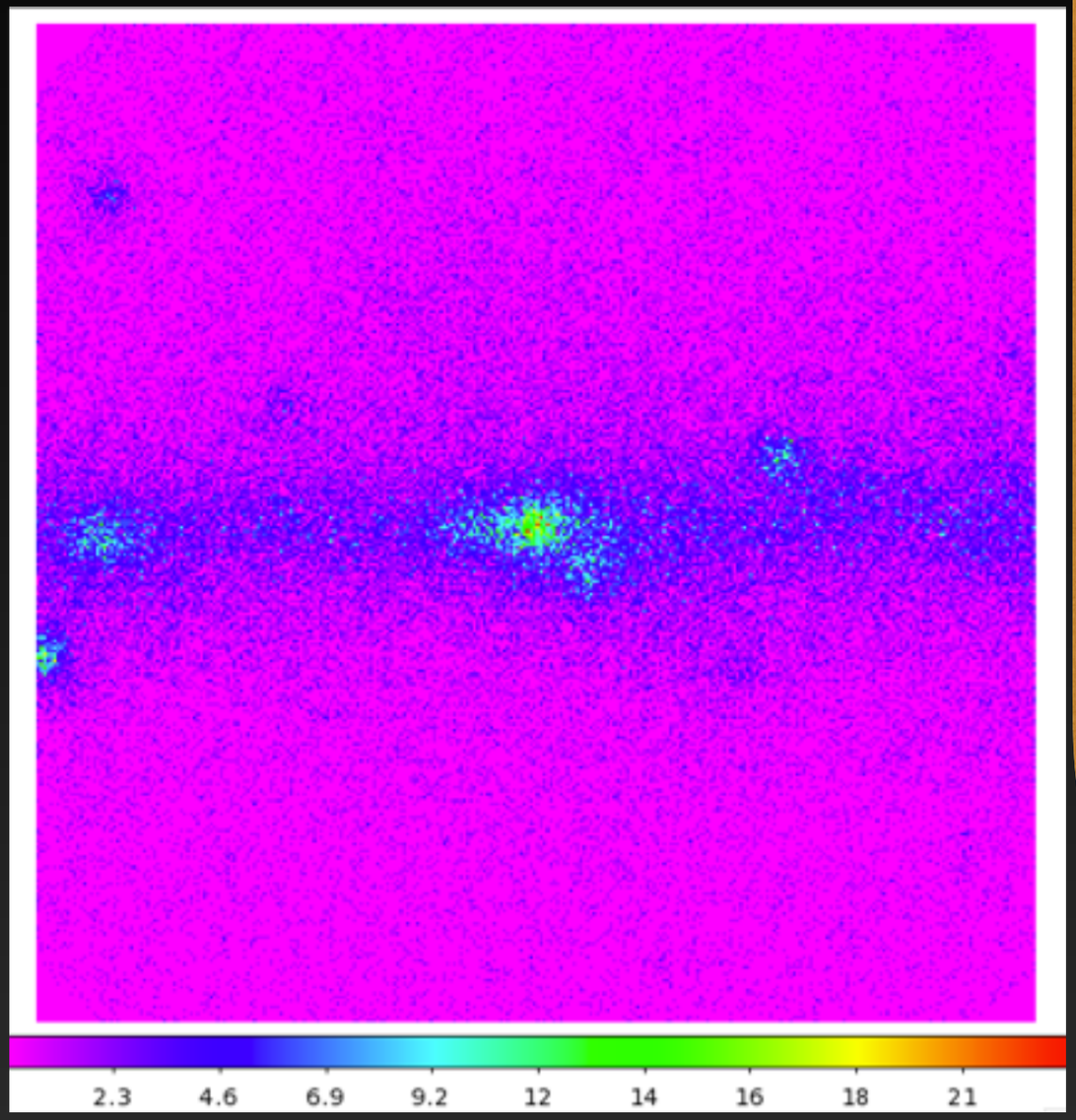

Data

750 — 950 MeV

Best Angular Resolution Cut

10^{o} x 10^{o} ROI

=

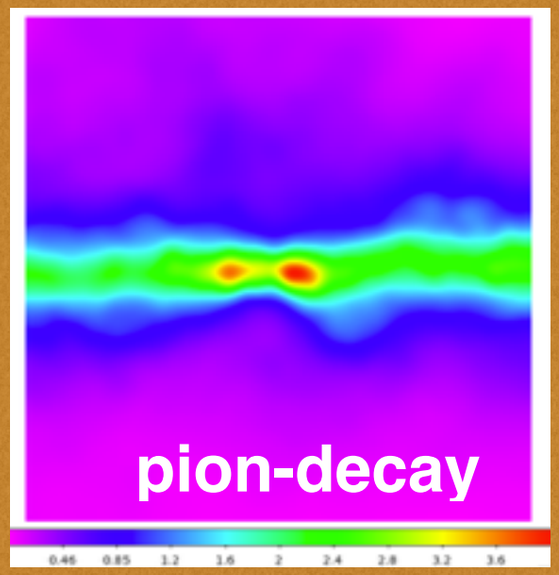

+

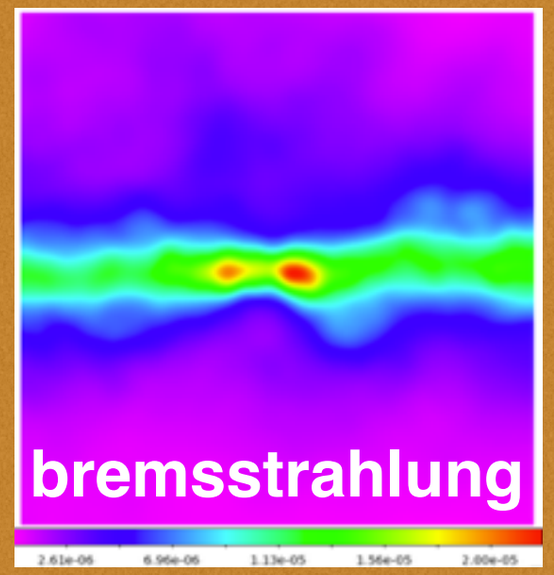

+

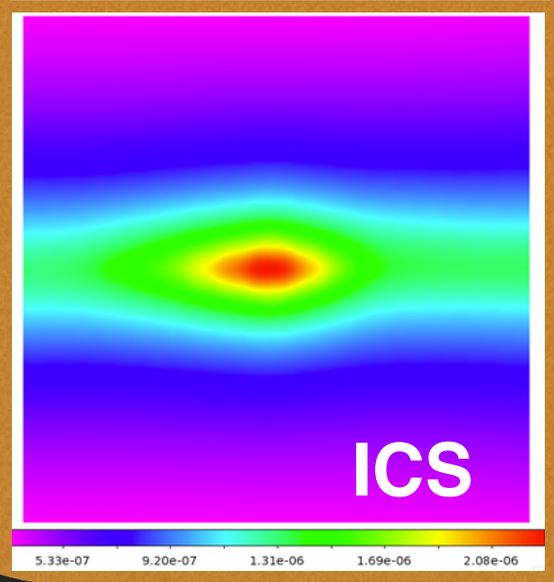

+

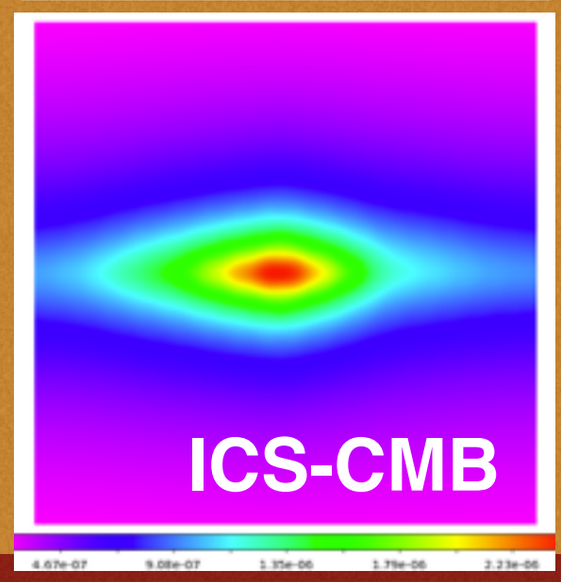

+

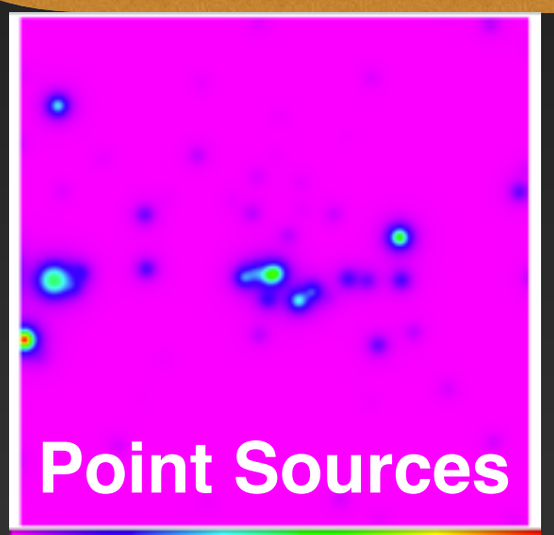

+

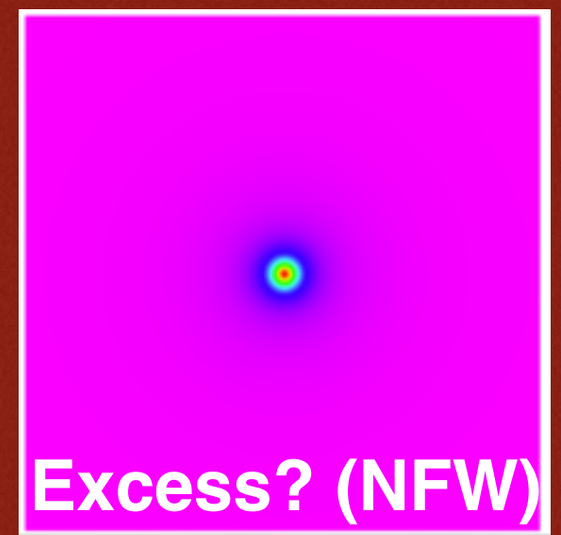

Effect on the GC Excess

IG

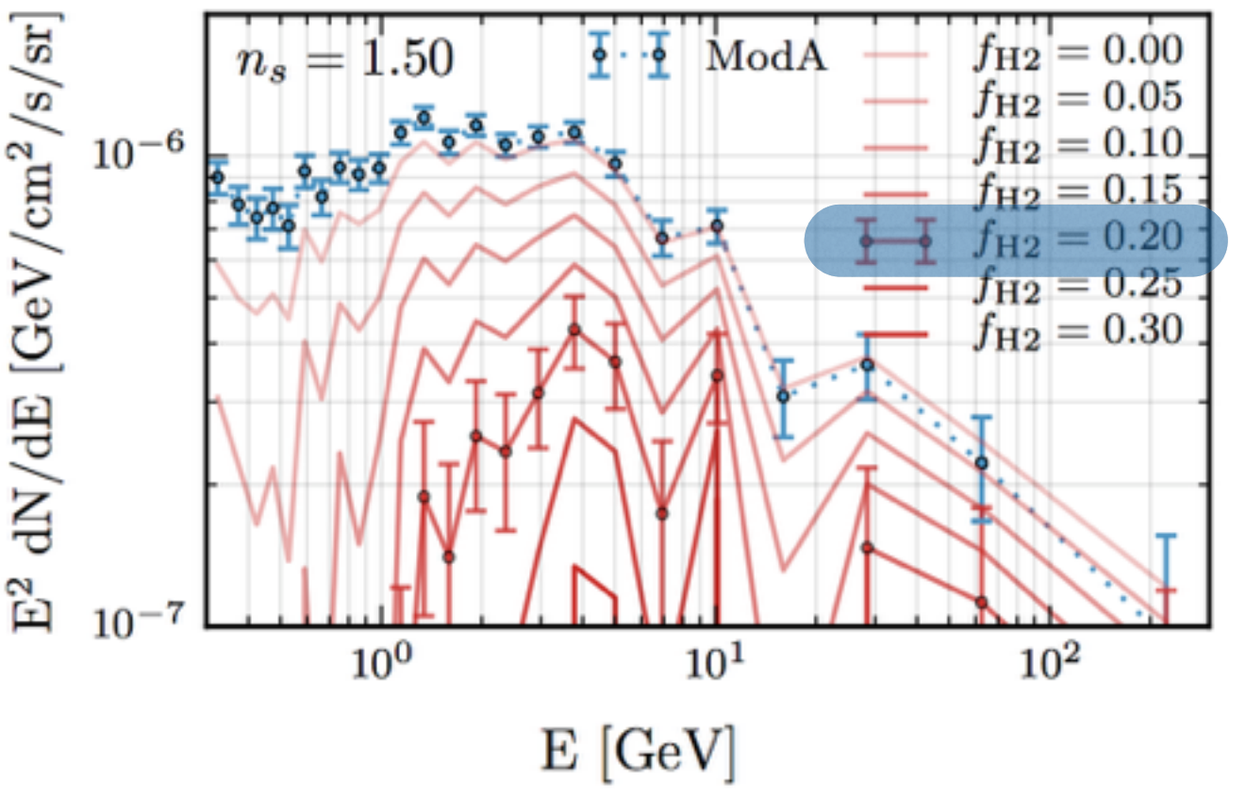

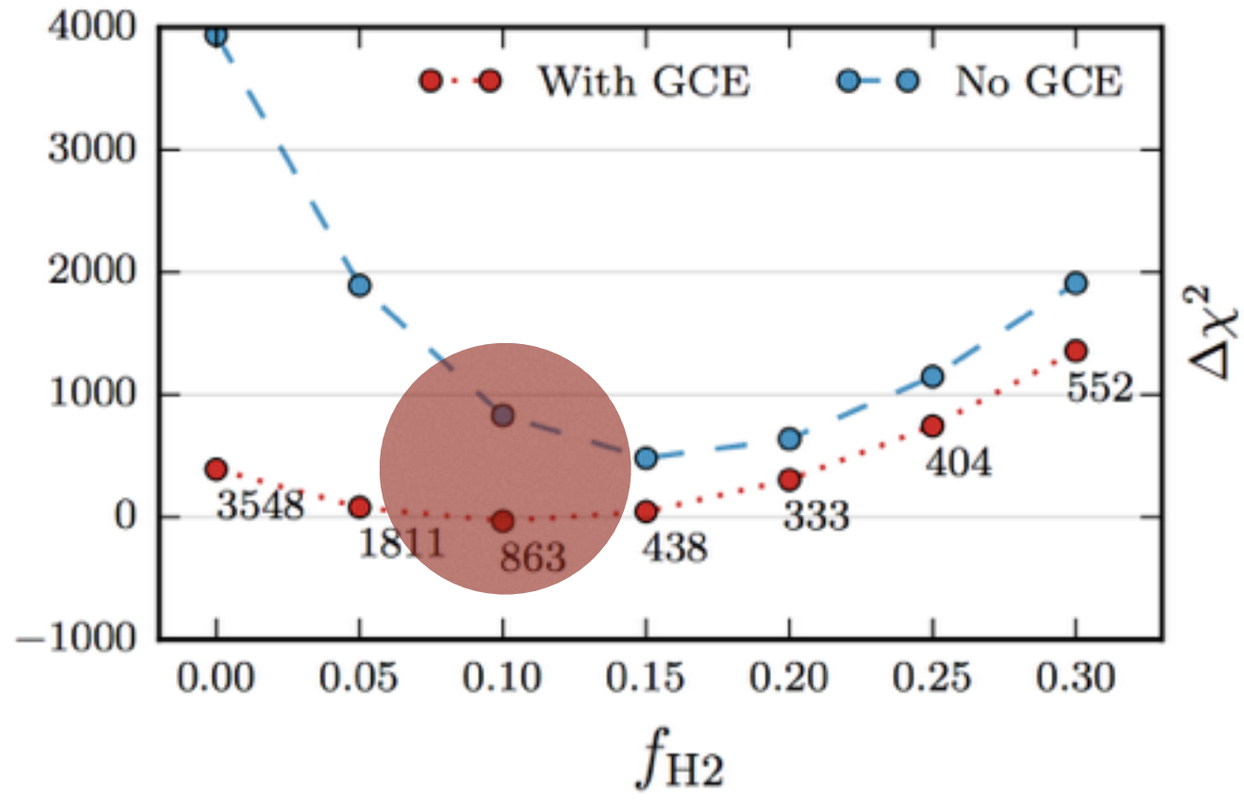

Increasing the value of f_{H2} decreases the intensity of the gamma-ray excess.

However, the best global fit is f_{H2} = 0.1, with a GC excess intensity that decreases by only ~30%.

Effect on the Excess Morphology

IG

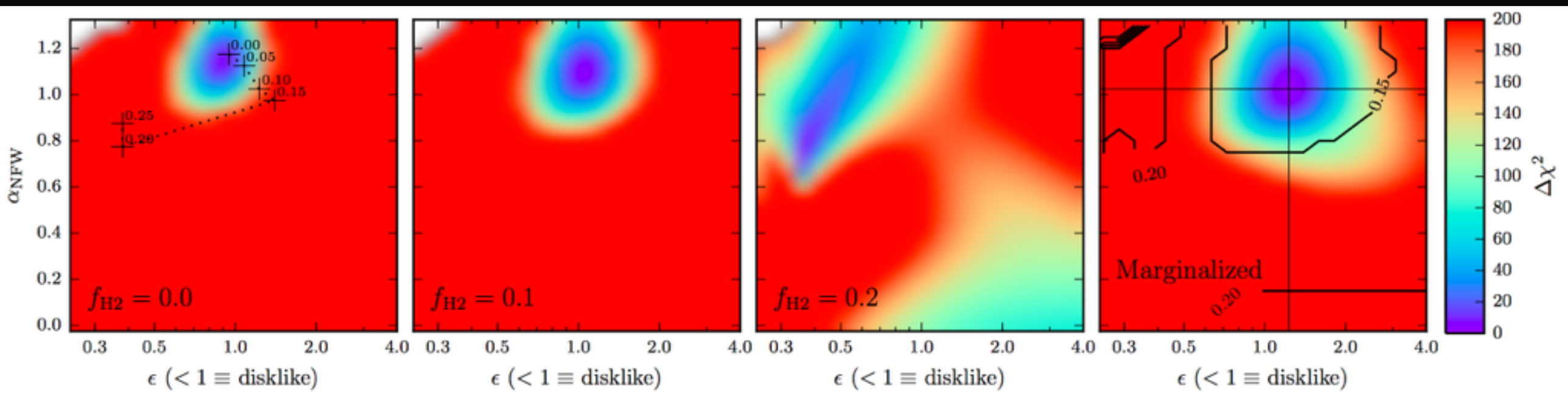

The morphology of the excess is also degenerate with f_{H2}.

As f_{H2} is increased, the best-fit morphology becomes stretched perpendicular to the galactic plane.

However, marginalized over all values of f_{H2}, the standard NFW template is still consistent with the data.

Analysis in the Galactic Center

GC

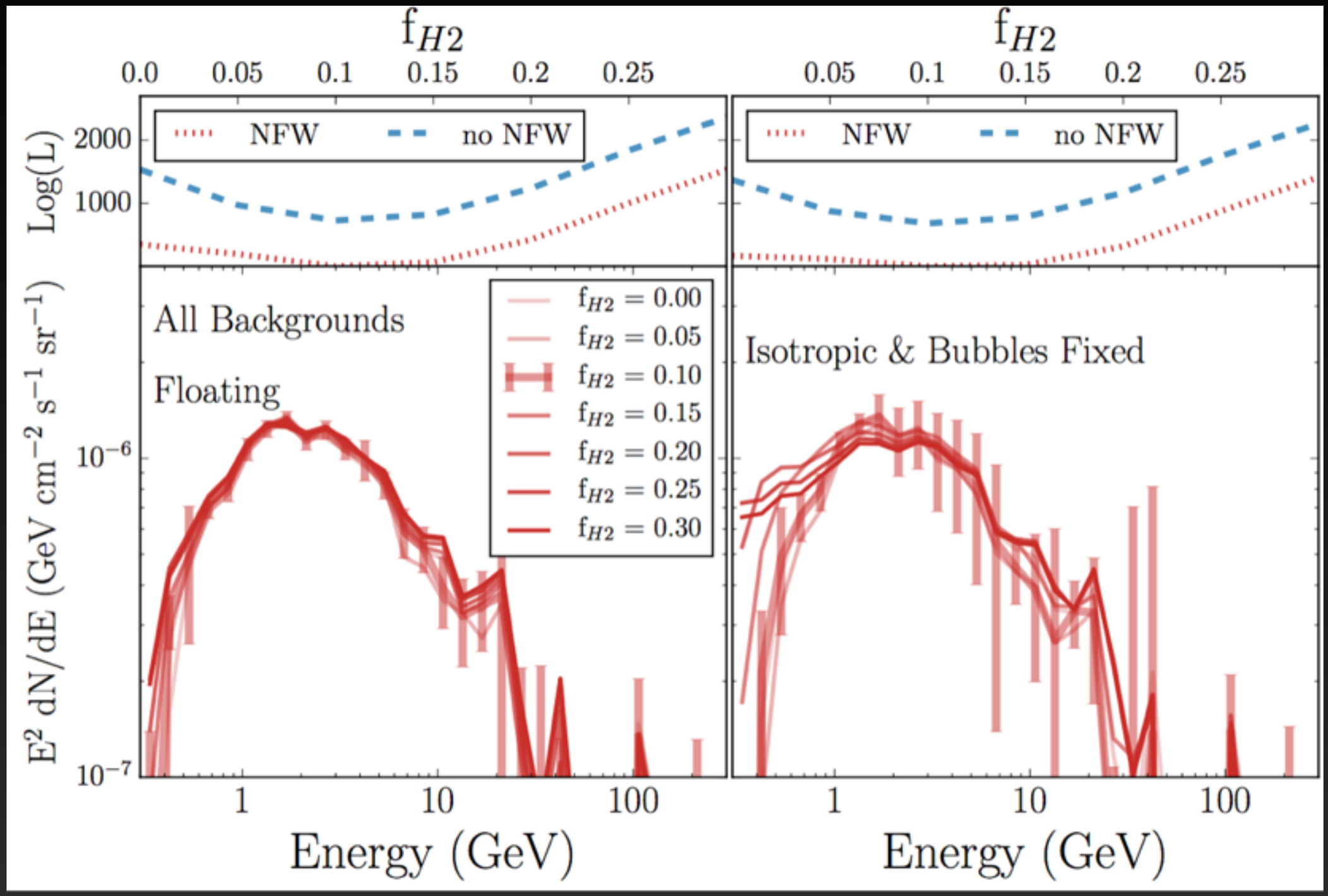

In this smaller region, the excess remains resilient to changes in diffuse emission modeling.

Galactic center excess is resilient....

IG

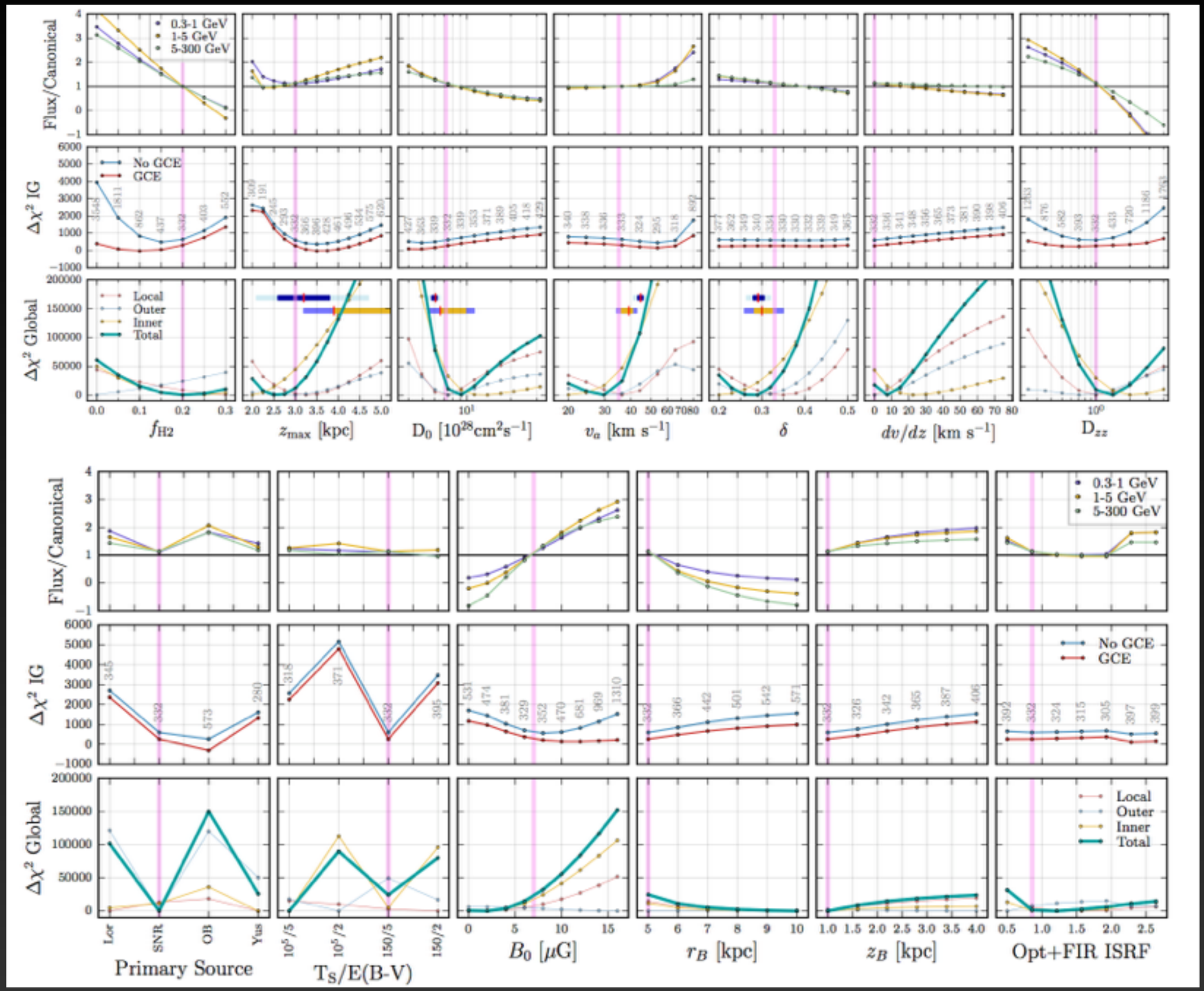

The Galactic Center Deficit?

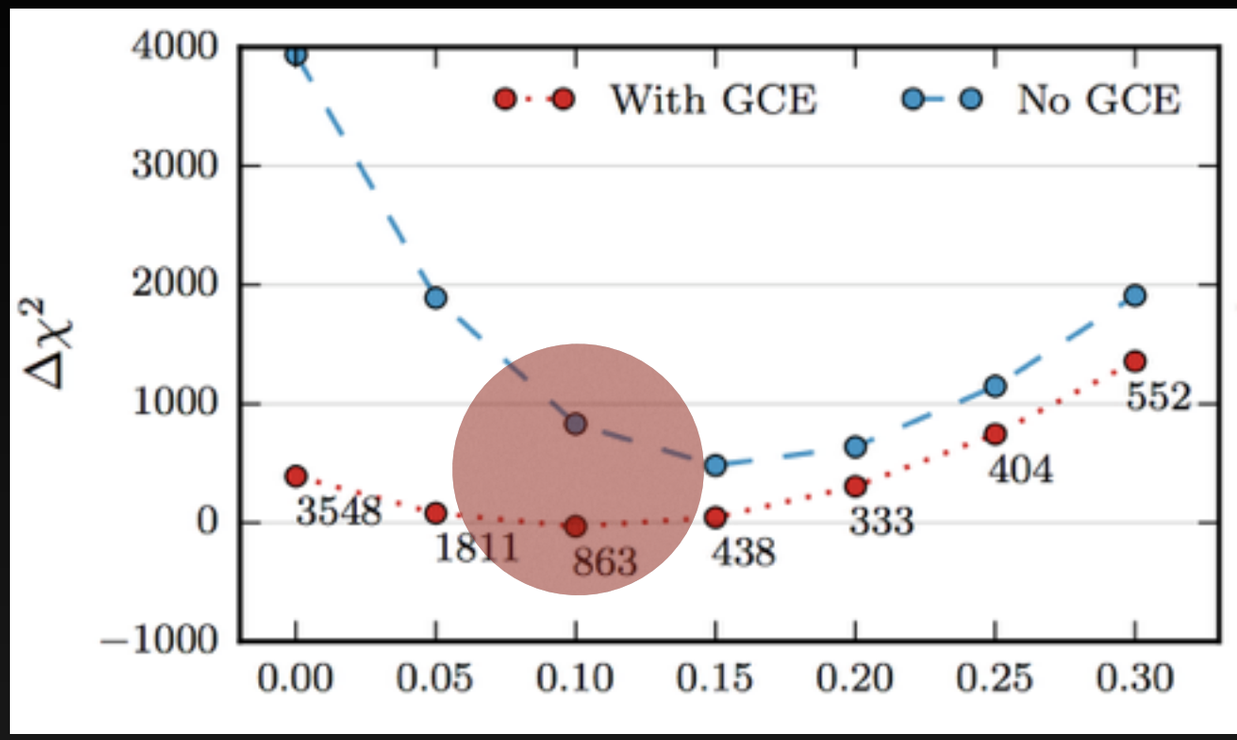

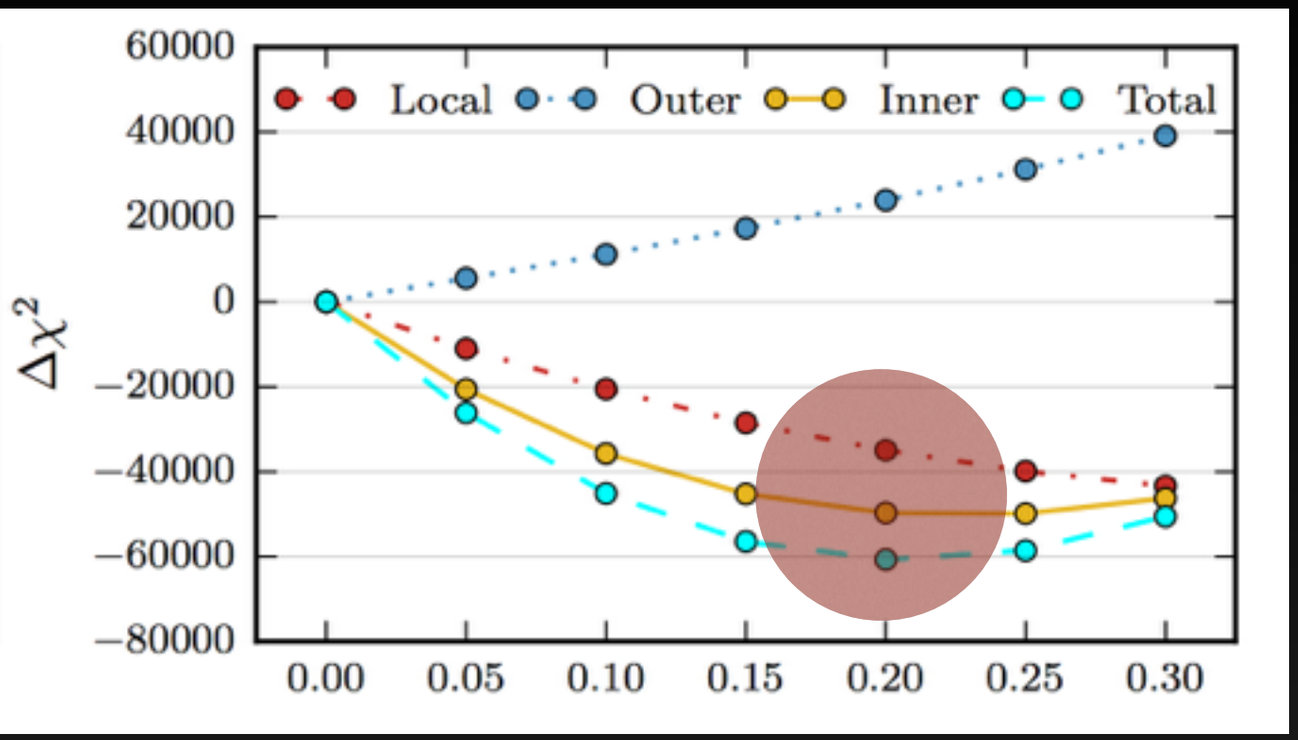

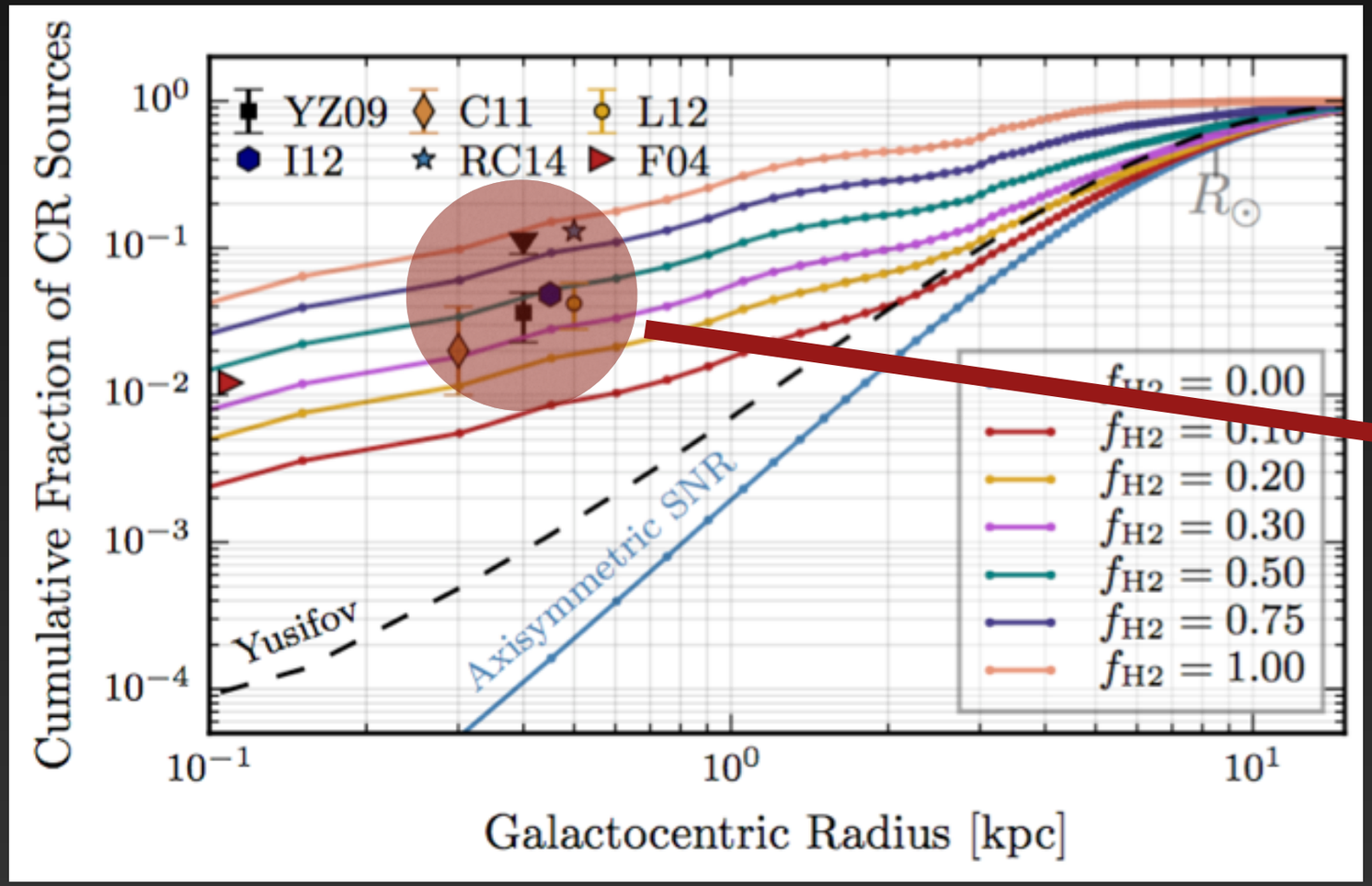

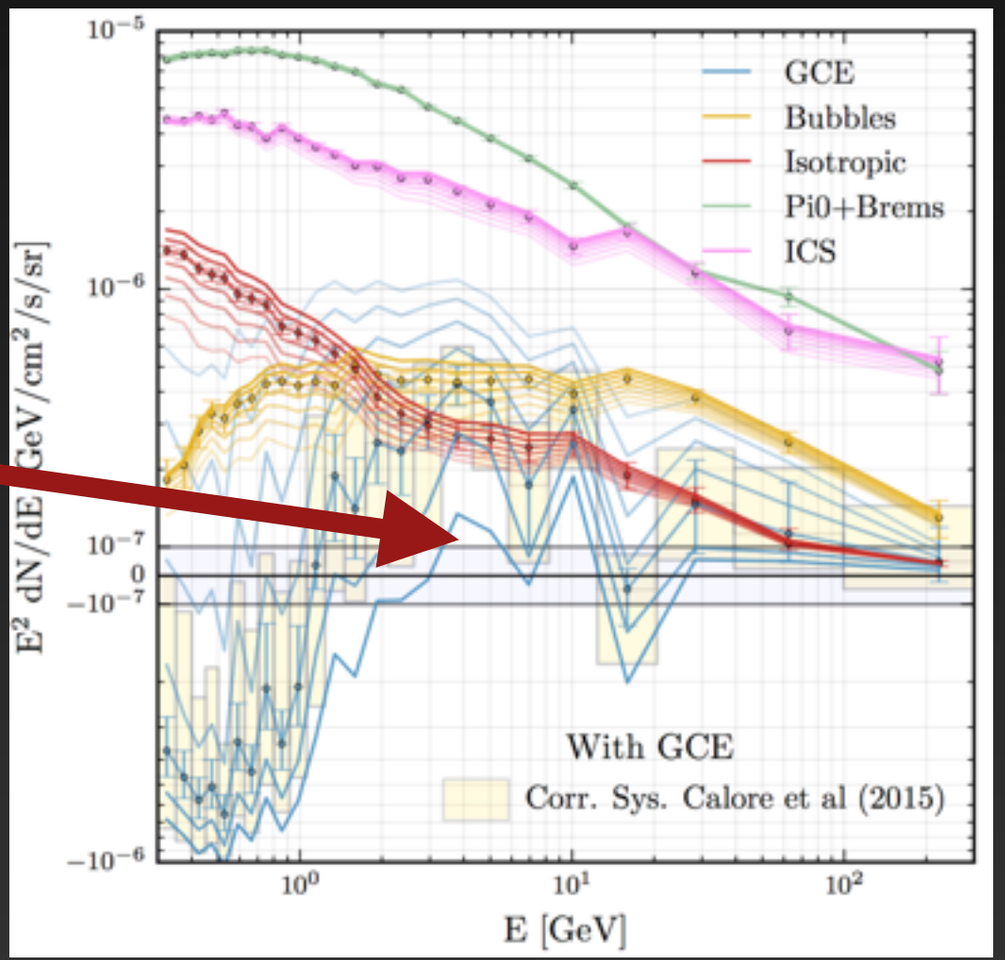

Advection and Convection in the Galactic Center

Crocker et al. (2011) demonstrated that the break in the GC synchrotron spectrum is best fit in the regime with:

a.) Large Magnetic Fields
b.) Large Convective Winds

Very different from typical Galprop diffusion scenario.

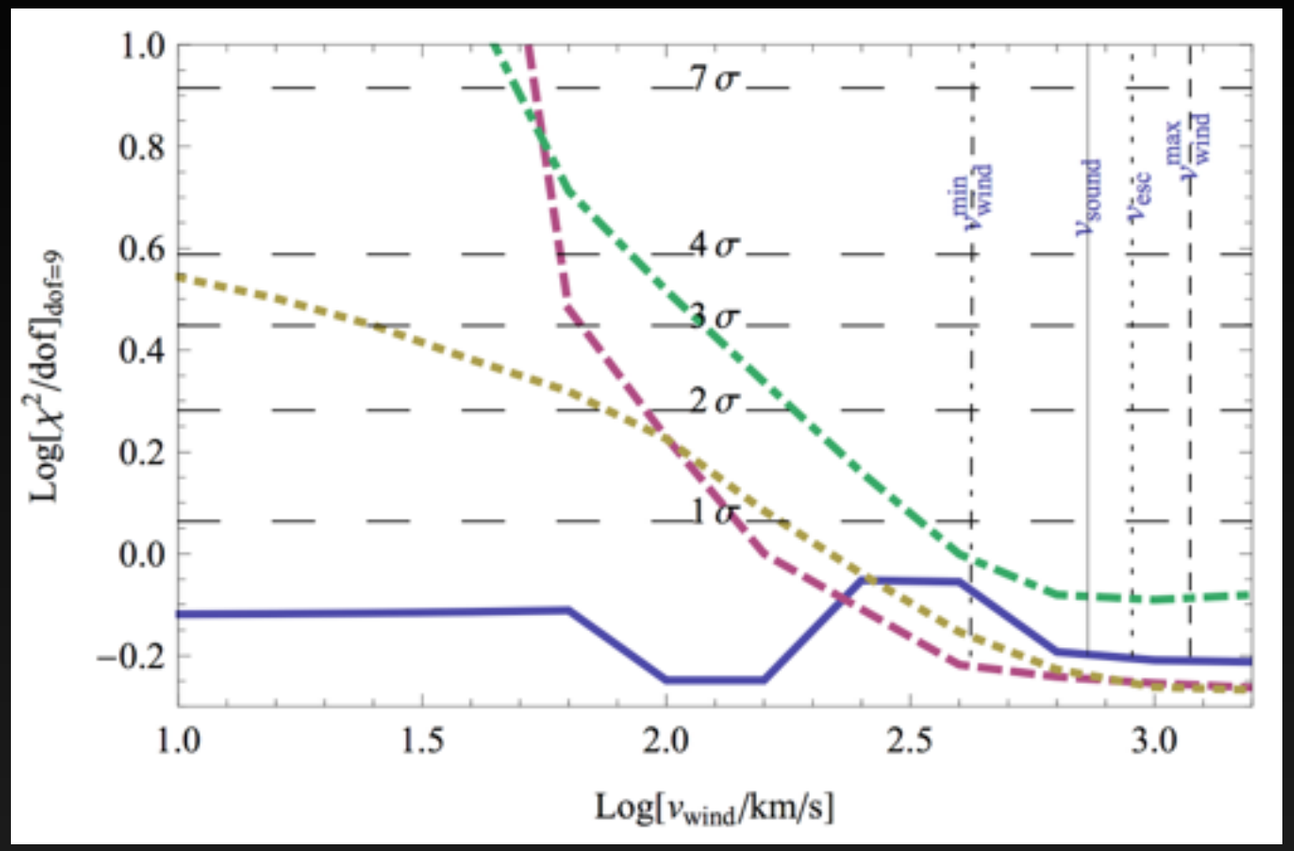

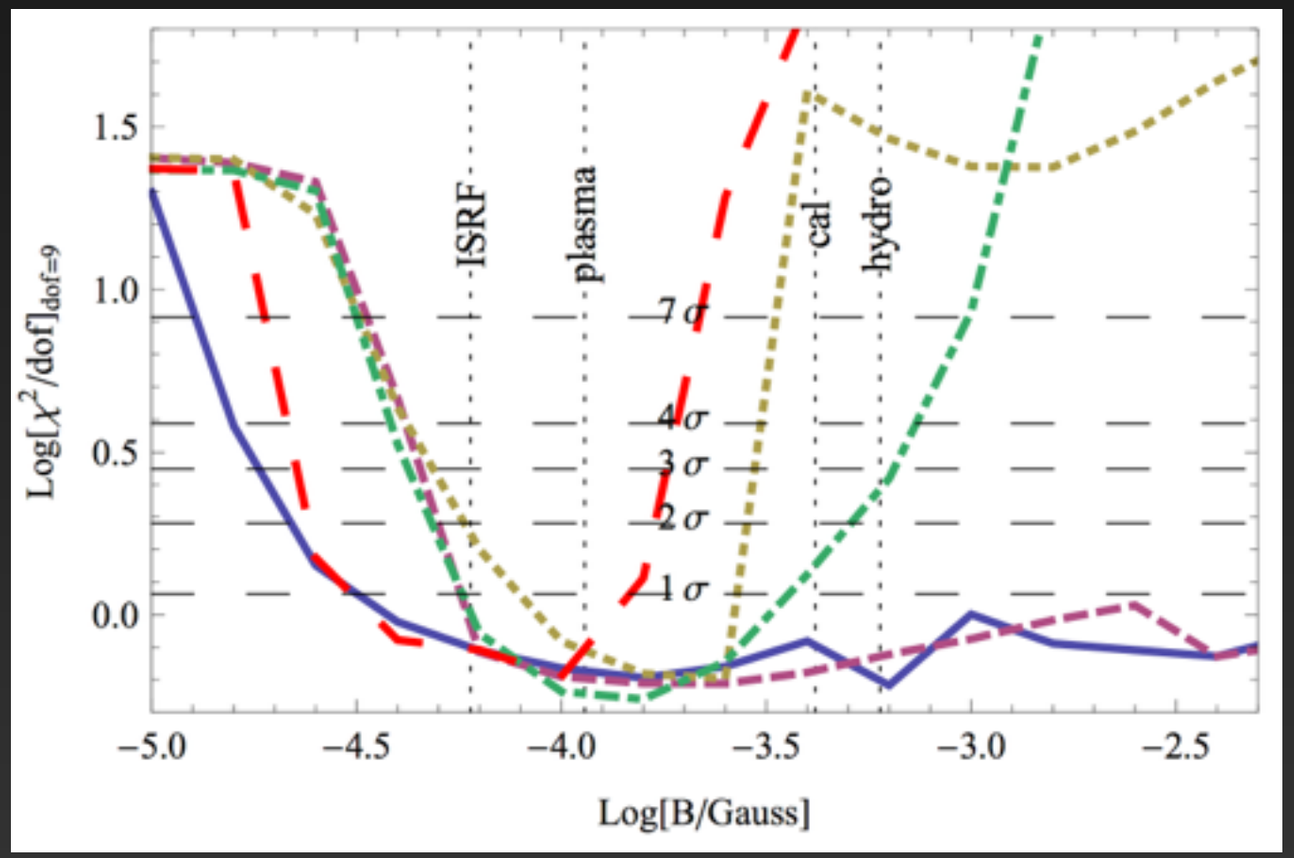

The Low Energy Spectrum

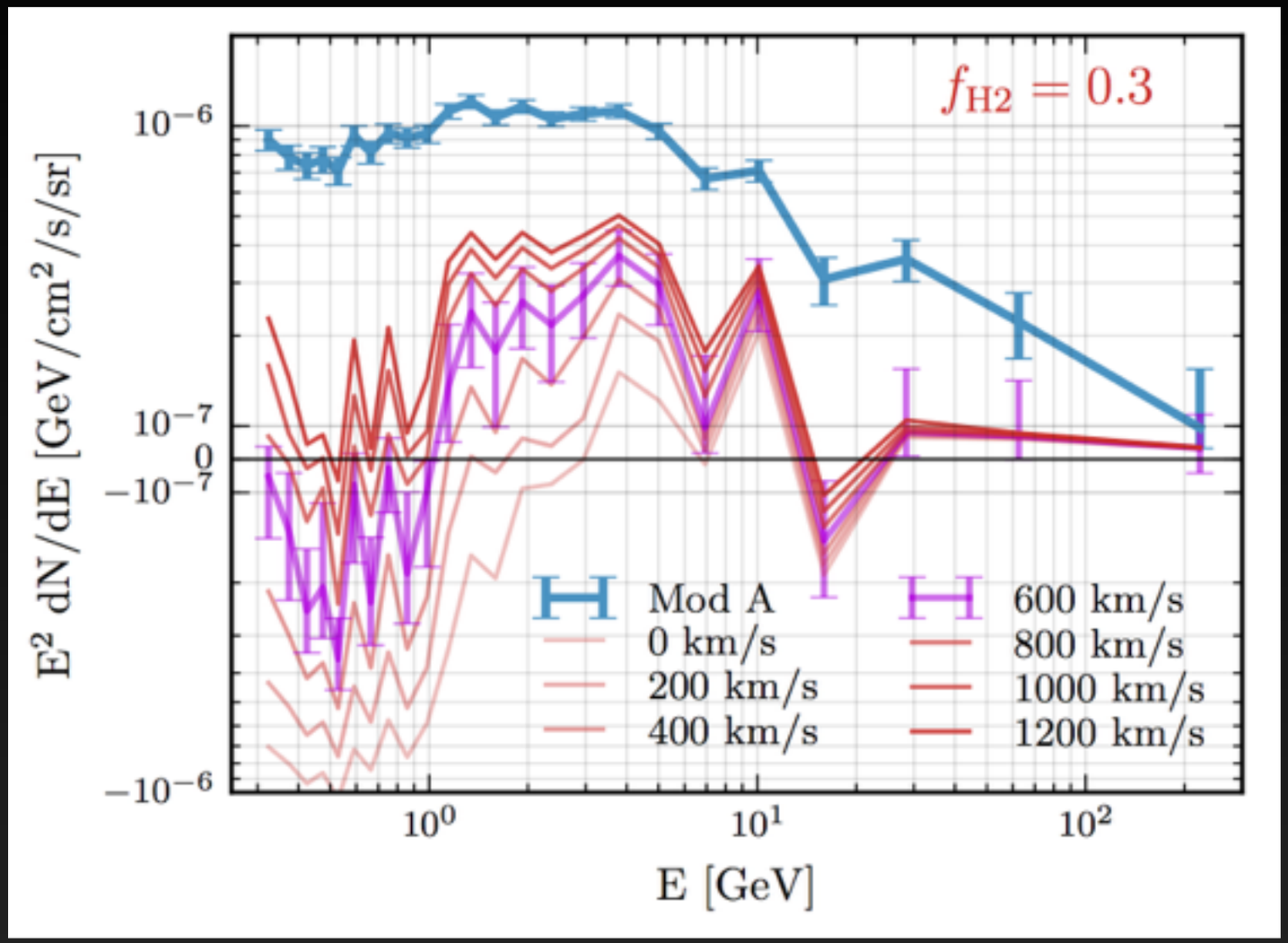

IG

Applying strong convective winds to the diffuse emission model fixes the low-energy over subtraction.

The intensity of the excess near the spectral peak also increases, up to ~50% of its nominal value.

The model produces a significantly better fit to the gamma-ray sky dataset - and also coincides better with multi wavelength data.

A Similar Result with Different Techniques

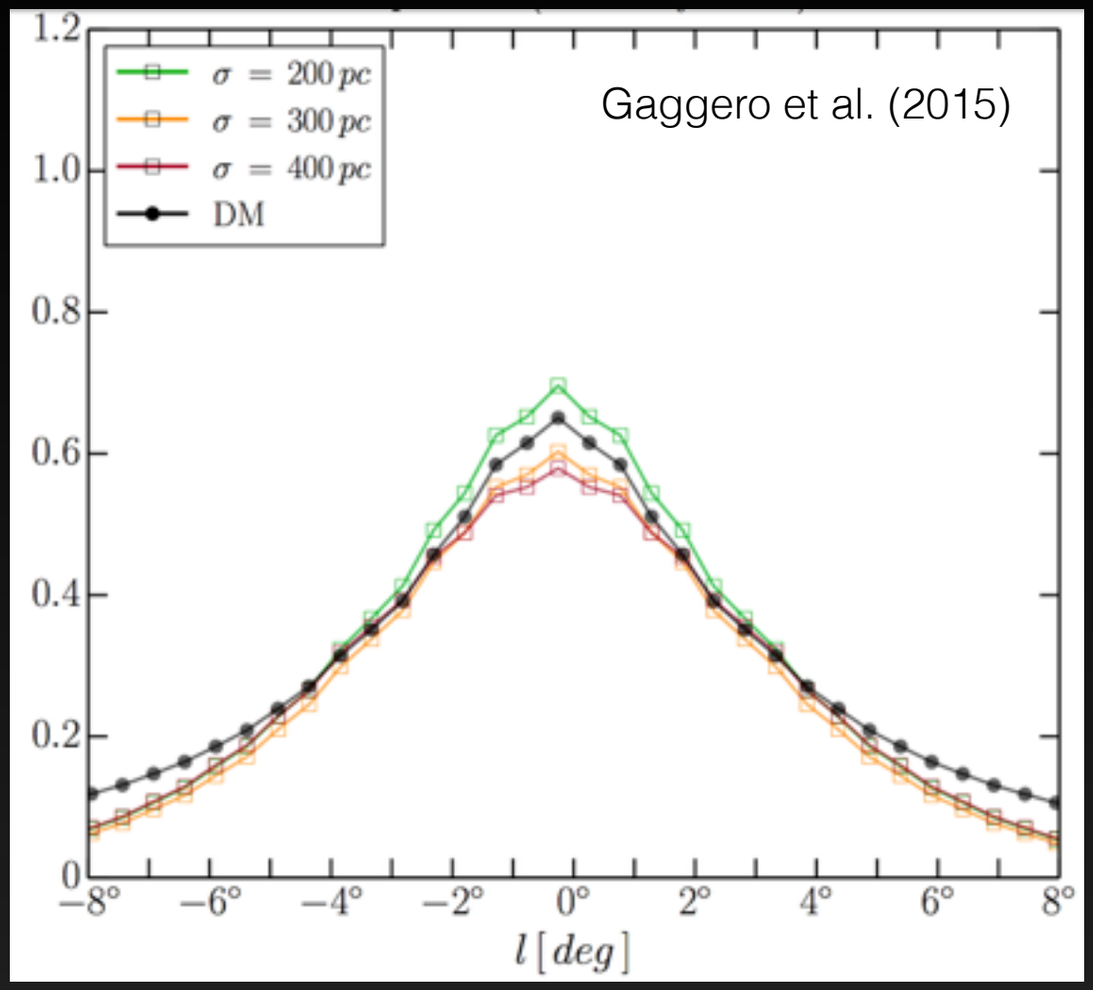

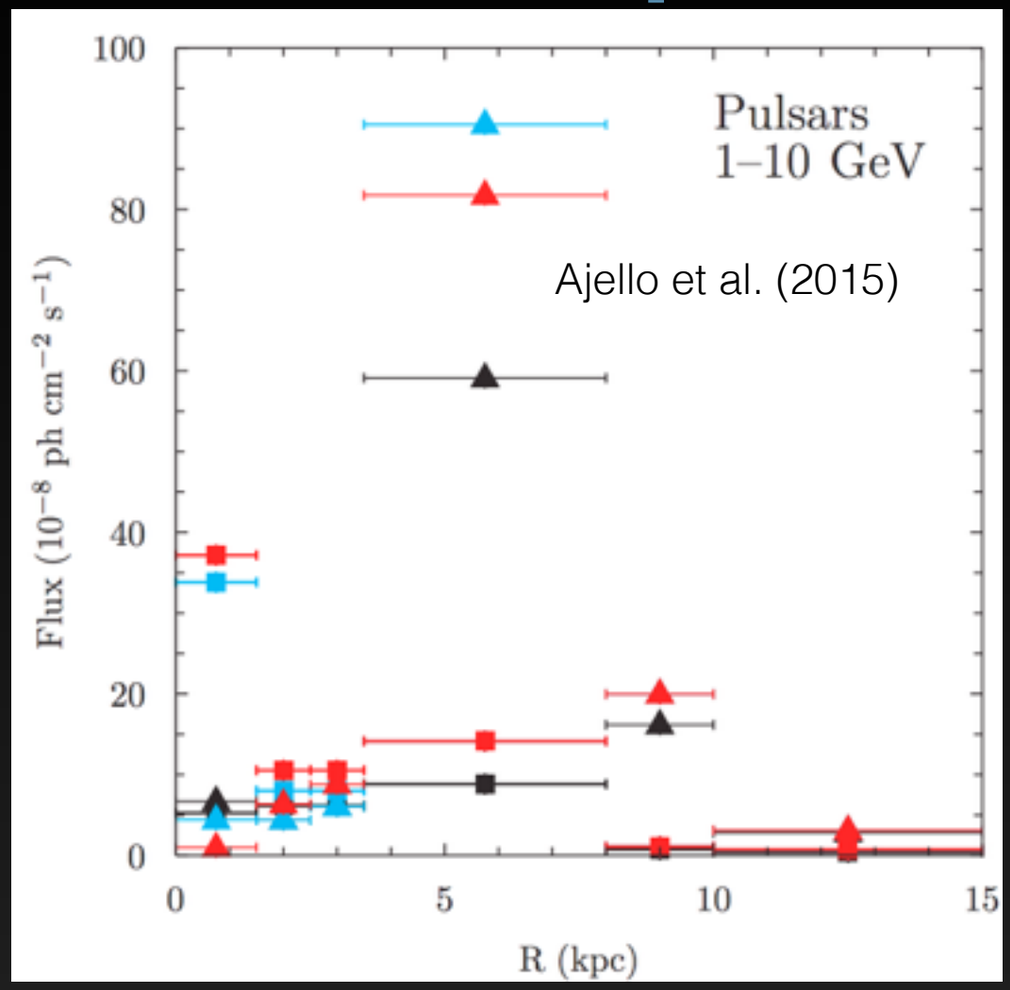

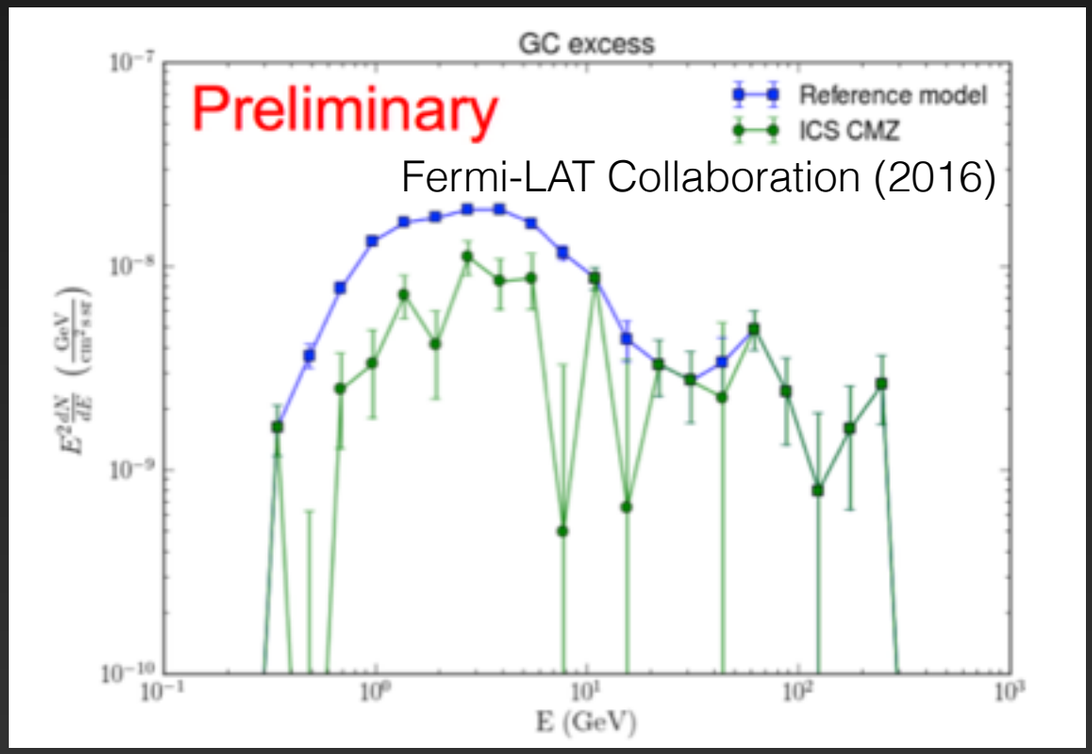

Leptonic Outbursts

The Galactic center is unlikely to be in steady state (e.g. Fermi bubbles).

An outburst of leptonic origin can produce the gamma-ray excess, but only if the injected electron spectrum is extremely hard (compared to observed blazar spectra).

Cholis et al. (2015, 1506.05119)

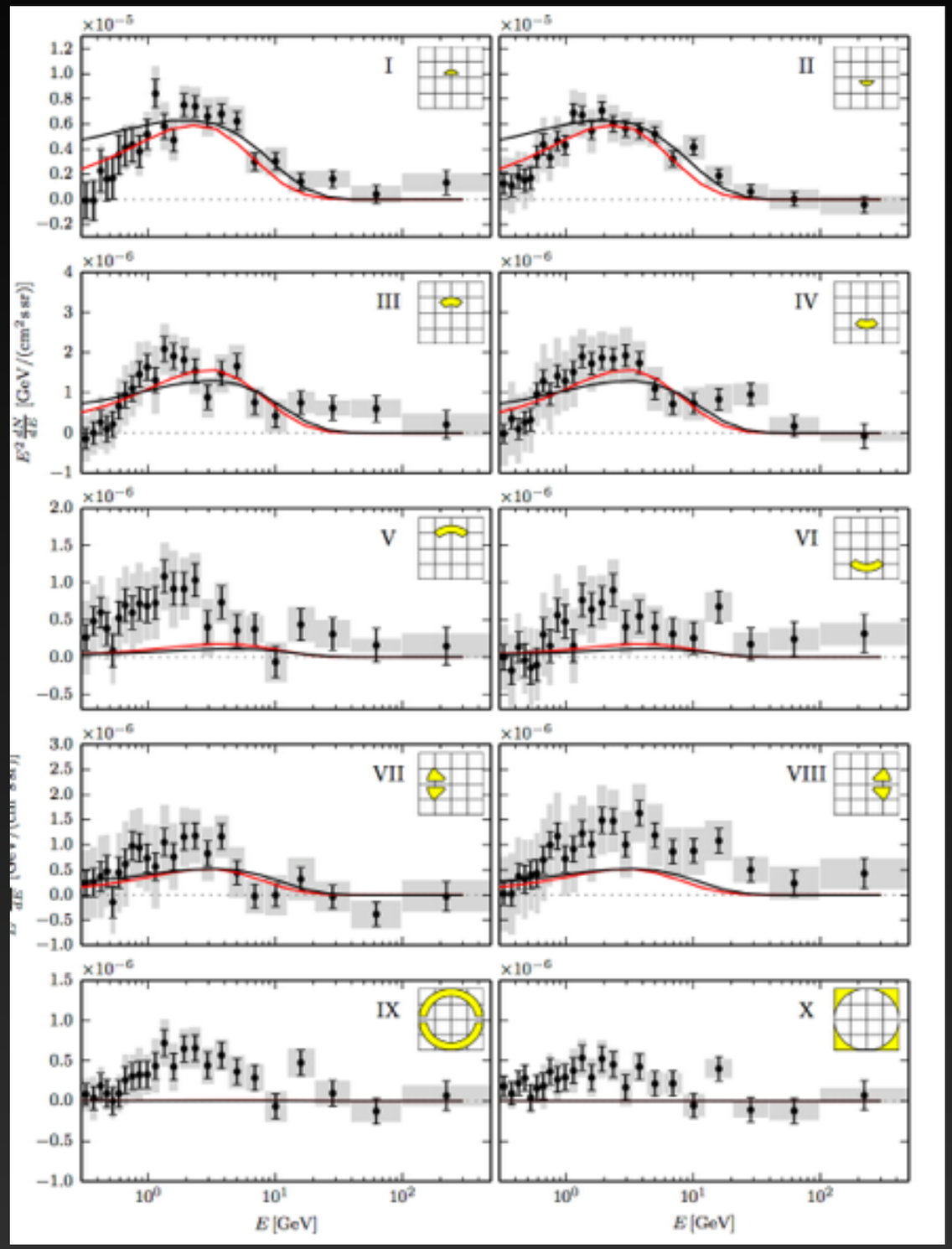

Petrovic et al. (2014, 1405.7928)
Cholis et al. (2015, 1506.05119)

IG

Upcoming Work

1.) Improved Models of Galactic Center Gas, especially within the CMZ.

2.) Joint analyses of the Fermi bubbles, WMAP Haze and GeV excess.

3.) Modeling the Gamma-Ray Accelerator at the Galactic Center.

The Sgr A* Source

Modeling The Galactic Center Point Source can give us direct information about the diffusion environment of the Galactic center.

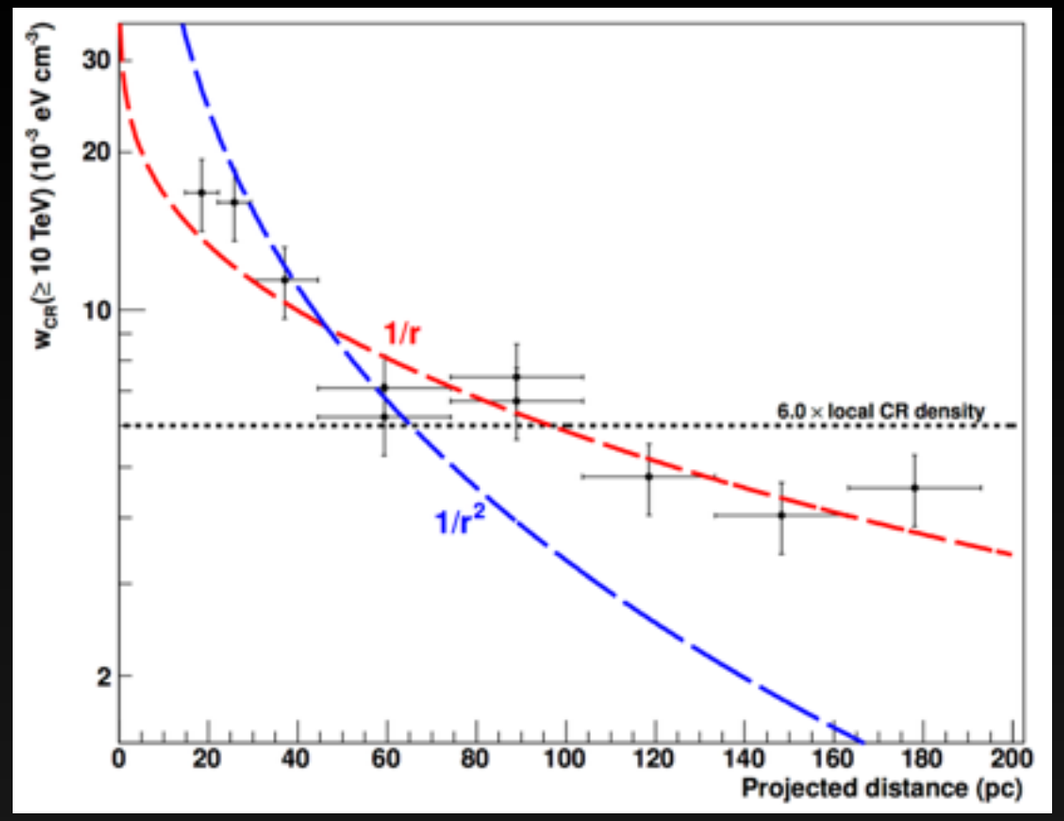

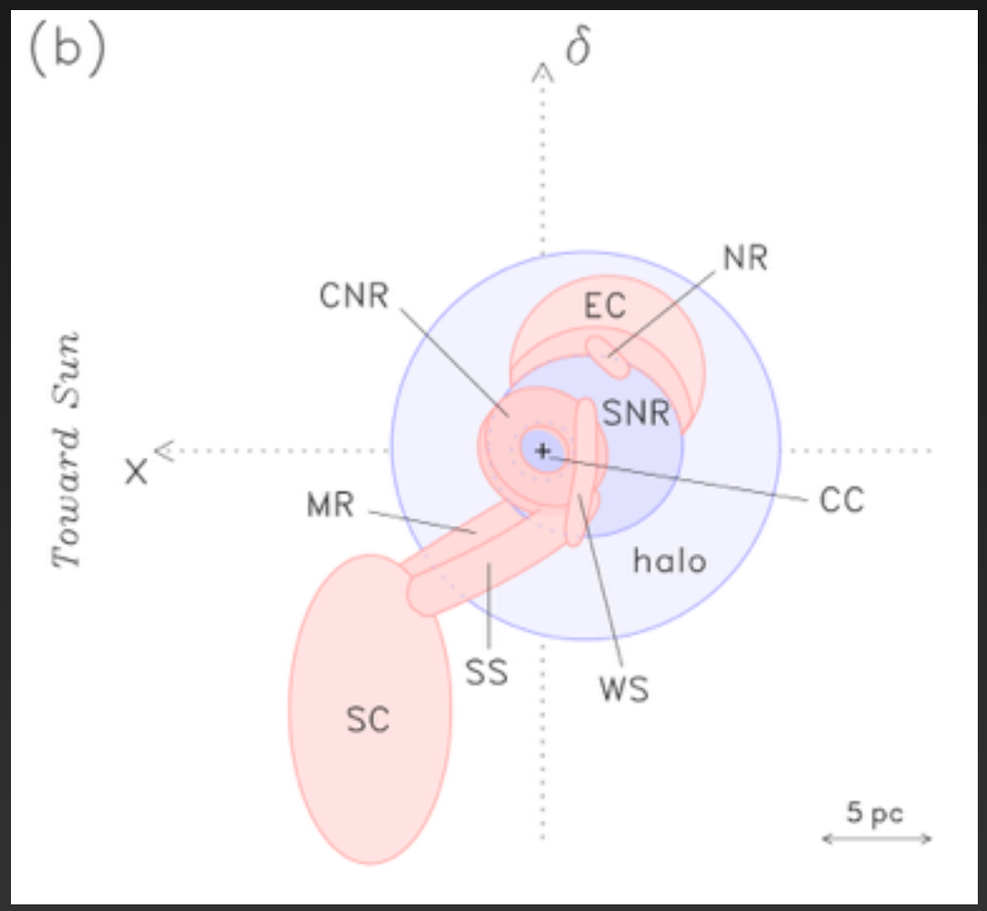

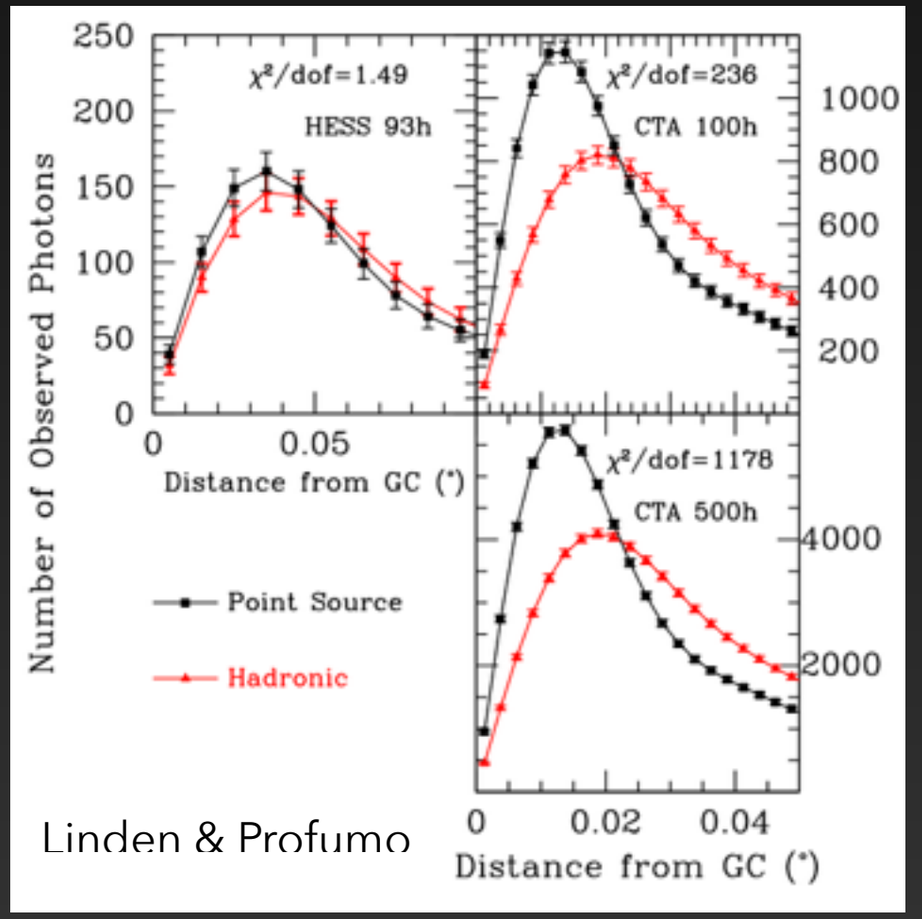

Waxing Philosophical.....

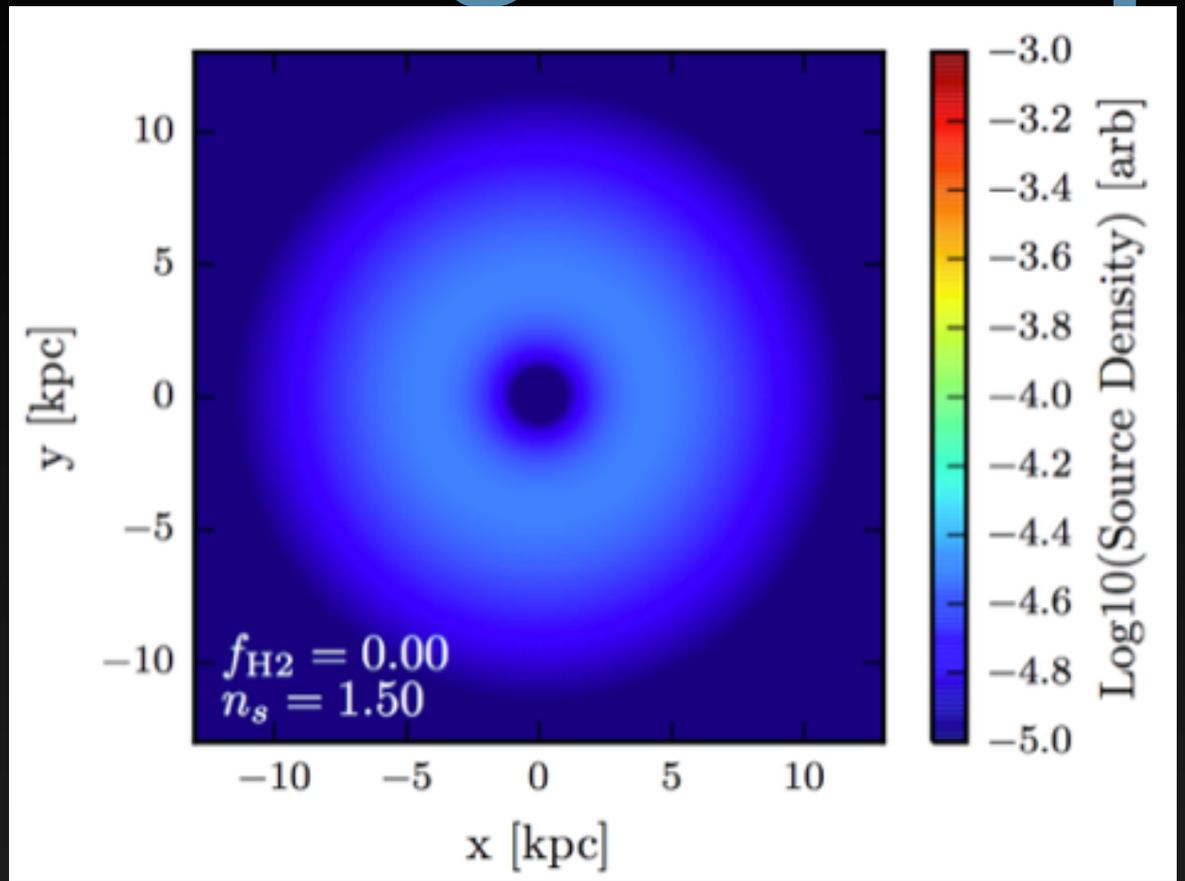

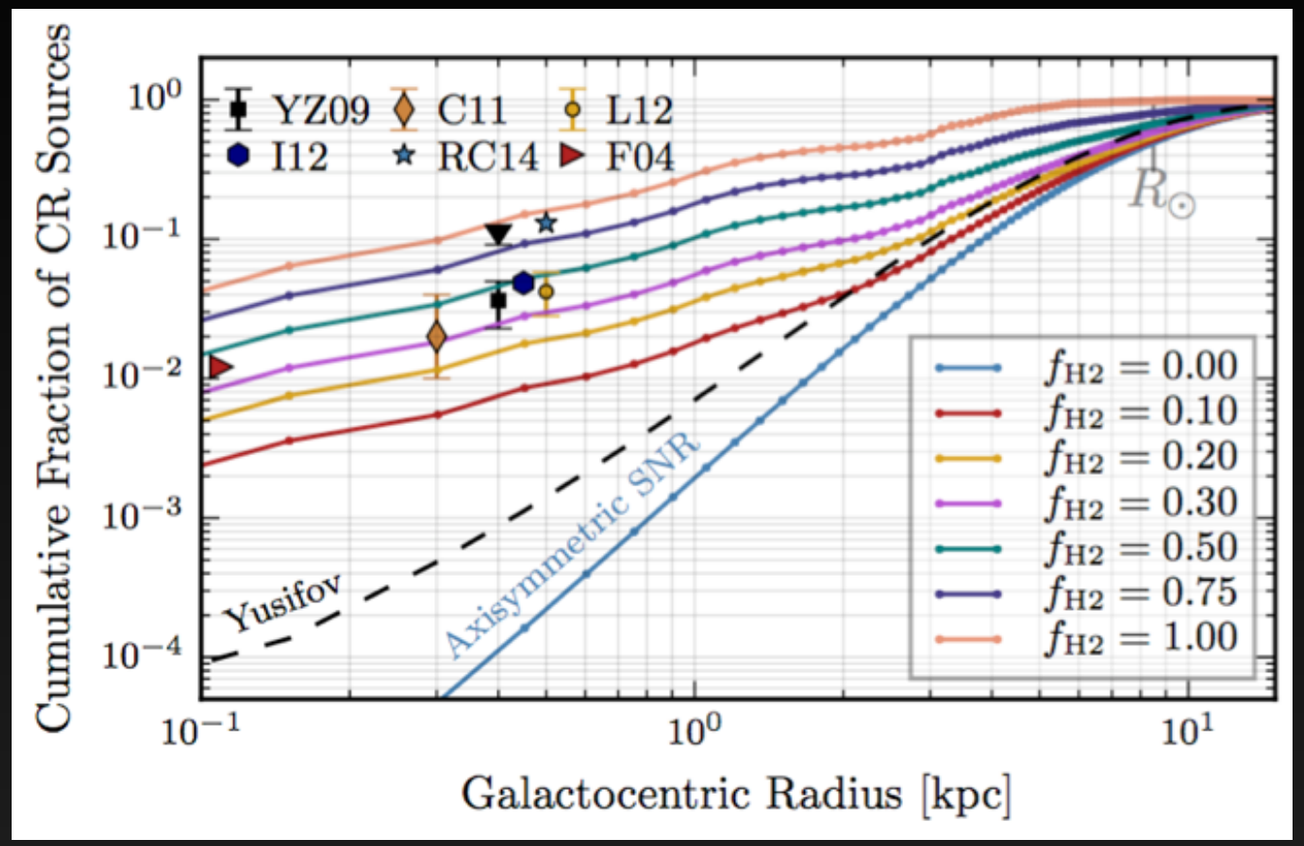

The lack of cosmic-ray injection in the GC should still be slightly disturbing. Especially when we try to answer the question: "excess compared to what?"

Our models indicate a degeneracy between cosmic-ray injection and the existence of a Galactic center excess template tracing an NFW profile. However, at present the best fit models still include a significant NFW component.

Not a Conclusion Yet...

1.) The Galactic Center is a complex, but exciting environment. Several significant excesses are tied to the dynamics of the Galactic center environment.

2.) The GeV excess is a robust component of the Galactic center emission profile. At present, no models have successfully eliminated the excess.

3.) Improving our diffuse emission modeling is imperative to understanding the properties of the excess.

Stay Tuned!

Extra Slides

Effect on the Excess Spectrum

IG

Changing the morphology of the excess has a significant effect on the spectrum of the gamma-ray excess.

The spectrum becomes extremely hard as f_{H2} is increased, most likely indicating that the GCE template is picking up mismodeling of some residual.

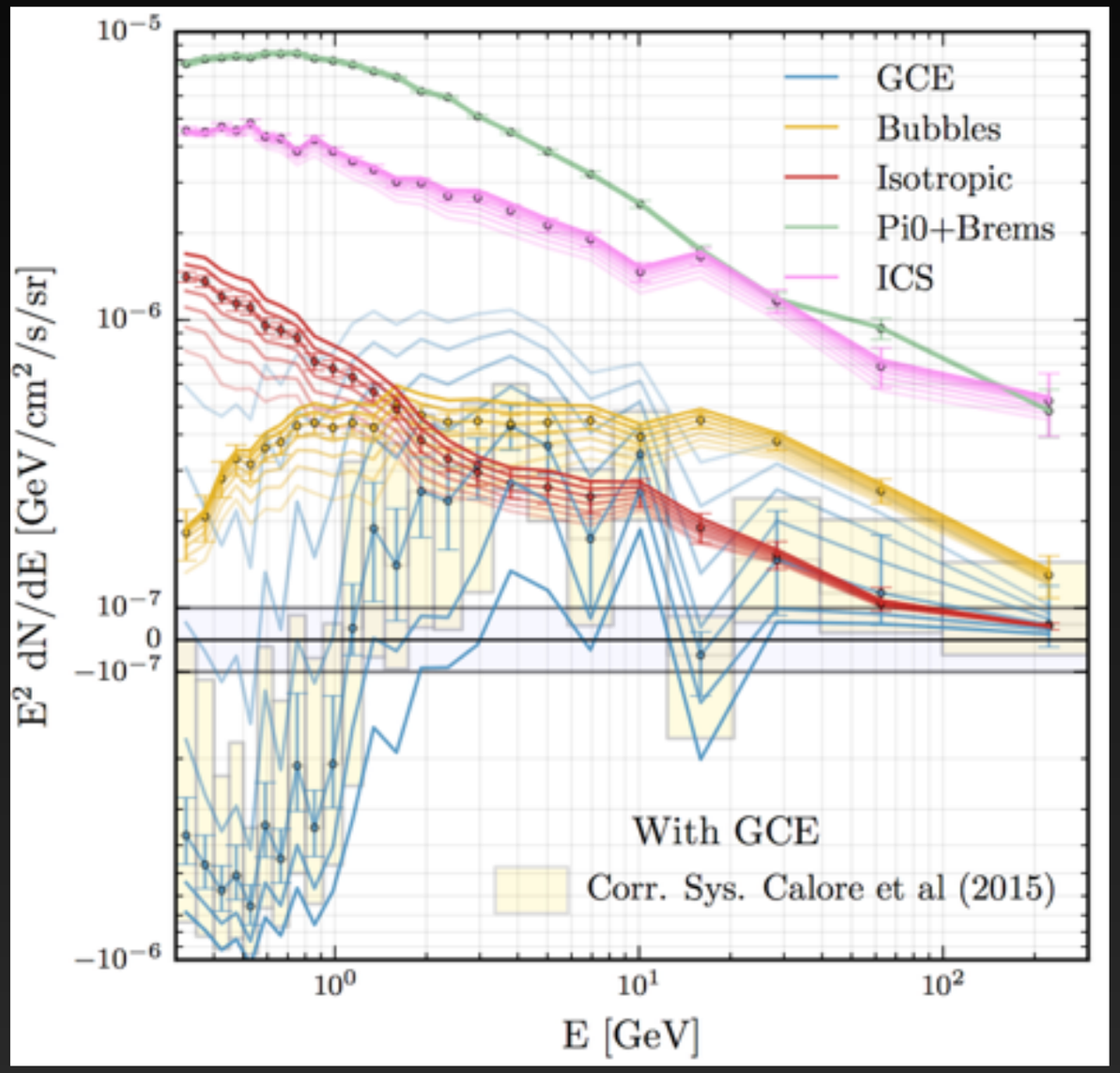

Dark Matter Annihilation?

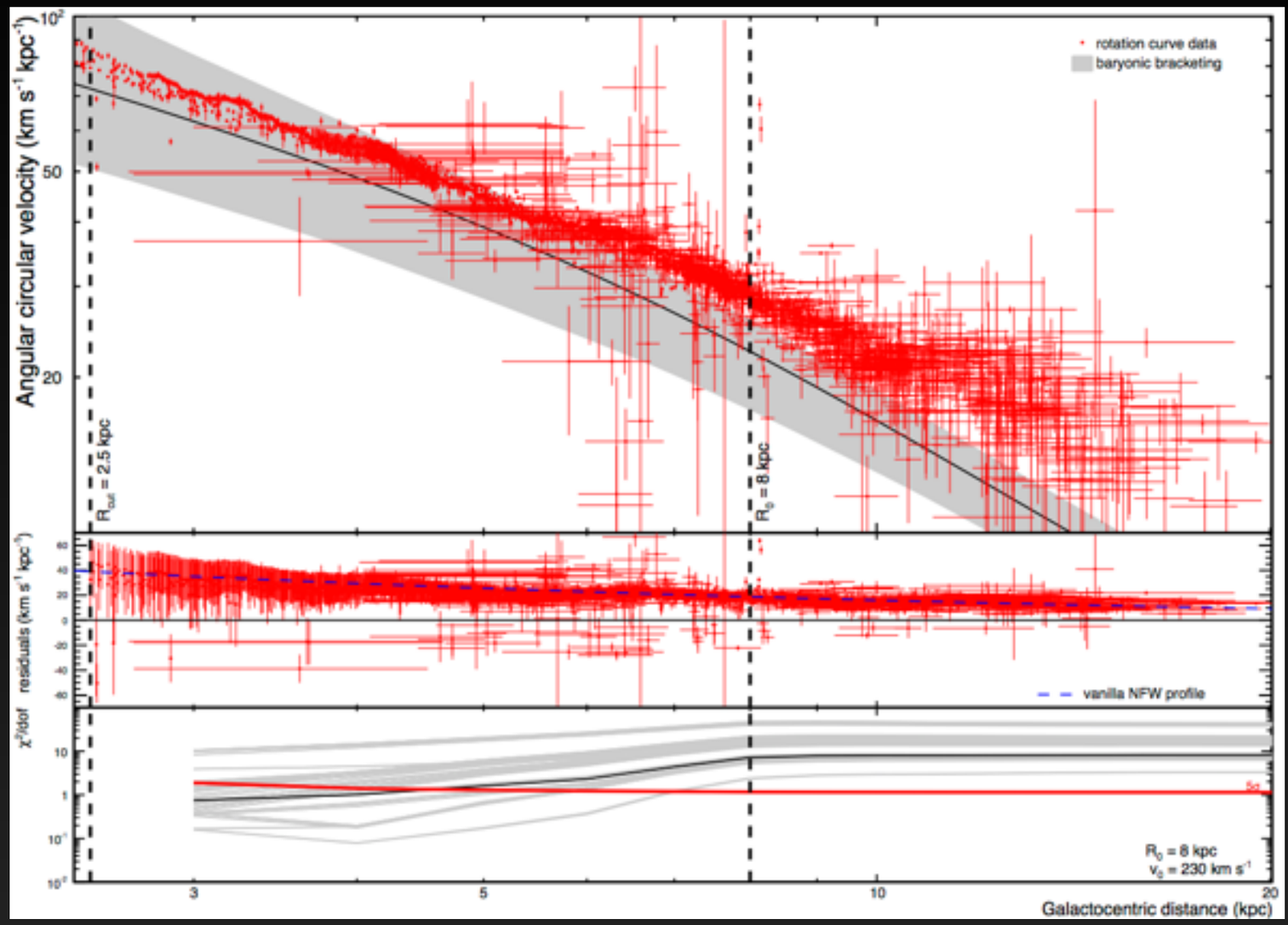

Recently, observations by Iocco, Pato & Bertone (2015) have used stellar velocity measurements to directly measure the dark matter density in the Milky Way (to within 3 kpc of the GC).

Future measurements (employing Gaia data) will have the ability to significantly improve these measurements.

Iocco, Pato & Bertone (2015)

Masking 1FIG Sources in the GC

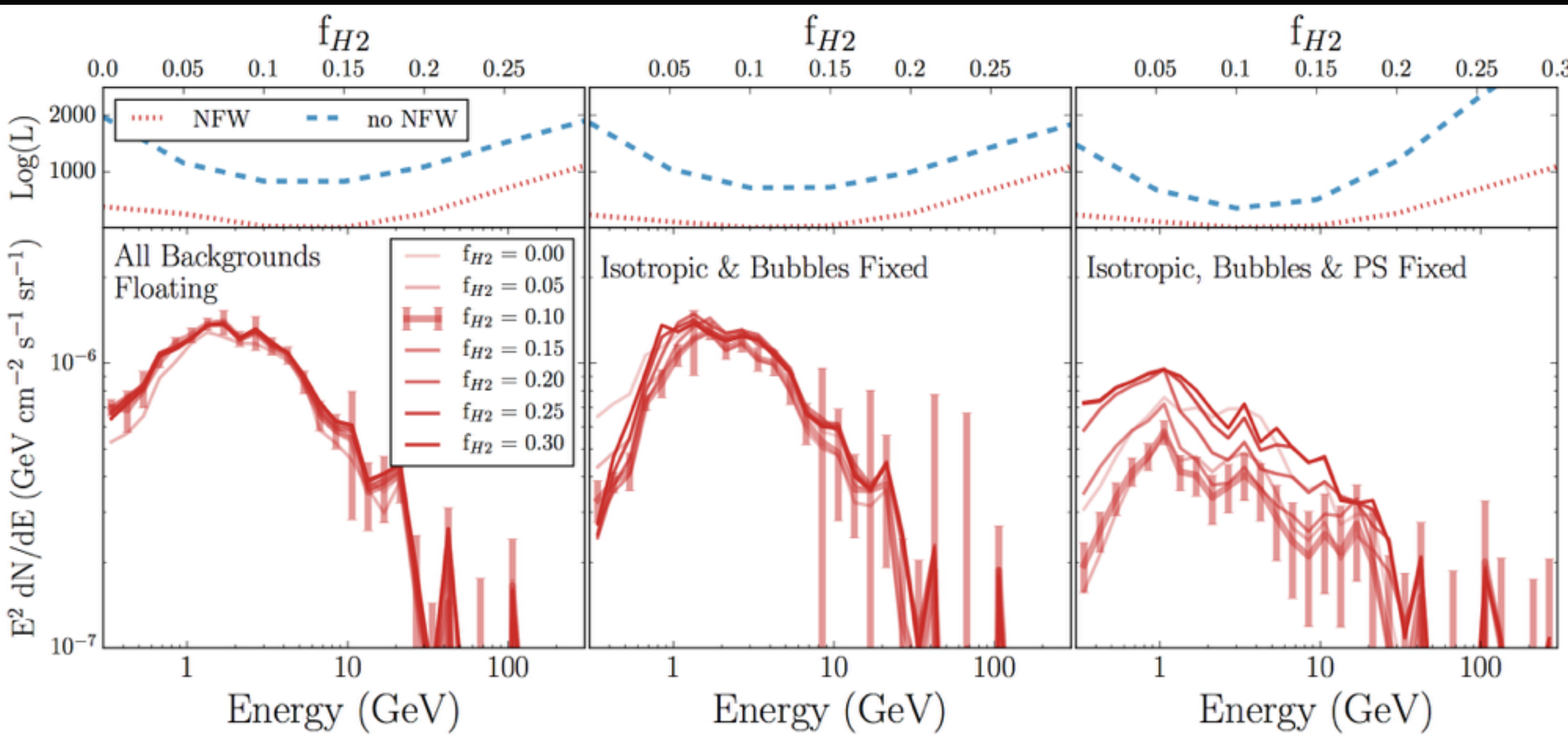

Changing the point source catalog from the 3FGL to the 1FIG has only a negligible effect on the gamma-ray excess.

The Effect on the Galactic center Excess (masking |b| < 2º)

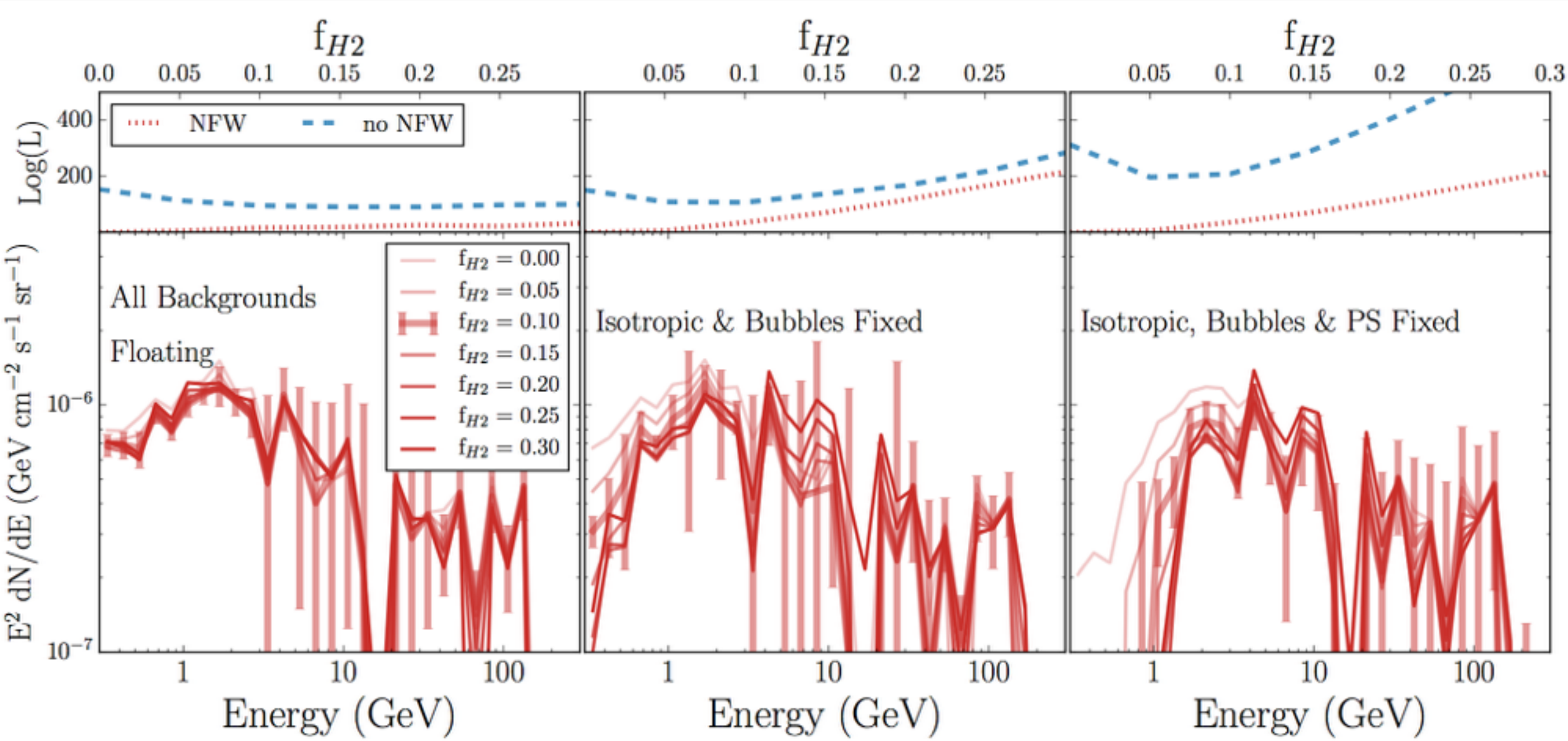

Intriguingly, this persists even when the inner 2º are masked - implying that analyses of small ROIs favors the excess.

The Low Energy Spectrum

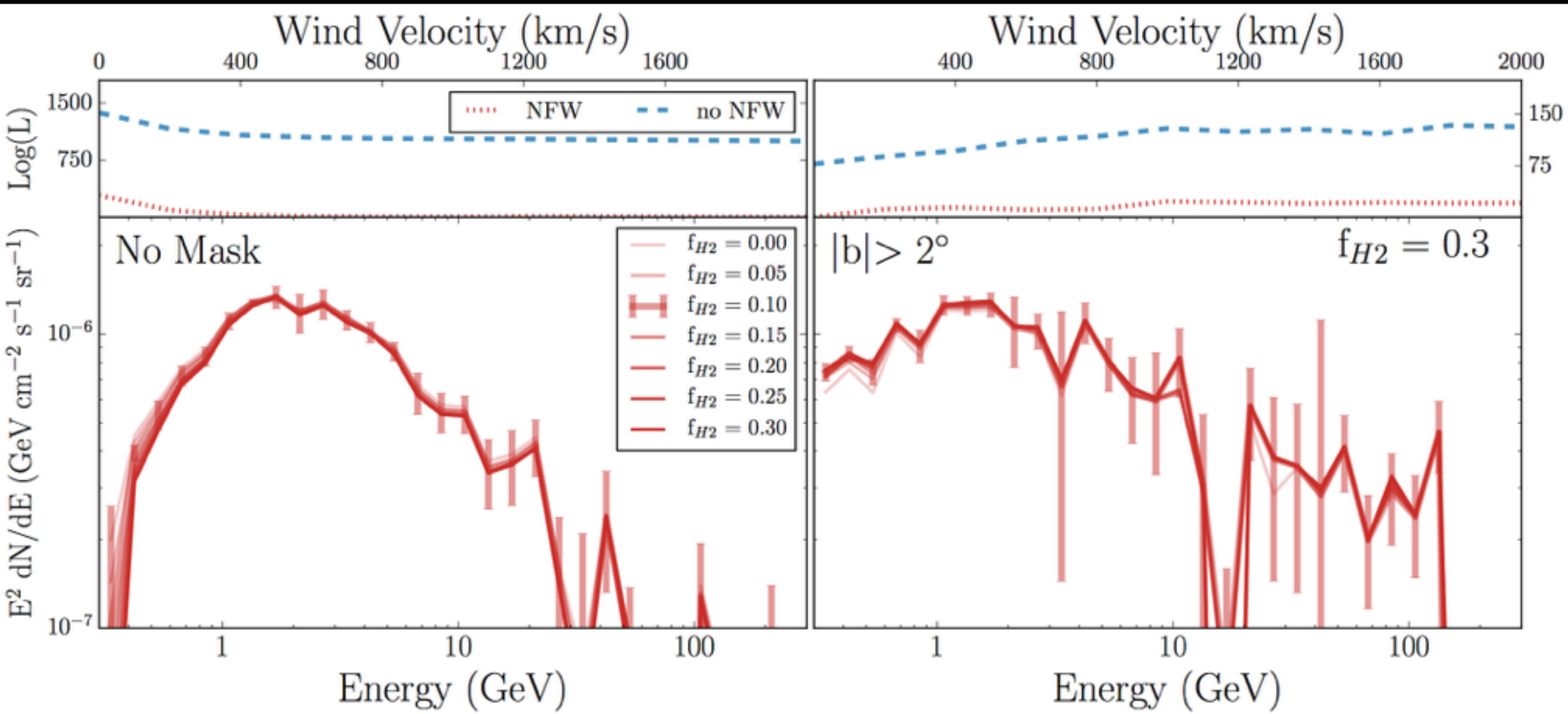

The Galactic Center models contain only a small preference for the convective winds, and the spectrum and intensity of the Galactic center excess component remains resilient.

Convection in the Galactic Center

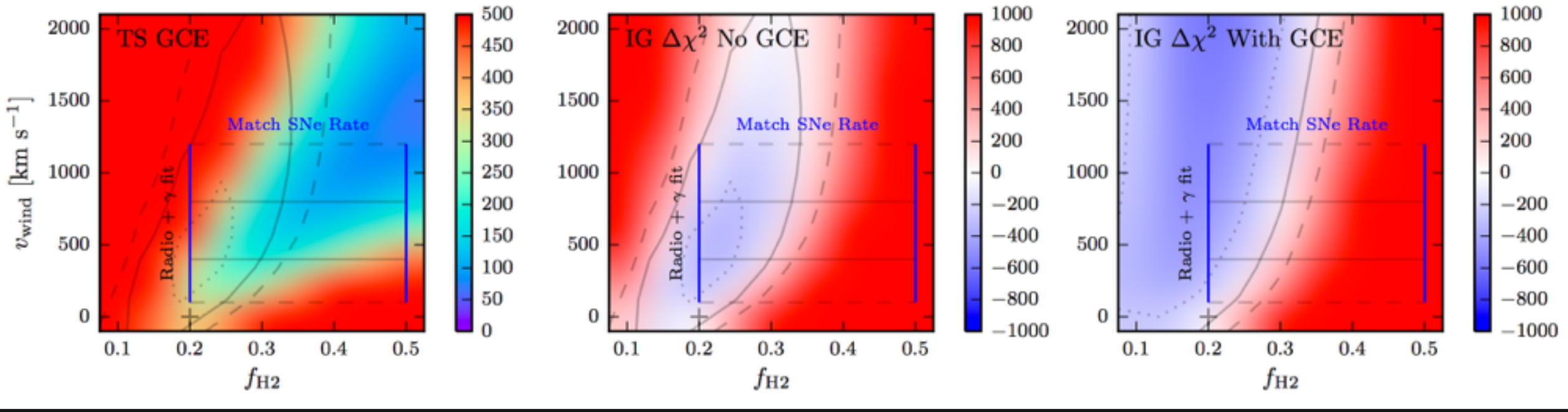

This increases the best fit value of f_{H2} for the GC data, bringing this value into agreement with the global best fit value.

Models with a GCE component still prefer slightly lower values of f_{H2}, but these have increased to 0.2 as well.

The Galactic Center Excess Morphology (masking |b| < 2º)

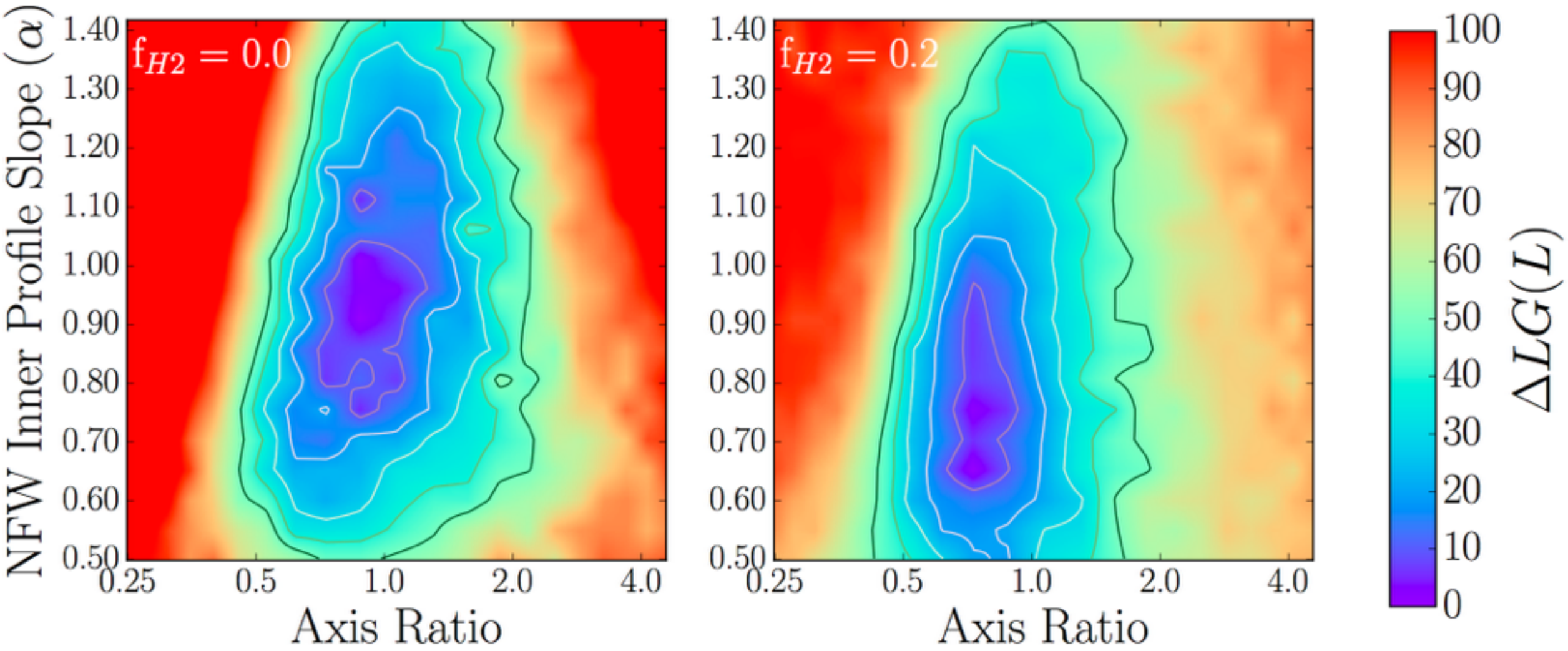

The deviations from typical NFW profiles are more extreme when the |b| < 2º is masked from the analysis, with a shallower emission profile preferred by the data.

Morphology in the Galactic Center

GC

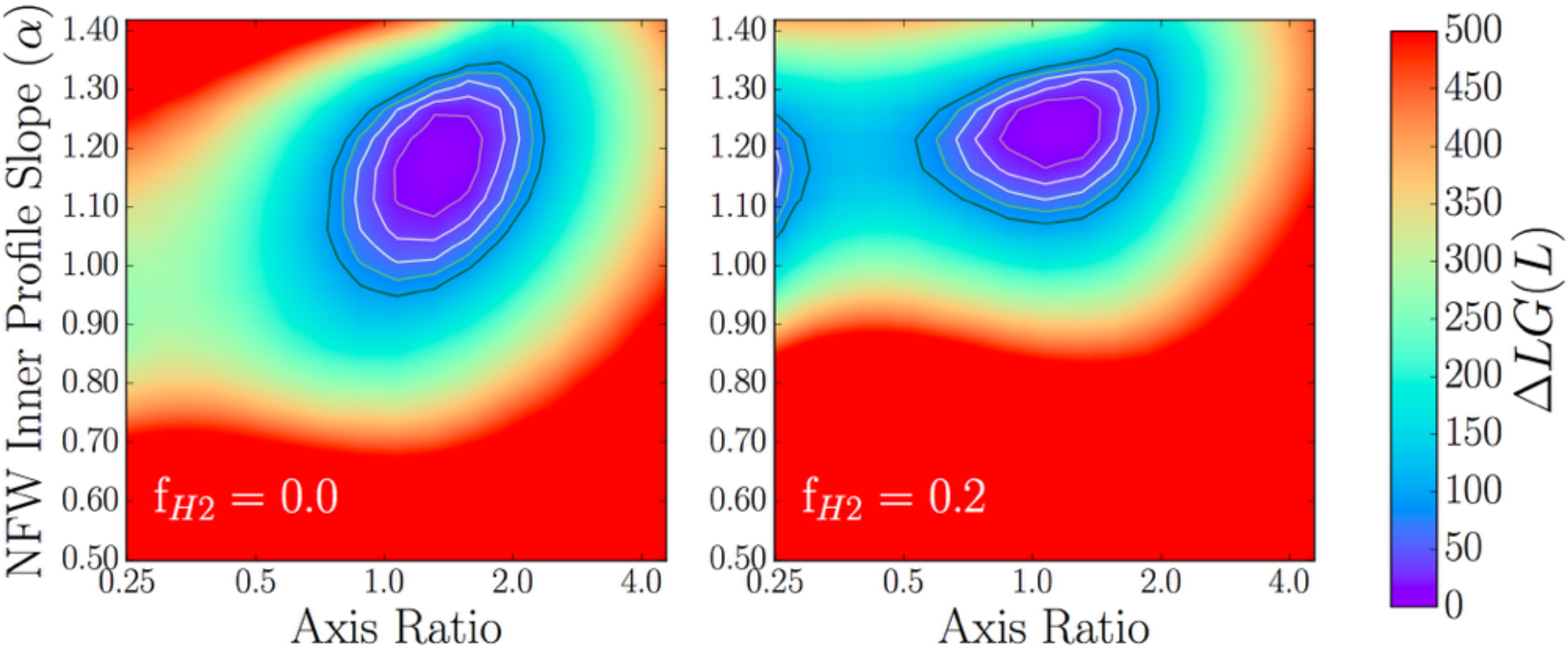

For the Galactic Center analysis, the morphology of the excess component remains relatively robust

Analysis Far from the GC

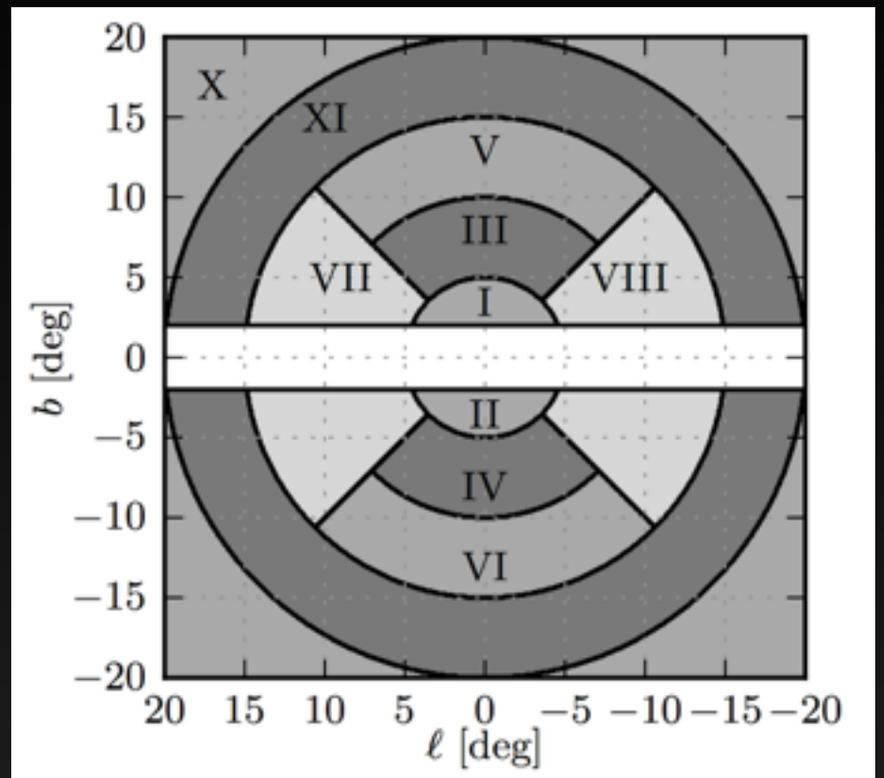

Analysis regions far from the GC also show an excess – not much star formation occurs a few degrees above the Galactic plane.

Calore et al. (2014, 1409.0042)

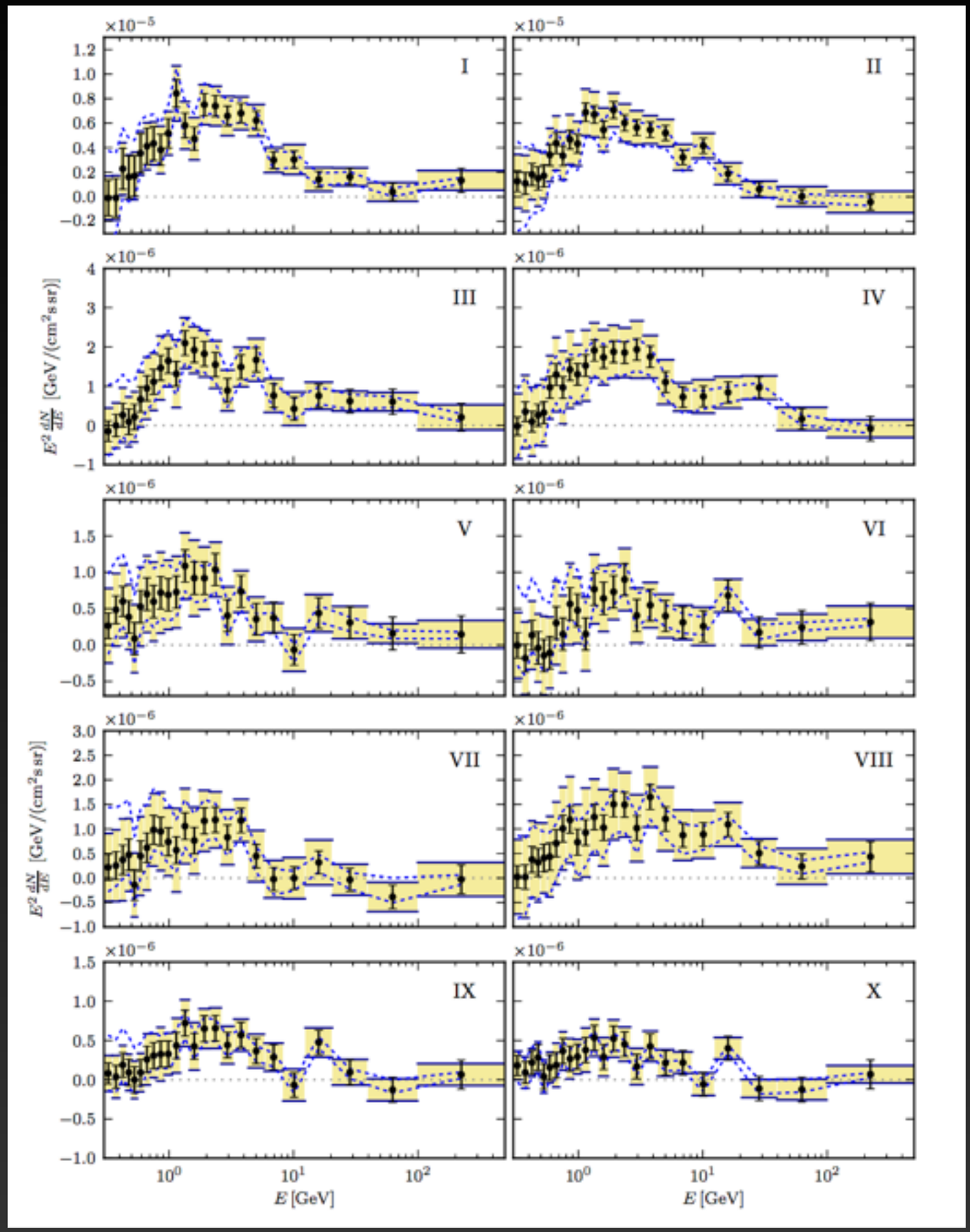

Comparison to Cygnus-X

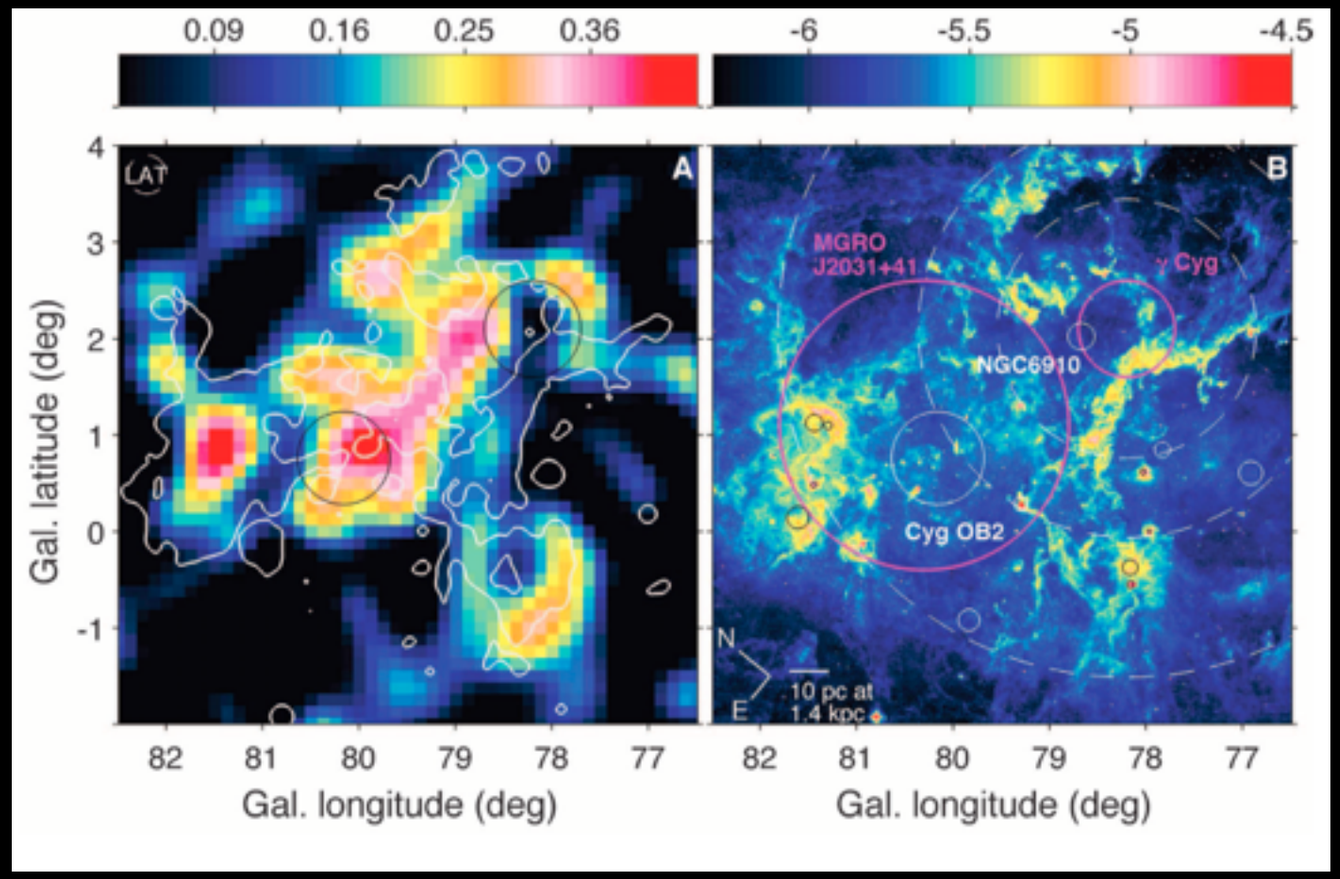

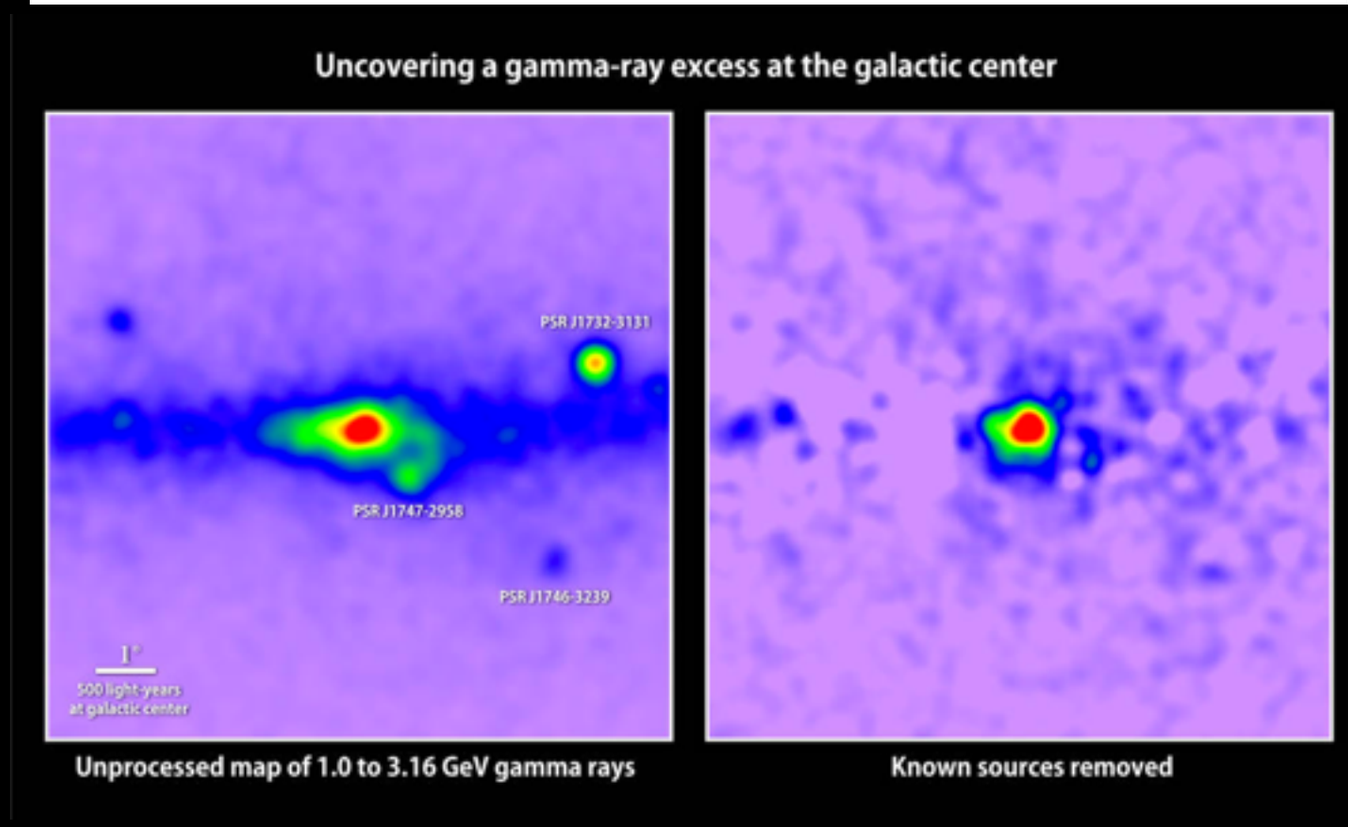

A Fermi-LAT Based Example

Total Gamma-Ray Flux (>1 GeV) in inner 1° is 1.1×10^{-9} erg cm^2 s^{-1}

Approximately half of this emission is produced along the line of sight towards the GC, and thus we approximate the total gamma-ray luminosity of the central one degree to be 5×10^{36} erg s^{-1}

Reacceleration

A 100 $M_\odot$ molecular cloud with a gas density of 200 cm^{-3} in a 10 μG B-field supports a Kinetic Energy transfer (via magnetic turbulence) of 5.0×10^{32} erg s^{-1}.

Given a total molecular cloud mass of 10^7 $M_\odot$, the total reacceleration of cosmic-ray electrons is 5.0×10^{37} erg s^{-1}.

If these electrons are trapped until losing their energy to bremsstrahlung and synchrotron emission with a standard spectrum):

A Fermi-LAT Based Example

Total Gamma-Ray Flux (>1 GeV) in inner 1° is 1.1×10^{-9} erg cm^2 s^{-1}

Approximately half of this emission is produced along the line of sight towards the GC, and thus we approximate the total gamma-ray luminosity of the central one degree to be 5×10^{36} erg s^{-1}

Reacceleration

A 100 $M_\odot$ molecular cloud with a gas density of 200 cm^{-3} in a 10 μG B-field supports a Kinetic Energy transfer (via magnetic turbulence) of 5.0×10^{32} erg s^{-1}.

Given a total molecular cloud mass of 10^7 $M_\odot$, the total reacceleration of cosmic-ray electrons is 5.0×10^{37} erg s^{-1}.

If these electrons are trapped until losing their energy to bremsstrahlung and synchrotron emission with a standard spectrum):

$$6.1 \times 10^{36} \text{ erg s}^{-1}$$ ✔

A Fermi Bubbles Component?

When the excess floats to the best fit morphological configuration, much of the excess intensity returns.

Most importantly, the over subtraction issue at low energies is fixed.

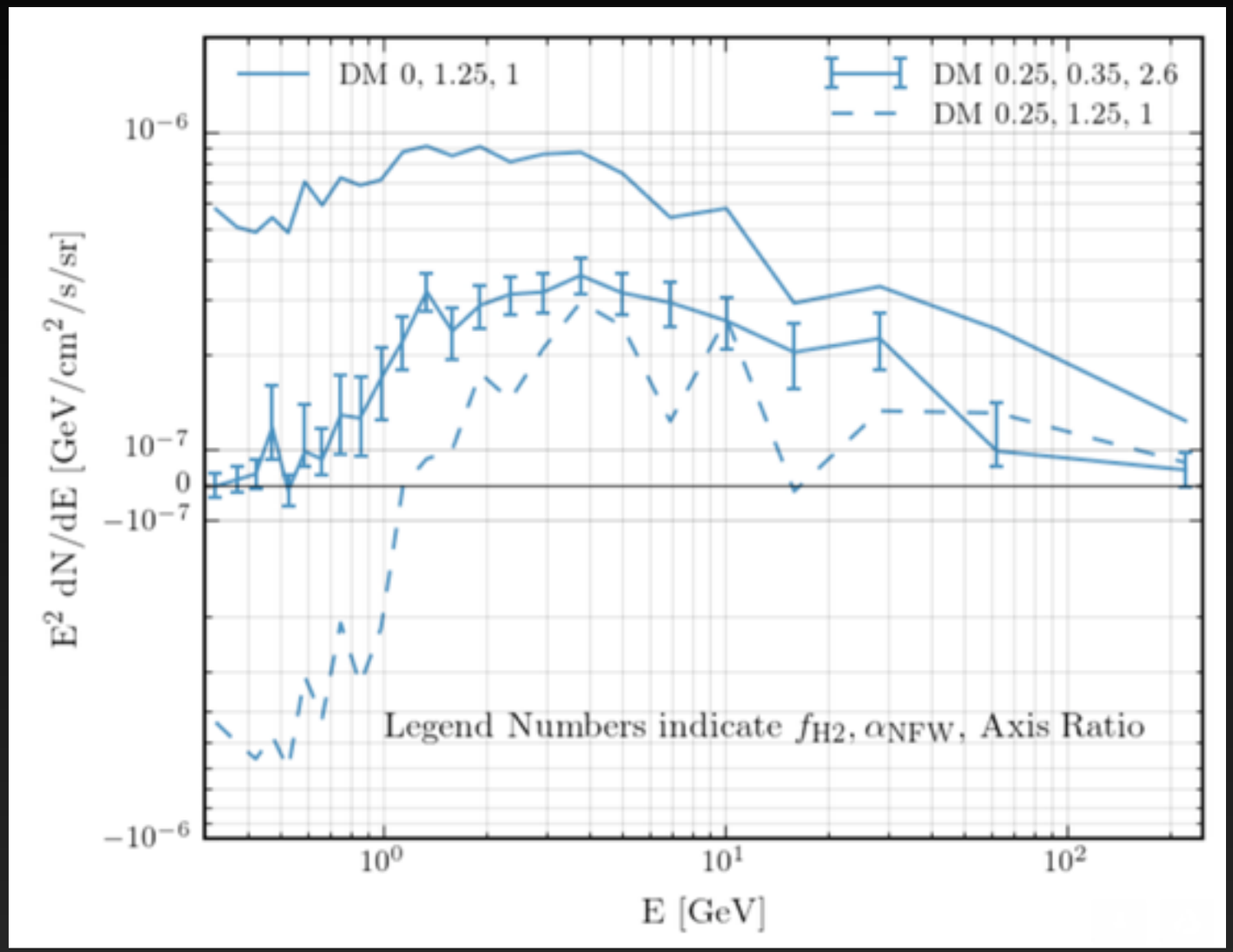

The Excess is Degenerate with f_{H2}

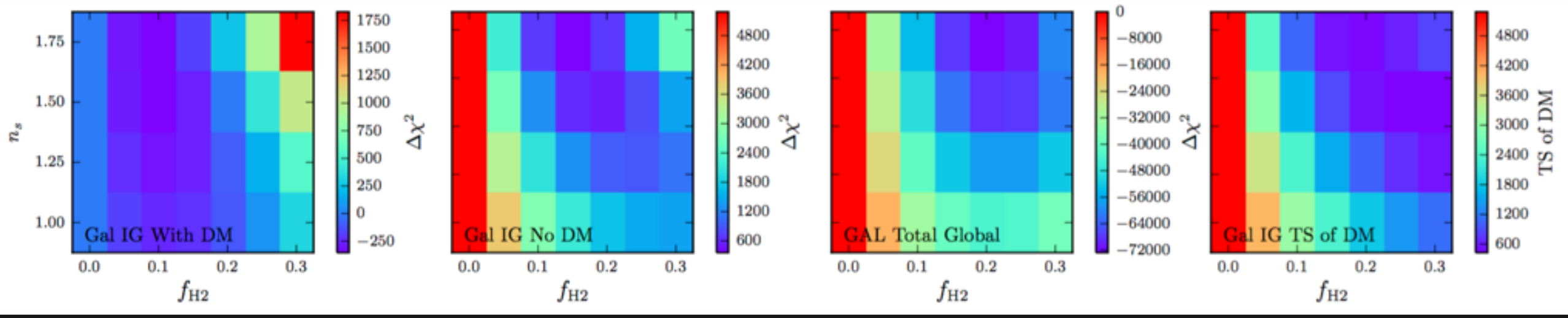

Models with no dark matter universally prefer f_{H2} ~ 0.2 for the 40ºx40º region surrounding the GC.

Models with an NFW emission template prefer f_{H2} ~ 0.1.

The reduction in the normalization of the NFW template is ~1.5 for f_{H2} ~ 0.1, instead of a factor of 3 at f_{H2} ~ 0.2.

Dark Matter Annihilation?

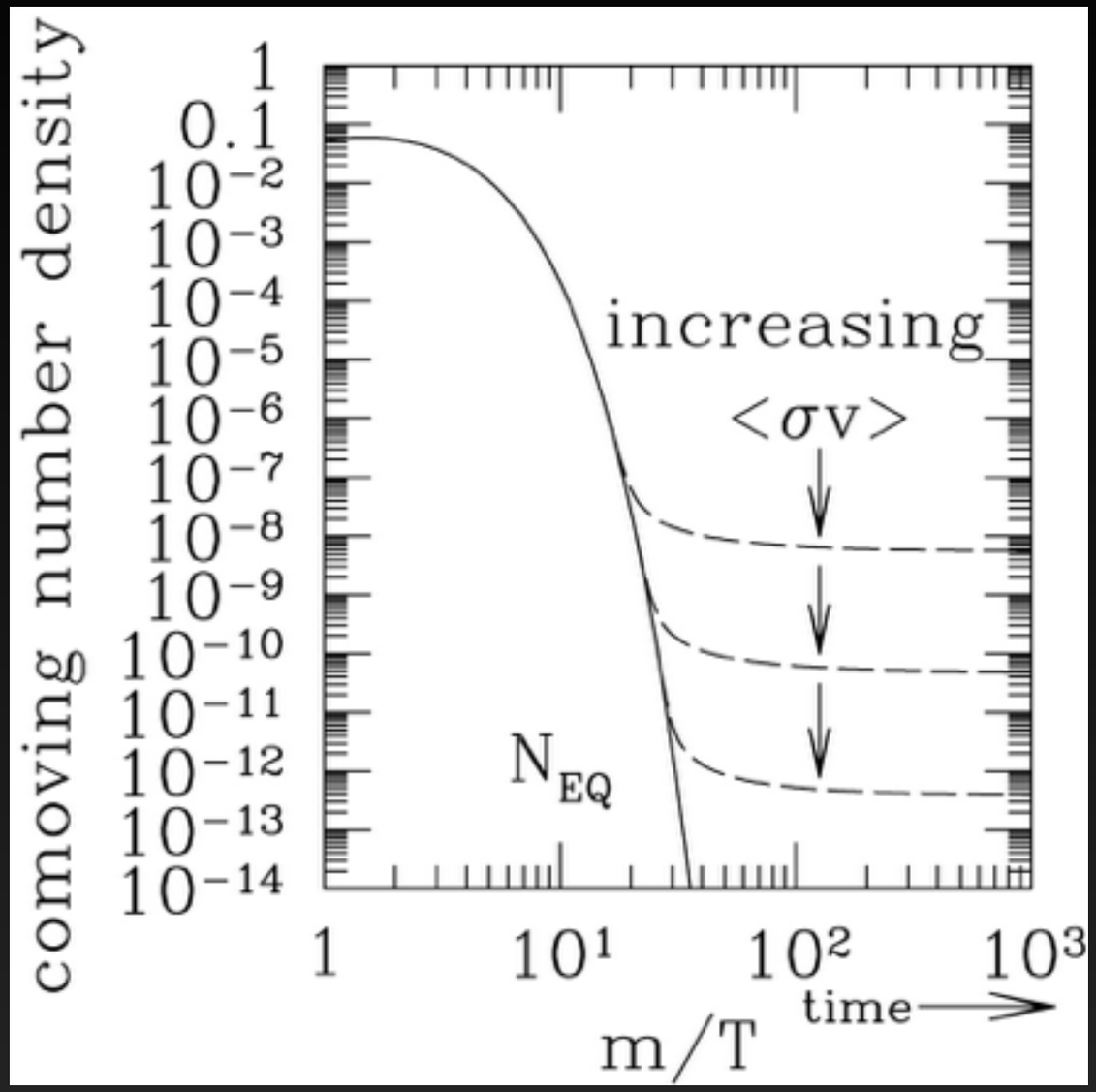

$$\left(\frac{\Omega_\chi}{0.2}\right) \simeq \frac{x_{\text{f.o.}}}{20}\left(\frac{10^{-8}\ \text{GeV}^{-2}}{\sigma}\right)$$

$$\langle\sigma v\rangle \sim 10^{-8}\ \text{GeV}^{-2}\left(3\times10^{-28}\ \text{GeV}^2\ \text{cm}^2\right)\ 10^{10}\ \frac{\text{cm}}{\text{s}} = 3\times10^{-26}\ \frac{\text{cm}^3}{\text{s}}$$

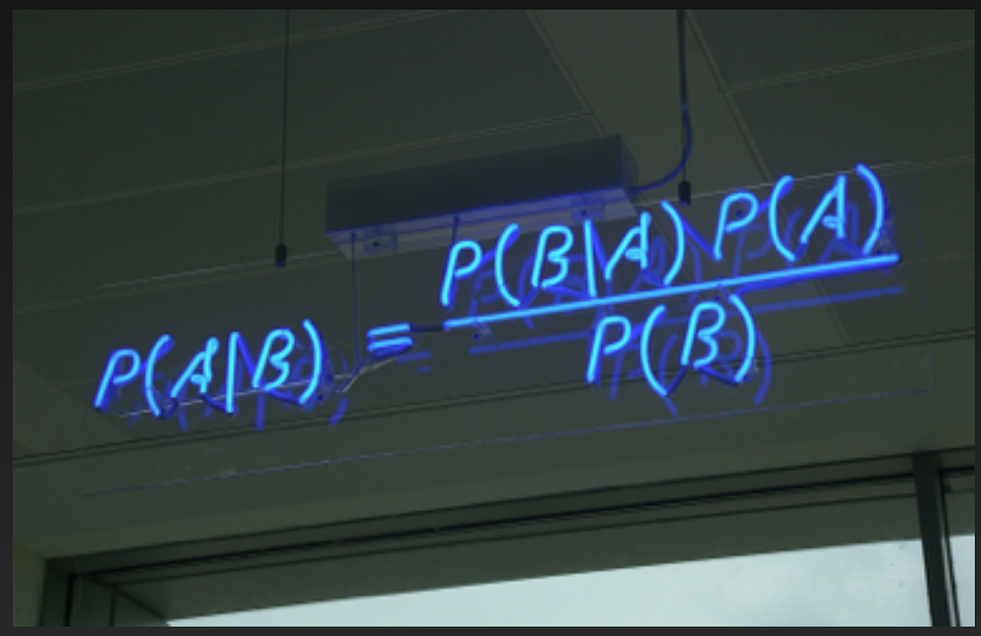

A particle with a weak interaction cross-section and a mass on the weak scale is expected to naturally obtain the correct relic abundance through thermal freeze-out in the Early Universe.